Microplastics in Freshwater Systems: Analysis, Occurrence, and Sorption of Organic Contaminants

Dissertation

by
Dipl.-Ing (FH) Sascha Klein
born on January 11th, 1986 in Wiesbaden, Germany

In Partial Fulfillment of the Requirements for the Degree of
Doctor rerum naturalium
(Dr.rer.nat.)

Submitted to
the Faculty of Environmental Sciences
of the Technische Universität Dresden

Supervisors/Examiners:
Prof. Dr. Eckhard Worch, Technische Universität Dresden
Prof. Dr. Thomas P. Knepper, Hochschule Fresenius, Idstein
Prof. Dr. Thorsten Reemtsma, Helmholtz-Zentrum für Umweltforschung, Leipzig

Day of Defense: December 15th, 2015

Erklärung des Promovenden

Die Übereinstimmung dieses Exemplars mit dem Original der Dissertation zu Thema

„Microplastics in Freshwater Systems:
Analysis, Occurrence, and Sorption of Organic Contaminants”

wird hiermit bestätigt.

Idstein, 14.03.2016
……………………………………….
Ort, Datum

Sascha Klein
………………………………………..
Unterschrift (Sascha Klein)

Die Wissenschaft, richtig verstanden, heilt den Menschen von seinem Stolz; denn sie zeigt ihm seine Grenzen.

- Albert Schweizer

Acknowledgement

First and foremost, I would like to thank Prof. Dr. Eckhard Worch for his supervision and the opportunity to carry out my PhD thesis with him.

I would like to express my special thanks to Prof. Dr. Thomas P. Knepper for his sincere and valuable scientific guidance as well as providing me with all the necessary facilities for my research.

All members of the Institute for Analytical Research contributed immensely to this work. During the last five years, the group of Dr. Tobias Frömel, Jutta Müller, Heike Weil, Dr. Ian Ken Dimzon, Marco Bernhard, Christoph Gremmel, and Daniel Zahn was a great source of incredibly helpful advices, support, and friendships. I enjoyed every day of the past five years working with you.

I am particular thankful to the German Water Chemistry Society for allowing me the PhD grant for two years of my experimental work.

I gratefully acknowledge the “Verband der Privaten Hochschulen e.V.” for awarding the proposal of this thesis with their “Promotionspreis”.

I would like to say thank you to my girlfriend Noreen Klein who has always been there for me. Thank you for your motivating and encouraging me during the past years. You were willing for endless discussions all night long, you were patient, when I needed some time and you gave me strength to move on.

I would also like to thank all of my friends who supported me in writing, and incented me to strive towards my goal. It was great to have you around and that you took my mind off things when it was necessary.

Finally, but by no means least, I would like to thank my family for their unconditional support. Words cannot express how grateful I am but I know that without your help I would not have been able to achieve what I have achieved.

Abstract

Synthetic polymers are one of the most significant pollutants in the aquatic environment, because of abilities such as buoyancy and extreme persistency. Serious effects are expected from so-called microplastics (particle size <5 mm) that are reported in rivers, lakes as well as the ocean and that accumulate in sediments worldwide.

In this thesis the abundance of microplastics in river shore sediments in the Rhine-Main area of Germany was studied. Therefore, a new method was developed that is based on a sodium chloride density separation with subsequent destruction of natural debris, and identification of the plastic particles by microscopy or Fourier transform infrared spectroscopy (FTIR).

Using the improved density separation, microplastics were separated from river shore sediments of 12 sites originating from the river Rhine, the river Main, and the stream Schwarzbach. Large amounts of microplastic particles of up to 1 g kg^{-1} or up to 4000 particles kg^{-1} were detected in the shore sediments. The identification by FTIR showed that polyethylene, polypropylene, and polystyrene were the most abundant polymer types in the sediments, covering over 75% of all plastics identified. Transport of microplastics from tributaries to main streams was indicated by the detection of identical pellets in the River Rhine and in the Main mouth. Comparable concentrations detected by sampling one site over a period of two years suggest a constant pollution of the river shore sediments with microplastics.

For deeper insights into the sorption process of organic contaminants to synthetic polymers in freshwater systems, batch experiments in synthetic freshwater were conducted to determine sorption kinetics and sorption isotherms for four selected glass state polymers (polycarbonate, poly(methyl methacrylate), polystyrene, and polyvinyl chloride) and six different model substances (carbamazepine, hexachlorocyclohexane (β/γ), 17α-ethynilestradiol, chlorpyrifos, and o,p-dichlorodiphenyltrichlorethane). Sorption to the polymer particles was observed for all contaminants increasing with the K_{OW} values of the contaminants. Because of losses of contaminants in control samples, sorption reaction models could be applied to four out of six contaminants, and isotherms were calculated for three contaminants. Furthermore, influences of the different polymer types used were observed in the experiments.

Finally, microplastics separated from sediments were extracted and analyzed by GC/MS and LC-MS/MS using target screening methods and non-target approaches. Different pesticides were identified in the polymer particles, suggesting that microplastics can act as a sink for hydrophobic contaminants. Moreover, several plastic additives such as phthalates or chlorinated flame retardants were identified. For this reason, it is very likely that microplastics act as a direct source for these chemicals in aquatic systems. The results of this thesis stress the urgency for the mitigation of the plastic particles in the aquatic environment.

Kurzfassung

Synthetische Polymere zählen zu den am häufigsten vorkommenden anthropogenen Schmutzstoffen im aquatischen Ökosystem. Besonders kritisch ist das sogenannte Mikroplastik (Partikelgröße <5 mm) anzusehen, das sowohl in Flüssen, Seen als auch dem Ozean nachgewiesen wurde, und in Sedimenten weltweit akkumuliert.

In dieser Arbeit wurde die Mikroplastik-Konzentration in Flussufersedimenten im Rhein-Main-Gebiet in Deutschland sowie die Sorption organischer Schadstoffe an Mikroplastikpartikeln untersucht. Dazu wurde eine Methode zur Abtrennung der Mikroplastikpartikel aus den Sedimenten basierend auf einer Dichtetrennung mit gesättigter Kochsalzlösung entwickelt.

Mit Hilfe dieser Methode wurde Mikroplastik aus 12 Flussufersedimenten der Flüsse Rhein, Main und dem Schwarzbach separiert. Dabei konnten hohe Konzentrationen an Mikroplastik von bis zu 1 g kg^{-1} oder 4000 Kunststoffpartikeln pro kg in den Sedimenten nachgewiesen werden. Messungen mittels Infrarotspektroskopie zeigten, dass über 75% aller detektierten Kunststoffe aus Polyethylen, Polypropylen und Polystyrol bestanden. Mikroplastikpartikel gleicher Form, Farbe und gleichen Polymertyps aus Sedimenten des Rheins und der Mainmündung deuten auf einen Transport von Mikroplastik aus den Nebenflüssen in die Hauptflüsse hin. Da über einen Zeitraum von zwei Jahren an einer Probennahmestelle eine gleichbleibende Mikroplastikkonzentration detektiert wurde, ist eine konstante Verschmutzung der Rheinsedimente anzunehmen.

Um das Sorptionsverhalten von organischen Schadstoffen an synthetische Polymere besser zu verstehen, wurde eine Laborstudie in Batchexperimenten durchgeführt und Sorptionskinetiken und Sorptionsisothermen für vier ausgewählte Polymere (Polycarbonate, Polymethylmethacrylat, Polystyrol und Polyvinylchloride) und sechs ausgewählte organische Schadstoffe (Carbamazepin, Hexachlorcyclohexan (β/γ), 17α-Ethinylestradiol, Chlorpyrifos und o,p-Dichlordiphenyltrichlorethan) bestimmt. Eine Sorption an die synthetischen Polymere konnte für alle Substanzen beobachtet werden. Die sorbierte Konzentration stieg mit ansteigenden K_{OW}-Werten der Substanzen. Aufgrund von Verlusten in einigen Kontrollproben konnten Sorptionskinetiken nur für vier und Sorptionsisothermen nur für drei der sechs Substanzen bestimmt werden.

Durch Extraktion der aus Flussufersediment separierten Mikroplastikpartikel konnte mit Hilfe von *Target*-Analytik und *Non-Target*-Analytik mittels GC/MS und LC-MS/MS verschiedene Pestizide und Umweltkontaminanten an den Mikroplastikpartikeln nachgewiesen werden. Daher ist anzunehmen, dass Mikroplastik als Senke für organische Schadstoffe fungieren kann. Des Weiteren wurden Kunststoffadditive wie Phthalate oder Flammschutzmittel nachgewiesen. Dies verdeutlicht, dass Mikroplastik auch als Quelle für Schadstoffe dienen kann. Die Ergebnisse dieser Arbeit legen die mit Mikroplastik verbundene Problematik dar und zeigen, dass der Kunststoffeintrag in die Umwelt reduziert werden muss ist.

1 Motivation 1

2 Introduction 2

2.1 Synthetic polymers 2

2.1.1 Production and use 2

2.1.2 Extends and impacts of the environmental pollution with plastics 4

2.1.3 Environmental degradation of synthetic polymers 5

2.2 Microplastics 6

2.2.1 Definition 6

2.2.2 Sources 7

2.2.3 Analysis of microplastics 8

2.2.3.1 Density separation 9

2.2.3.2 Identification of microplastics 10

2.2.4 Occurrence in the environment 10

2.2.5 Environmental effects of microplastics 11

2.2.5.1 Effects on organisms 11

2.2.5.2 Sorption and desorption of organic contaminants 12

2.3 Sorption 13

2.3.1 Adsorption 14

2.3.2 Sorption isotherms 15

2.3.2.1 Henry sorption model 15

2.3.2.2 Freundlich isotherm 16

2.3.2.3 Langmuir isotherm 16

2.3.2.4 BET isotherm 16

2.3.3 Kinetics of sorption processes 17

2.3.4 Glass transition temperature 18

2.3.5 Analytical determination of sorption processes 19

3 Objectives 22

4 Materials and Methods 23

4.1 Materials 23

4.1.1 Chemicals, solutions, consumables materials, and instruments 23

4.1.2 Polymers 23

4.2 Investigation of plastic particles in sediments 24
4.2.1 Area of investigation..24
4.2.2 Sampling strategies...25
4.2.2.1 Sampling of Site R4 and R5 in May 2013 25
4.2.2.2 Sampling of shore sediments from the river Rhine, river Main, and stream Schwarzbach from December 2013 until February 2015..25
4.2.3 Sieving 26
4.2.4 Density separation 26
4.2.4.1 Density separation by Thompson *et al.* (2004)..26
4.2.4.2 Vacuum-enhanced separation of plastic artefacts.......................................27
4.2.5 Analysis...28
4.2.5.1 Determination of weight and numerical abundance of plastic particles.........28
4.2.5.2 Microscopic analysis...28
4.2.5.3 Fourier transform infrared spectroscopy 29
4.2.6 Method validation 29
4.2.6.1 Determination of blank values...29
4.2.6.1.1 Blank determination of the density separation 29
4.2.6.1.2 Storage of sediment in HDPE wide neck cans.......................................30
4.2.6.1.3 Blank determination of the complete procedure.....................................30
4.2.6.2 Recovery of the density separation...30
4.2.6.3 Influence of hydrogen peroxide and sulfuric acid on natural debris and synthetic polymer particles..30
4.3 Sorption experiments 31
4.3.1 Investigation of the sorption kinetics..31
4.3.1.1 Sample preparation of the supernatant of CBZ and EE2 solutions...............32
4.3.1.2 Sample preparation of the supernatant from β-HCH, γ-HCH, chlorpyrifos, and DDT solutions 32
4.3.1.3 Extraction of the polymer particles 32
4.3.2 Acquisition of the sorption isotherms 33
4.3.2.1 Sample preparation of CBZ for LC-MS/MS measurements..........................33
4.3.2.2 Sample preparation of γ-HCH and chlorpyrifos for GC/MS measurements ..33
4.4 LC-MS/MS and GC/MS analysis 34
4.4.1 Calibration...34
4.4.2 Method validation 34

4.5 Extraction of the polymer particles from sediment samples 34
4.5.1 Extraction of PS particles 34
4.5.2 Extraction of PE particles 35
4.5.2.1 Extraction method 35
4.5.2.2 Sample preparation for and measurement via LC-MS/MS 35
4.5.2.3 Sample preparation and measurement via GC/MS 35
4.5.3 Blank preparations 35
4.6 Data analysis 36
4.6.1 Statistical analysis 36
4.6.2 Modelling of isotherms and sorption kinetics 36
4.6.3 Principle component analysis 36
5 Results 37
5.1 Microplastic particles in inland water sediments 37
5.1.1 Initial investigations on microplastic abundance in river sediments 37
5.1.2 Method development for the analysis of microplastics in sediments 38
5.1.2.1 Improvement of the density separation 39
5.1.2.2 Removal of natural debris in the filter residues 40
5.1.2.3 FTIR measurements for the identification of plastic particles 41
5.1.2.4 Sampling method 43
5.2 Microplastic abundance in shore sediments sampled in December 2013 44
5.2.1 Abundance of shapes 45
5.2.2 Spatial distribution of microplastics 46
5.2.2.1 Correlation of particle numbers and particle weight 48
5.2.2.2 Correlation of population density and microplastics 49
5.2.3 Abundance of polymer types 49
5.3 Annual variation of the microplastic concentration at site R4 52
5.4 Sorption of contaminants to polymer particles in freshwater systems 53
5.4.1 Determination of sorption kinetics of different organic contaminants to PE, PC, PMMA, PS, EPS, and PVC 53
5.4.1.1 Carbamazepine 53
5.4.1.2 β-HCH and γ-HCH 54
5.4.1.3 Ethinylestradiol 57

5.4.1.4 Chlorpyrifos 58
5.4.1.5 DDT 59
5.4.2 Modelling sorption kinetics for CBZ, γ-HCH, EE2, and Chlorpyrifos 60
5.4.3 Extraction of polymer particles 61
5.4.4 Sorption isotherms 64
5.4.5 Principle components analysis of contaminant sorption to polymer particles ...67
5.5 Extraction of PE and PS particles separated from sediments 69
5.5.1 Screening for contaminants using GC/MS and LC-MS/MS....................69
5.5.2 Screening for contaminants by GC/MS measurements in Scan mode....................70
6 Discussion 73
6.1 Microplastics in freshwater sediments 73
6.1.1 Method development to improve microplastic separation 73
6.1.1.1 Sampling strategy....................73
6.1.1.2 Sodium chloride for density separation 74
6.1.1.3 Natural debris removal....................75
6.1.1.4 Polymer analysis by FTIR....................75
6.1.2 Occurrence and spatial distribution of microplastics along the river Rhine, the river Main, and the stream Schwarzbach....................76
6.1.2.1 Concentration of microplastics in the river shore sediments....................76
6.1.2.2 Particle shape of microplastics....................78
6.1.2.3 Polymer types in the sediments 79
6.1.2.4 Spatial distribution of microplastics 79
6.1.3 Consistency of the microplastic pollution 83
6.2 Sorption of contaminants to polymer particles 83
6.2.1 Sorption in dependence on K_{OW} values 83
6.2.2 Sorption isotherms and sorption kinetics of CBZ 84
6.2.3 Sorption kinetics and sorption isotherms of γ-HCH....................85
6.2.4 Sorption kinetics and sorption isotherms of chlorpyrifos 86
6.2.5 Sorption kinetics of β-HCH and DDT and losses in control samples....................87
6.2.6 Possible mobilization of sorbed β-HCH by microplastics 87
6.2.7 Determination of contaminant sorption via a direct and an indirect method – A comparison via polymer extraction 89

6.3 Environmental contaminants in microplastics from sediments of the river Rhine, river Main, and stream Schwarzbach 91

6.4 Conclusion 92

7 Perspectives 94

8 Summary 96

9 Annex 98

9.1 Materials and Methods 98

9.1.1 Consumable materials 98

9.1.2 Instruments 98

9.1.3 Solutions 99

9.1.3.1 Saturated sodium chloride solution 99

9.1.3.2 Synthetic freshwater 99

9.1.4 Reference materials and stock solutions 100

9.1.5 Separation of microplastics from shore sediments 100

9.1.6 Sorption isotherm experiments 101

9.1.7 Instrument parameters 101

9.1.7.1 GPC Parameters 101

9.1.7.2 LC-MS/MS analysis 102

9.1.7.2.1 LC-MS/MS analysis for the determination of sorption kinetics and sorption isotherms 102

9.1.7.2.2 LC-MS/MS parameters for the target screening of extracted microplastics 103

9.1.7.3 GC/MS analysis 105

9.1.7.3.1 GC/MS method for the analysis of the laboratory sorption experiments 105

9.1.7.3.2 GC/MS screening method for analysis of microplastic extracts in SIM mode and Scan mode 106

9.2 Investigations on microplastic abundance in river shore sediments 110

9.2.1 Identification of microplastics via FTIR 110

9.2.2 Investigations on blank values 110

9.2.3 Analysis of microplastics in shore sediments 111

9.3 Investigation on sorption of contaminants on microplastics 113

9.3.1 Polymer particle characterization 113

9.3.2 Control samples of the sorption kinetics experiments 114

9.3.3 Determination of sorption kinetics 116

9.4 Extraction via dissolution with subsequent GPC clean-up 118

10 References 122

List of Figures

Figure 1: (A) Production of synthetic polymers worldwide (blue line) and in European countries (green line) starting in 1950. (B) European plastic demand and relative demand in percent of the most important countries. Data from PlasticsEurope (2015, modified).[3] 2

Figure 2: Possible degradation pathways of synthetic polymers in the environment. Solid lines show degradation processes of intact polymer products resulting in fragments or smaller molecular units. Dashed lines assign degradation processes of polymer fragments that are involved in the degradation of polymer fragments in monomers, dimers, or oligomers. From Gu (2003, modified)[37] 6

Figure 3: Possible routes described in literature for the analysis of microplastics in sediment samples starting sample pre-treatment to the report of the results. The sample preparation is split in pre-treatment, the density separation, and the post treatment of the separated microplastics. Fourier transform infrared spectroscopy (FTIR), scanning electron microscopy-energy dispersive X-ray spectroscopy (SEM-EDS)........ 8

Figure 4: Possible impacts of microplastics on aquatic environments divided into microplastics acting as transporter or source. Impacts are shown for the water column as well as the sediment compartment. Dashed arrows show additional routes that do not necessarily involve microplastics. 12

Figure 5: Basic terms of adsorption of molecules from a liquid phase to a solid surface. Worch (2012, modified).[110] 14

Figure 6: Scheme of the isotherm models which were are known as the Henry model, Freundlich model, Langmuir model, and the BET model. 15

Figure 7: Different approaches to determine sorption in laboratory batch experiments or in environmental samples. Accelerated solvent extraction (ASE), microwave-assisted extraction (MAE), solid phase extraction (SPE), solid phase micro extraction (SPME), matrix-assisted laser desorption ionization-time of flight (MALDI-TOF), direct analysis in real time (DART), fluorescence detector (FLD). 20

Figure 8: Detailed map of the sampling sites in the Rhine Main area in Germany. Sampling sites are marked by circles; (S1) Astheim, (S2) Ginsheim-Gustavsburg Schwarzbach, (R1) Ginsheim-Gustavsburg, (M1) MZ-Kostheim 1, (M2) MZ-Kostheim 2, (R2) MZ-Kastel 1, (R3) MZ-Kastel 2, (R4) WI-Biebrich, (R5) WI-Schierstein, (R6) Walluf, (R7) Erbach, (R8) Geisenheim. Grey-shaped areas represent settled areas. Arrows mark the locations of municipal sewage treatment plants........24

Figure 9: Schematic of the vacuum-enhanced density separation of plastic artefacts. Floating particles are transferred by addition of saturated sodium chloride solution by means of a vacuum directly to the glass fiber filter. 28

Figure 10: Analysis of river shore sediments sampled in May 2013. The mass fraction and particle numbers of microplastics separated from sediments from site R4 and site R5. The sampling was done in triplicates, and the density separation was carried out after Thompson *et al*. (2004). 37

Figure 11: Abundance of polymer types by weight (A) and by number (B) in the sediment samples from R4 and R5. Identification of the polymer type was carried out by ATR-FTIR spectroscopy. Polymers identified were PE, PP, PS, and PET. Non-identified particles are marked as “unknown”. 38

Figure 12: (A) Recovery rates of PE pellets, PC, PMMA, PS, and PVC separated from clean sand by two different density separation methods. Density separations were carried out in triplicates. Microscopic analysis of PC (B), PVC (C), PS (D), and PE (E) used for the recovery experiments. 40

Figure 13: Influence of the treatment with hydrogen peroxide and sulfuric acid on the mass of natural debris (black diamonds) and on the polymers PC (red squares), PMMA (yellow triangles), PS (green diamonds), and PVC (cyan circles). The reaction was carried out over 24 h in duplicates. 41

Figure 14: ATR-FTIR spectrum of a green polymer pellet scanning the aged polymer surface (A) and fresh polymer surface (B). Blue lines represent measured spectra; red lines represent the respective database spectra with the best match factors. A microscopic image of the surface at a 40-old magnification is provided on the right hand-side. 42

Figure 15: Design for the different sampling procedures of river shore sediment. Random, triplicate sampling of sediment along the sampling site is shown by green circles. Theoretical coverage of zone sampling of distinct areas (0.5 m x 0.25 m) is represented by red rectangles. 43

Figure 16: Weight abundance (A) and numerical abundance (B) of microplastic particles from twelve sediments (R1-R8, M1, M2, S1, S2) determined in the size fraction 63-200 µm, 200-630 µm and 630-5000 µm. Black rectangles represent the average of the data. Data is plotted in logarithmic scale (n=12). 45

Figure 17: (A) Abundance of plastic pellets (P), fragments (F), spheres (S), and fibers (Fi) in the size fractions 63-200 µm (blue), 200-630 µm (red), and 630-5000 µm (green). (B) Microscopic image of the size fraction 63-200 µm at a magnification of 100-fold to show exemplarily the classification of the particle shape. Numbers in parenthesis represent the size of the particles in µm measured by the lengths of the red lines. 46

Figure 18: Spatial distribution of microplastics in terms of mass fraction and numerical abundance. Microplastics were separated from sediments of the stream Schwarzbach (S1, S2) the river Main (M1, M2), and the river Rhine (R1-R8), sampled on 3th December 2013. Data is shown for the size fractions 63-200 µm (blue bars), 200-630 µm (red bars), and 630-

5000 µm (green bars) in logarithmic scale. The flow direction of the river is displayed by a blue arrow. 47

Figure 19: Correlation of total particle number and total particle weight at the sampling sites S1, S2, M1, M2, and R1-R8......48

Figure 20: Correlation of population density with mass fraction of microplastics (A) and numerical abundance of microplastics (B). Sampling sites are marked in the plots (S1, S2, R1-R8, M1, and M2). 49

Figure 21: Relative abundance of each polymer type in terms of weight and numbers at the sampling sites from the stream Schwarzbach (S1, S2), the river Main (M1, M2), and river Rhine (R1-R8). The flow direction of the the river is shown by the blue arrow. 50

Figure 22: Identification of optical identical polymer pellets at sampling sites M2, R2, and R3 (A) as EPDM (B) and PP (C) by ATR-FTIR spectroscopy......51

Figure 23: Mass fraction of microplastics separated from sediments of site R4 over a time period of approximately 2 years (grey bars, n=3). The water level of the river Rhine is shown by the blue dotted line (note that it does not represent the exact course of the the water level). 52

Figure 24: Sorption of CBZ to the polymers PE, PC, PMMA, PS, EPS, and PVC depending on time. The experiments were carried out in duplicates over 30 days. The decrease of CBZ is shown relatively to the initial concentration of CBZ. 54

Figure 25: Sorption of β-HCH to the polymers PE, PC, PMMA, PS, EPS, and PVC in dependence on time. The experiments were carried out in duplicates over 30 days. The decrease of β-HCH is shown relatively to the initial concentration of β-HCH. Average concentration of the control sample after two days is shown as dashed line......55

Figure 26: Concentration of β-HCH in the supernatant of five samples without polymer over 27 days. PC, PMMA, PS, or PVC particles, respectively, were added after 27 days to four samples......56

Figure 27: Sorption of γ-HCH to the polymers PE, PC, PMMA, PS, EPS, and PVC in dependence on time. The experiments were carried out in duplicates over 30 days. The decrease of γ-HCH is shown relatively to the initial concentration of γ-HCH. 57

Figure 28: Sorption of EE2 to the polymers PE, PC, PMMA, PS, EPS and PVC in dependence on time. The experiments were carried out in duplicates over 30 days. The decrease of EE2 is shown relatively to the initial concentration of EE2. 58

Figure 29: Sorption of chlorpyrifos to the polymers PE, PC, PMMA, PS, EPS, and PVC in dependence on time. The experiments were carried out in duplicates over 30 days. The decrease of chlorpyrifos is shown relatively to the initial concentration of chlorpyrifos. 59

Figure 30: Decrease of DDT concentration in samples containing the polymers PE, PC, PMMA, PS, EPS, and PVC in dependence on time. The experiments were carried out in

duplicates over 30 days. The decrease of DDT is shown relatively to the initial concentration of DDT. Average concentration of the control sample after two days is shown as dashed line. 60

Figure 31: Concentration of the organic contaminants CBZ, HCH, HCH, EE2, chlorpyrifos, and DDT sorbed to the polymers PC, PMMA, EPS, PS, and PVC in 30 days. The amount of sorbed contaminant was determined by measurement of the supernatant (indirect method; orange bars) and by extraction of the polymer particles (direct method; blue bars). 63

Figure 32: Sorption efficiency PC, PMMA, EPS, PS, and PVC in dependence to the contaminants CBZ, γ-HCH, β-HCH, EE2, chlorpyrifos, and DDT. Data is normalized to highest sorption of each contaminant. Contaminants are listed in order of increasing K_{OW}. ..64

Figure 33: Sorption isotherms of CBZ, γ-HCH, and chlorpyrifos for the synthetic polymers PC, PMMA, PVC, and PS. Symbols represent experimental data and lines represent the best fit for the Henry model (blue), Freundlich model (red), Langmuir model (orange), and BET model (green). Only curves of models with reasonable fits are shown. Data are shown in double logarithmic scale. 65

Figure 34: (A) Factor loading plot and (B) factor scores plot of the PCA with the K_D values of CBZ, γ-HCH, and chlorpyrifos as well as the polymer parameters T_g and the C/H and O/C ratios, respectively. Polymers used were PC, PMMA, PS and PVC. 68

Figure 35: GC/MS total ion chromatogram of PE extract obtained in SIM mode. The details show exemplary extracted ion chromatograms of the detected substances TCEP (A), chlorpyrifos (B), and TPP (C). 70

Figure 36: GC/MS total ion chromatogram of PE extract obtained in SCAN mode. Details show exemplary mass spectra of the substances DnPP (A), M2EHP (B), and B2INP (C), which were identified by database comparison with the highest match factors. 71

Figure 37: Proposed mobilization of β-HCH sorbed to glass in an initial step by the addition of polymer particles (data of PMMA shown). 88

Figure 38: IR spectra of PE, PP, PS, acrylic polymer, PA, and EVA, compared to reference spectra (REF). Match factors are shown in brackets. 110

Figure 39: Particle size distribution based on the particle number of the polymer powders PC (green) PMMA (yellow), PS (teal), and PVC (red). Size distributions were obtained by microscopic measurement of 200 particles. 113

Figure 40: Particle density distribution based on the particle number of the polymer powders PC (green) PMMA (yellow), PS (teal), and PVC (red). The particle density distributions were obtained by microscopic measurement of 200 particles. 114

Figure 41: Control samples of the sorption kinetics experiments of CBZ (A), β-HCH (B), γ-HCH (C), EE2 (D), chlorpyrifos (E), and DDT (F). Measurements were done with two independent controls samples for each substance. 115

Figure 42: Sorption kinetics model curves applying a pseudo-first-order rate law for the polymers PMMA and PVC and the model substances CBZ, γ-HCH, EE2, and chlorpyrifos. 116

Figure 43: Sorption kinetics model curves applying a pseudo-first-order rate law for the polymers PS and EPS and the model substances CBZ, γ-HCH, EE2, and chlorpyrifos......117

Figure 44: Sorption kinetics model curves applying a pseudo-first-order rate law for the polymer PVC and the model substances CBZ, γ-HCH, EE2, and chlorpyrifos....................118

Figure 45: Elution time of CBZ on a GPC system equipped with a PSS SDV linear M column using THF as eluent. CBZ was measured by LC-MS/MS after collecting 12 fractions between 8.5 and 12.5 min....................119

Figure 46: (A) GPC chromatogram of the separation of PMMA (1) and CBZ (2) after detection by a refractive index detector. (B) LC-MS/MS chromatogram of 0.1 ng mg^{-1} CBZ after measured after GPC separation from PMMA. Chromatograms of the quantifier ion (blue line) and the qualifier ion (red line) including the signal-to-noise ratio (S/N) of the quantifier ion are shown....................120

List of Tables

Table 1: Polymer types in the order of European plastic demand including density, structure, and abbreviation used in this thesis. 3

Table 2: Polymers used in this work, including abbreviation used, glass transition temperature (T_g), formulation, molecular mass (M_W) with polydispersity index in parenthesis, and supplier. 23

Table 3: Details of the sampling campaigns at the river Rhine, river Main, and stream Schwarzbach including dates of sampling, water levels of the rivers, and further processing. The processing includes sieving (S) ,density separation described by Thopmson *et al.* (2004) (DST), or vacuum-enhanced separation of plastic artefacts (VESPA), visual identification of plastic particles by microscopy (Mic), and FTIR (IR). 26

Table 4: Contaminants used for sorption experiments, including log K_{OW} values, water solubility Concentration of the contaminants in synthetic freshwater used for the kinetic experiments. The references are provided in parentheses. 31

Table 5: Mass fraction and item numbers of the triplicate analysis from sediment samples which were taken at the sampling sites R4 and R8 by random sampling. Data are shown as means and relative standard deviation in parentheses. 44

Table 6: Parameters of a first order rate law for the sorbates CBZ, γ-HCH, EE2, and chlorpyrifos and sorbents PC, PMMA, PS , EPS, and PVC. q_{eq} is the equilibrium concetration in the polymer particle in ng mg^{-1}, k is the rate constant in h^{-1}, and $t_{1/2}$ is the half-life period in h. Errors of the parameters are shown in parantheses. 61

Table 7: Parameter of Henry, Freundlich, BET, and Langmuir model fits for CBZ, γ-HCH, and chlorpyrifos isotherms for PC, PMMA, PS, and PVC. K_D is the distribution coefficient in L g^{-1}, K_F is the Freundlich coefficient in (µg g^{-1})(µg L^{-1})$^{-1/n}$, n^{-1} is the Freundlich exponent, K_L is the Langmuir constant in L mg^{-1}, q_{max} is the maximum monolayer coverage capacity in mg g^{-1}, K_B is the BET sorption coefficient, q_m is the concentration of a monolayer, and C_s the saturation concentration. The quality of the model fit is represented by R². (N=10) 67

Table 8: Summary of the substances identified in the extracted polymers listed by the origin of their sampling location. 71

Table 9: Consumable materials used in this work. 98

Table 10: Instruments used in this work. 98

Table 11: Reference materials used in this work. Solvent of BPA-D16 and CBZ-D10 was acetonitrile. 100

Table 12: Sampling sites at the river Rhine, the river Main, and the stream Schwarzbach with abbreviation used and coordinates of the sites. 100

Table 13: Concentration and sampled volume of CBZ, γ-HCH, and chlorpyrifos in the sorption isotherm experiments. 101

Table 14: Conditions of the GPC clean-up for the extraction of contaminants from THF-soluble polymer particles 101

Table 15: Settings of MS parameters used for the analysis of CBZ, EE2, and the mass-labeled internal standards CBZ-D10 and BPA-D16. 102

Table 16: Gradients for the chromatographic separation of CBZ and EE2. 103

Table 17: Chromatographic conditions of the LC-MS/MS target screening method. 103

Table 18: Ion source parameters of the LC-MS/MS target screening method. 104

Table 19: MRM parameters of the LC-MS/MS screening method including substance name, *m/z* ratios selected in Q1 and Q3, as quantifier and qualifier ion, respectively, as well as the respective declustering potential (DP), and collision energy (CE). 104

Table 20: Parameters for the GC/MS analysis. 105

Table 21: GC parameters used in the SIM method. 106

Table 22: Substances comprised and *m/z* ratios used in the GC/MS screening method as quantifier and qualifier ions. 107

Table 23: GC/MS parameters for the GC/MS analysis in Scan mode 108

Table 24: Blank values obtained after sieving of clean sand, shaking of wide-neck cans filled with clean sand, blank values of the density separation only and the blank values of the complete method. Control samples that were analyzed with the sediment samples are shown as “Mean blank value”. Blank values are given as absolute particle numbers. Standard deviation is shown in parentheses. 111

Table 25: Mass fraction of plastic in the sediments analyzed. All values are given in mg kg^{-1}. 111

Table 26: Number of plastic items in the sediments analyzed. All values are given as plastic particles kg^{-1} except the estimation of total amount of microplastics for area-related results. Although exact numbers are provided, these should be considered as estimation. 112

Table 27: Recovery of the substances CBZ, β-HCH, γ-HCH, EE2, chlorpyrifos, and DDT after GPC clean-up and analysis by LC-MS/MS or GC/MS, respectively. Recovery was determined with and without the use of an internal standard (ISTD). GC/MS analysis was additionally carried out with an internal calibration. Standard deviation of a triplicate analysis is shown in parentheses. 121

List of Abbreviations

ANOVA	Analysis of variation
ASE	Accelerated solvent extraction
ATR	Attenuated transverse reflectance
B2INP	1-Butyl-2-isononylphthalat
CBZ	Carbamazepine
CE	Collision energy
DART	Direct analysis in real time
DBP	Dibutylphthalate
DDT	o,p’- Dichlorodiphenyltrichloroethane
DNP	Dinonylphthalate
DnPP	Di-n-pentylphthalate
DP	Declustering potential
EDS	Energy dispersive X-ray spectroscopy
EE2	17α-Ethinyl estradiol
EPDM	Ethylene propylene diene rubber
EPS	Expanded polystyrene
EVA	Ethylene vinyl acetate
FLD	Fluorescence detector
FTIR	Fourier transform infrared spectroscopy
GC	Gas chromatography
GPC	Gel permeation chromatography
ISTD	Internal standard
LC	Liquid chromatography
M2EHP	Methyl-2-ethylhexylphthalate
MAE	Microwave-assisted extraction
MALDI	Matrix-assisted laser desorption ionization
MRM	Multiple reaction monitoring
MS	Mass spectrometry
n/a	Not applicable
PA	Polyamide
PAH	Polycyclic aromatic hydrocarbon
PC	Polycarbonate
PCA	Principle component analysis
PCB	Polychlorinated biphenyl
PE	Polyethylene
PET	Polyethylene terephthalate
PMMA	Polymethacrylate
POM	Polyoxymethylene

PP	Polypropylene
PS	Polystyrene
PSS	Polymer Standard Services
PU	Polyurethane
PVC	Polyvinyl chloride
Pyr	Pyrolysis
REF	Reference Spectra
RSD	Relative standard deviation
SD	Standard deviation
SEM	Scanning electron microscopy
SIM	Single ion monitoring
SPE	Solid phase extraction
SPME	Solid phase micro extraction
TCEP	Tris(2-chloroethyl) phosphate
TCPP	Tris(2-chloroisopropyl) phosphate
T_g	Glass transition temperature
THF	Tetrahydrofuran
TOF	Time of flight
TPP	Triphenyl phospate
UK	United Kingdom
UV	Ultraviolet
VESPA	Vacuum-enhanced separation of plastic artefacts
β-HCH	β-Hexachlorocyclohexane
γ-HCH	γ-Hexachlorocyclohexane

Parts of this thesis have been published in the following articles

Klein, S., Worch, E., Knepper, T. P. (2015) Occurrence and spatial distribution of microplastics in river shore sediments of the Rhine-Maine area in Germany. Environmental Science and Technology, 49, 10, 6070-6077.

Klein, S., Worch, E., Knepper, T. P. (2015) Belastung von Mikroplastik aus Flussufersediment mit organischen Schadstoffen. Jahrestagung der Wasserchemischen Gesellschaft, Wasser 2015, Tagungsband (ISBN 978-3-936028-90-4), 396-398.

Klein, S., Worch, E., Knepper, T. P. (2014) Mikroplastik in aquatischen Ökosystemen: Vorkommen in Flusssedimenten und Belastung mit organischen Schadstoffen. Jahrestagung der Wasserchemischen Gesellschaft, Wasser 2014, Tagungsband (ISBN 978-3-936028-83-6), 443 -446.

Klein, S., Worch, E., Knepper T. P. (2013) „Microplastics“ in aquatischen Ökosystemen: Untersuchung der Sorption organsicher Schadstoffe an synthetische Polymere in Süßwasser. Jahrestagung der Wasserchemischen Gesellschaft, Tagungsband (ISBN 978-3-936028-71-3), 142-146.

1 Motivation

Synthetic polymers in the form of plastic debris are one of the most significant pollutants in the aquatic environment. Extremely durable, lightweight, and mostly buoyant, plastic particles spread in the aquatic environment and last for several decades. For this reason, it is not surprising that plastic particles are reported in different sizes and shapes in all marine compartments all over the world.

In the recent years, small plastic particles, so-called microplastics came into the focus of scientists more and more. The elevated abundance compared to larger particles in marine systems underlines the serious concerns about microplastic particles. These anthropogenic microparticles possibly interfere in natural systems and might be harmful after ingestion by organisms. Even though freshwater systems are of particular concern, as they possibly act as transport vectors for plastic particles or are used for drinking water production the majority of scientific reports concentrates on the plastic pollution of the marine environment. For this reason, data of the microplastic pollution of freshwater ecosystems were very rare. To the best of the author’s knowledge no publications on the microplastic burden of inland waters were available by 2010. Consequently, no estimation about the pollution of freshwater systems with microplastics was possible, and the relevance of microplastics for inland waters remained unclear.

Furthermore, it is known that organic contaminants present in the aqueous system sorb to particles made from synthetic polymers, leading to enrichment on the polymer surface. For this reason synthetic polymers are a suitable material for passive sampling devices. However, contaminants sorb to plastic debris of aquatic systems likewise to the sorption to the passive samplers. Thus, different organic contaminants have already been detected in marine plastic debris.

For the production of commercial products, a variety of different polymer types is used. Hence, highly diverse polymers might be present in the environment. As these polymers differ in their chemical and mechanical properties, it is likely that they offer different sorption characteristics. However, the sorption process was mainly studied for polyethylene or polypropylene particles, as they are expected to be the most important polymer types in the environment. For this reason, the sorption to other polymer particles is not fully understood, yet. Moreover, the relevance of contaminant sorption to microplastics in freshwater systems might still be overlooked.

2 Introduction

2.1 Synthetic polymers

Synthetic polymers are organic macromolecules that are composed of several monomeric units, and are formed by a polymerization reaction of the monomers. The general definition of the term polymer is met, if the properties of the macromolecule do not change by the addition of one monomer unit to the polymer chain.[1]

Synthetic polymers, or so-called plastics, were first discovered with the inventions of vulcanized rubber and polystyrene in the 19th century.[2] Nowadays synthetic polymers play an integral role in both, technological advancement and everyday life.

2.1.1 Production and use

During the first 60 years of the 20th century, the expansion of synthetic polymers was initiated by the discovery of different important polymer types such as polyethylene (PE), polypropylene (PP), polystyrene (PS), polyvinyl chloride (PVC), and polyurethane (PU). Starting the 1940s to 1950s, synthetic polymers were produced in high amounts and distributed all over the world. Since the beginning of the mass production of polymers, the production volume of synthetic polymers increased to more than 150-fold to 299 Mt per year until 2013 (Figure 1A).[3]

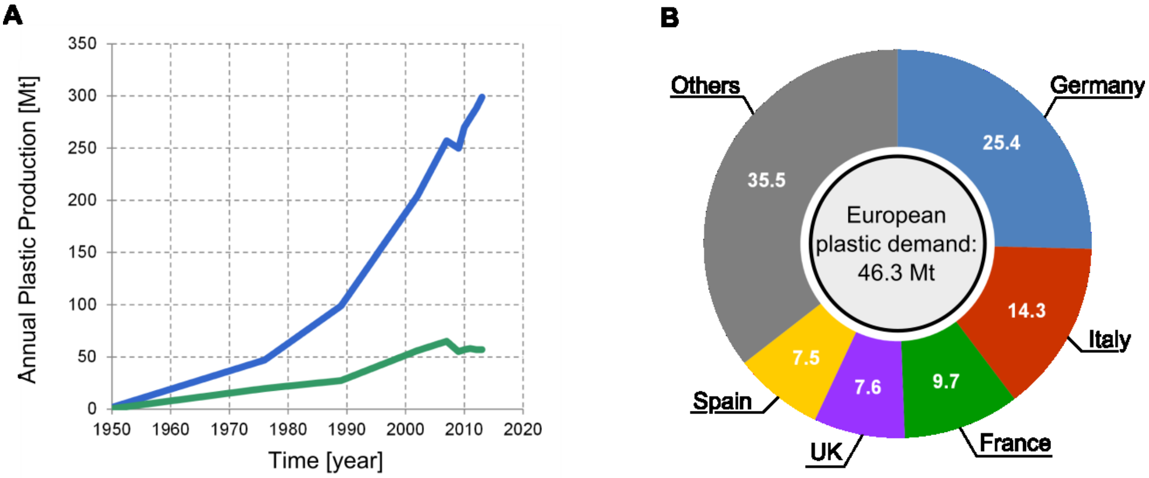

Figure 1: (A) Production of synthetic polymers worldwide (blue line) and in European countries (green line) starting in 1950. **(B)** European plastic demand and relative demand in percent of the most important countries. Data from PlasticsEurope (2015, modified).[3]

Besides with China and North America, Europe is one of the most important markets for plastics having currently a constant production of synthetic polymers of 57 Mt per year and a plastic demand of 46.3 Mt per year. Leading countries of the European plastic demand are Germany, Italy, France, the United Kingdom (UK), and Spain. Among those countries

Germany poses the highest demand accounting for approximately 25%, underlining the urgency for monitoring studies of plastic debris in the environment (Figure 1B).[3]

The high versatility of synthetic polymers can be easily explained by their unique material properties. On the one hand-side plastics are lightweight and resistant to mechanical, chemical and biological stress. The cheap production and easy processing of plastics on the other hand are further reasons for the success of synthetic polymers.

Albeit the availability of many hundreds of different polymer types, only a few plastics cover over 75% of the total plastic demand. These commodity plastics are namely, PE, PP, PS, PET, PVC, and PU (Table 1). Besides commodity plastics, different engineering polymers are used for important applications such as clothing (polyamide; PA), as safe replacement for soda-lime glass in building and construction, or automotive production (polycarbonate; PC and poly(methyl methacrylate); PMMA). Plastics are used in many fields, but the main purposes are packaging (39.6%) as well as building and construction (20.3%).[3] For example, foamed PS is a versatile material that is used to create lightweight and shock resistant packaging.

Often, the synthetic polymers do not directly provide the desired material properties and polymer additives must be used to alter or to improve the plastic properties for the intended purpose. These additives comprise for example, softeners that decrease the brittleness of the plastics, stabilizers that prohibit oxidation of the synthetic polymers or of the additives, respectively, blowing agents that are necessary for the further processing or flame retardants to meet purpose criteria.[1]

Table 1: Polymer types in the order of European plastic demand including density, structure, and abbreviation used in this thesis.

Polymer	**Abbre-viation**	**Demand (EU) [%]**[3]	**Density**[4, 5]	**Structure**
Polyethylene	PE	29.6	0.91-0.96	$-\!\!\left[CH_2-CH_2\right]_n\!\!-$
Polypropylene	PP	18.9	0.90-0.91	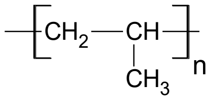 $-\!\!\left[CH_2-\underset{CH_3}{CH}\right]_n\!\!-$
Polyvinyl chloride	PVC	10.7	1.16-1.58	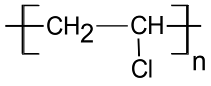 $-\!\!\left[CH_2-\underset{Cl}{CH}\right]_n\!\!-$
Polyurethane	PU	7.4	1.20	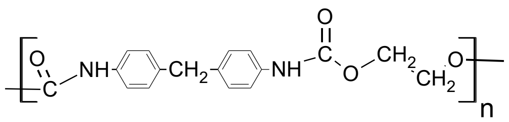
Polystyrene	PS	7.1	1.04-1.10	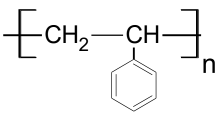

Polymer	Abbre-viation	Demand (EU) [%][3]	Density[4, 5]	Structure
Polyethylene terephthalate	PET	6.9	1.37-1.45	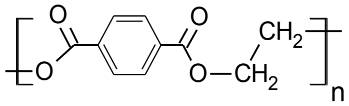
Polyamide	PA	2.0	1.02-1.05	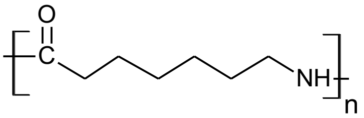
Polycarbonate	PC	1.3	1.20-1.22	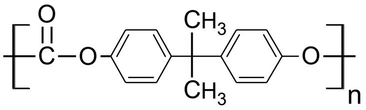
Poly(methyl methacrylate)	PMMA	0.6	1.17-1.20	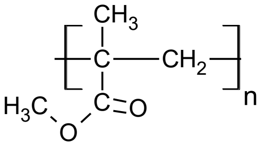

2.1.2 Extends and impacts of the environmental pollution with plastics

First reports of plastic marine litter were published in the 1970 years.[6-8] However, these reports have drawn only little attention from the scientific community. Over the years, plastics accumulated in the environment and are nowadays present in every environmental compartment. Thus, plastic debris is reported at beaches, coastal sediments, the Antarctica, or the open ocean itself.[9-13] Very high amounts of plastic debris are found in the ocean, specifically in the regions of the great ocean gyres, as plastic are transported and gathered in these region by currents.[14-17] Noteworthy, the plastic particles are floating several meters below the sea surface, invisible from above, and should not be regarded as one large accumulation covering the sea surface.

Plastic litter in the aquatic environment can be either discharged directly in the marine and freshwater systems or are transported from the mainland. For this reason sources can be distinguished between sea-based sources and land-based sources. Sea-based sources are mainly represented by oil and gas platforms, commercial fishing, and tourism, where plastic debris are dumped or incidentally lost at sea.[18] However, it was estimated that the majority of the marine litter, approximately 80%, is delivered into the ocean by land-based sources.[19] Many routes of land-based litter are known. Public littering, improper waste disposal, waste dump run-offs, tourism, industrial activity, and combined sewer systems contribute dramatically to the pollution of the aquatic environment with plastics.

Jambeck *et al.* (2015) estimated the input of plastic litter from land-based sources into the ocean with 4.8 to 12.7 Mt in 2010, corresponding to 1.7-4.6% of the estimated total plastic waste generated (275 Mt).[20] It was further predicted that the cumulative amount of plastics available to enter the ocean will increase by one order of magnitude by 2025, assuming no improvement of the waste management infrastructure. From the inland, plastic litter can be transported and introduced into the ocean by rivers and streams. This influence of rivers as transport vector for plastic debris into the oceans was further discussed by Rech *et al.* (2014).[21]

Plastic litter is of serious concern because of economic and ecological reasons. Aesthetically distasteful plastic debris pollutes shores and beaches, and will therefore negatively affect the tourism industry.[9] Furthermore, floating plastic debris can damage equipment.[22] Since synthetic polymers are generally nontoxic, freshwater and marine biota is mainly threated mechanical. Animals can entangle in plastic bags, nets, or packaging material, what results in higher mortality due to movement impairing effects.[23, 24] Furthermore, plastics are confounded with food by several species, such as fish, turtles, and birds.[25-29] Once consumed, the plastics cannot be excreted and are blocking the gastro-intestinal system, finally leading to death of the animals. Many of the synthetic polymers used for the production of plastic products do not possess any nutritive value and cannot be degraded by microorganisms.

2.1.3 Environmental degradation of synthetic polymers

One of the reasons for the great versatility of many synthetic polymers is their high resistance against environmental influences. However, this fact leads to extremely low degradation and long half-life periods of synthetic polymers under environmental conditions. Degradation of synthetic polymers can generally follow five different mechanisms, possibly ending in complete mineralization (Figure 2)[30]:

- Biodegradation by organisms
- Photo degradation (usually by UV light)
- Chemical degradation (oxidation or hydrolysis)
- Thermal degradation
- Mechanical degradation

Biodegradation of polymers mainly dependents on their chemical structure and is well described for poly(ε-caprolactam) or water-soluble polyethylene glycol.[31] However, the environmentally particular occurring plastics are water-insoluble, and many of the synthetic polymers present in the aquatic environment, such as PE, PP, PS, and PET are not or only very slowly biodegradable. For this reason the first step of the degradation of these polymers is initiated by UV radiation (photo oxidation) and is eventually followed by chemical oxidation.[32] If the polymers are oxidized, their molecular weight is decreased and oxidized groups might become available for a microbial degradation. It needs to be addressed that photo degradation of plastics floating in the aquatic environment is decelerated compared to degradation in outdoor exposure.[33] For this reason many plastics can stay in the aquatic environment for decades.

Furthermore, under environmental conditions temperatures are not high enough to start chemical changes of synthetic polymers, thus thermal degradation does not play an important role for aquatic systems.[34, 35]

Mechanical degradation is an important factor with regards to plastics in the aquatic environment. In most cases, aging of the polymer by environmental influences, such as photo or chemical degradation of polymer additives, changes the polymer properties and leads to embrittlement of the polymer.[36] The recalcitrant material is then shredded into smaller particles by friction forces occurring during the movement through the different environmental habitats. Admittedly, this degradation generally leads to smaller plastic particles, so-called microplastics, which can cause new problems in aquatic environments.

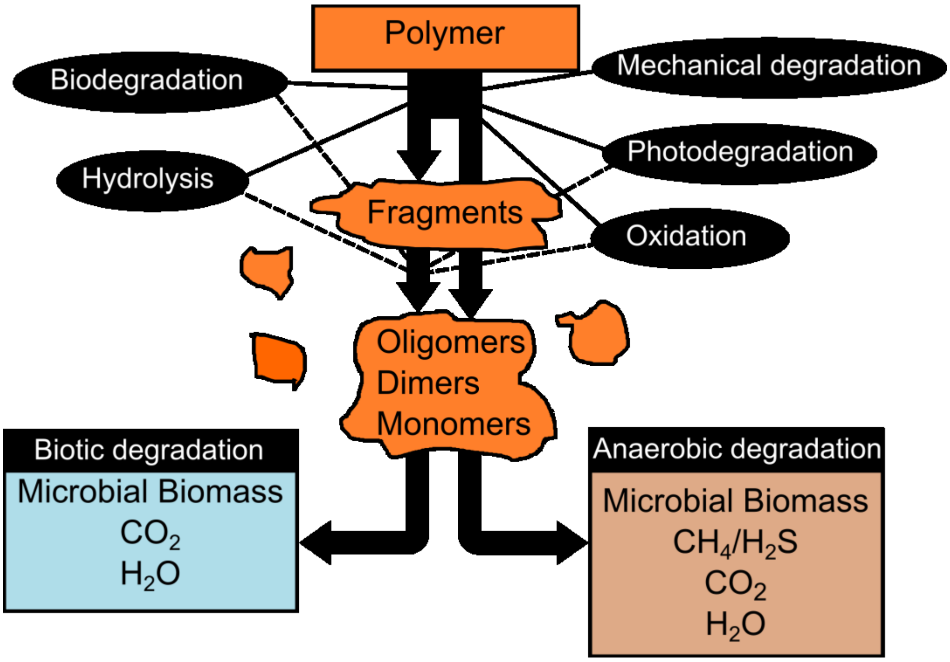

Figure 2: Possible degradation pathways of synthetic polymers in the environment. Solid lines show degradation processes of intact polymer products resulting in fragments or smaller molecular units. Dashed lines assign degradation processes of polymer fragments that are involved in the degradation of polymer fragments in monomers, dimers, or oligomers. From Gu (2003, modified)[37]

2.2 Microplastics

2.2.1 Definition

The term microplastics was first defined by the scientific community as particles smaller than 5 mm in size at a workshop on the “Occurrence, Effects, and Fate of Microplastic Marine

Debris” in 2009.[38] A lower limit for the size of microplastics was defined as 0.33 mm corresponding to the common mesh size of the Neuston nets, which were used for the sampling of sea surface microplastic. However, the lower boundary is not applied in recent microplastic studies, and particles down to 1 µm in diameter are usually described as microplastics. Nowadays the size limit of 5 mm for microplastics is widely accepted, even though some scientists use other definitions such as particles smaller than 1 mm.[39, 40] Recent developments indicate that 5 mm might become the official size limit for microplastics, as support for this definition was provided by the National Oceanic and Atmospheric Administration and in the marine strategy framework directive of the European parliament.[41, 42] Furthermore, additional classifications besides microplastics and macroplastics are used in literature. Recently, microplastics were discerned again into large microplastics (1-5 mm) and small microplastics (<1 mm) in several studies.[43-45] The term mesoplastics is used to describe plastic particles in the size range of 4 to maximal 25 mm. [46-48]

Despite the availability of several definitions for microplastic particles, further size limits, such as 0.2-2 mm for small microplastics and 5-10 mm for mesoplastics, are still defined in newer studies.[49] For this reason, it is essential to harmonize research on the plastic pollution by the introduction of official definitions rather than guidelines to guarantee best comparability between results of the investigation of plastic particles in water and sediments.

2.2.2 Sources

Microplastic particles enter the aquatic environment in various forms, shapes, and colors, derived from several different sources.

Microplastic particles are divided depending on their origin into two groups: Primary microplastics and secondary microplastics. The term “secondary microplastics” describes small plastic particles, which are formed by the break-down of larger plastic items. Embrittlement and following size reduction of larger plastic particles is expedited by aging of the polymer due to environmental influences such as UV radiation or biological degradation and mechanical deterioration by friction forces (refer to 2.1.3).

Primary microplastics are manufactured microparticles of synthetic polymers, which are produced for further processing or are added to products to enhance their abilities. This includes on the one hand plastic pellets, which are used to produce larger plastic objects and are incidentally lost during transport or enter the environment through run-offs of processing facilities.[50, 51] On the other hand microplastic particles are used in cosmetic formulations such as exfoliants or in cleansers as abrasive scrubbers.[52, 53] These particles can enter the environment via sewage treatment plants together with synthetic fibers which are released from synthetic textiles during the washing process.[54] Noteworthy, these fibers can be considered as primary or secondary microplastics.

2.2.3 Analysis of microplastics

The small size of microplastics complicates their determination in environmental samples compared to macroplastics and demands for higher requirements regarding the analytical approaches. Depending on the sampling compartment of the aquatic environment, the application of different sampling methods and sample treatments is necessary (Figure 3). Microplastic particles are generally too small to differentiate them with the naked eye from sediments or floating natural debris.

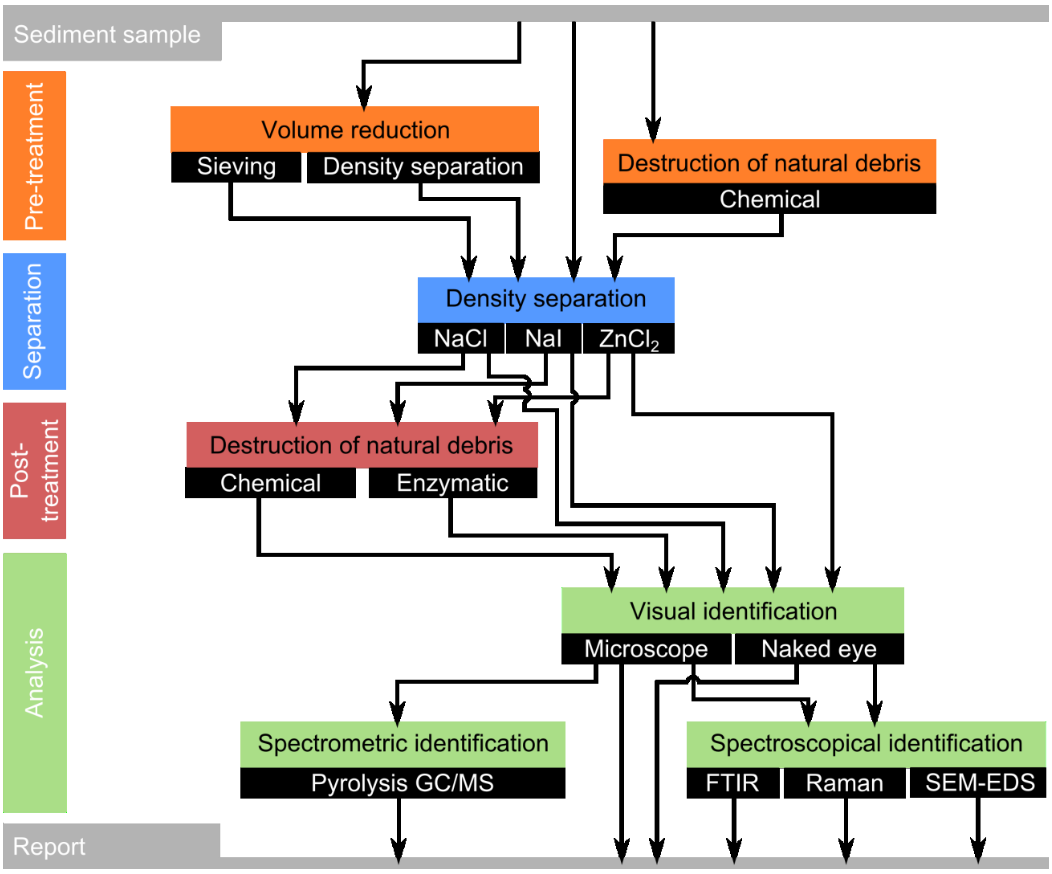

Figure 3: Possible routes described in literature for the analysis of microplastics in sediment samples starting sample pre-treatment to the report of the results. The sample preparation is split in pre-treatment, the density separation, and the post treatment of the separated microplastics. Fourier transform infrared spectroscopy (FTIR), scanning electron microscopy-energy dispersive X-ray spectroscopy (SEM-EDS)

Even plastic pellets, counting to the larger microplastics, are difficult to separate between sediment particles with the naked eye, especially after aging or fouling of the polymer particles. For this reason different methods were developed that allow the mechanical separation of microplastics from the sediment, followed by an analysis of the separated particles. A variety of different techniques is reported and used during all steps of the sample treatment or the microplastic identification. As not all studies conducted extensive method validation including the determination of recovery of the microplastic particles or did not provide experiments with blank samples, the resulting data can lack comparability.

2.2.3.1 Density separation

A commonly used technique for the separation of plastic particles is the density separation. The usage of a heavy liquid enables the microplastic particles to float in the solution whereas the sediment particles settle due to their higher density. Numerous different techniques are described in literature, many of them based on the separation introduced by Thompson *et al.* (2004).[55] Alterations to this method comprise the usage of different salts to create the heavy liquid used for separation, the development of different instrumental setups, and different pre-treatment and post-treatment steps of the samples (compare Figure 3).

In addition to sodium chloride, which was used by Thompson *et al.* (2004) and different other studies, the usage of sodium iodide and zinc chloride is reported.[56-58] Sodium iodide and zinc chloride offer the possibility to produce solutions with higher densities than sodium chloride. As the density of a saturated sodium chloride solution ($\rho \approx 1.2\ \text{g cm}^{-3}$) is rather limited and does not offer consistent separation of higher density polymers such as polyoxymethylene, PVC, and PET, sodium iodide and zinc chloride are viable choices. Sodium iodide is usually combined with a pre-separation, based on elutriation that separates less dense particles from heavier particles in an upward directed stream of gas or water. This procedure is necessary to minimize the volume needed for the density separation due to the high costs of sodium iodide.[56, 59] Using zinc chloride, solutions with densities of $\rho > 1.6\text{-}1.7\ \text{g cm}^{-3}$ can be obtained, but the ecological hazards of zinc chloride complicates the disposal of used solutions and contaminated sediments.

The identification of microplastic particles is often prevented by natural debris that floats in saturated salt solutions and accompanies the microplastics during the density separation. Thus, the destruction of natural debris or biological material is unavoidable to minimize the possibility of misidentifications or underestimation of small plastic particles. This can be carried out by chemical or enzymatic catalyzed reactions. Chemical destruction of natural debris is often achieved via the treatment of the sample with hydrogen peroxide, mixtures of hydrogen peroxide and sulfuric acid, and Fenton-like reactions prior or after the density separation.[44, 58, 60] To avoid possible loss of synthetic polymers, which are not resistant against acidic treatments, usage of sodium hydroxide was proposed. However, it is reported by Cole *et al.* (2014), that alkaline treatment could damage some of the synthetic polymers as well.[61] For biota rich samples, enzymatic treatments were developed, which grant the detection of pH-sensitive polymers.[61]

2.2.3.2 Identification of microplastics

In most studies microplastics are first identified visually. Larger particles might be identified with the naked eye, whereas small microplastics are identified using binocular microscopes or scanning electron microscopy (SEM).[62-64] Depending on the efficiency of the sample treatment visual identification might not be sufficient, and further spectroscopic or spectrometric methods are needed to ensure unambiguous identification of particles made from synthetic polymers.

Fourier transform infrared (FTIR) spectroscopy and Raman spectroscopy are often employed for the identification of synthetic polymers. For larger particles (approximately >500 µm), FTIR can be carried out using an attenuated transverse reflection (ATR) unit.[51, 65] Coupling of FTIR instruments to microscopes such as reflectance micro-FTIR allows the detection of smaller microplastics.[66] Both, FTIR-based and Raman-based methods are limited in the minimal particles size, which can be determined. Furthermore, these methods are susceptible to fouling and soiling of the polymer particles, or colored plastics as the pigments or microorganisms interfere with the reflection or excitation of the polymer molecules.[67]

The application of pyrolysis-gas chromatography/mass spectrometry (Pyr-GC/MS) allows the simultaneous determination of the polymer type and polymer additives by desorption of the thermal degradation products of the polymers.[56, 68] In contrast to the above mentioned techniques Pyr-GC/MS is a destructive method, preventing any further analysis of the plastic particles.

SEM can be coupled with X-ray detection (SEM-EDS), which produces high-resolution images of the particles and provides an elemental analysis of the measured objects. By Using SEM-EDS it is possible to distinguish between microplastics and particles, which are composed of inorganic elements, such as aluminum silicates.[69]

If no identification via the above mentioned techniques is possible, hardness tests of the particles are reported, to preclude misidentifications with fragile carbon particles or carbonate particles that are not removed or formed during the sample treatment.[70]

2.2.4 Occurrence in the environment

Microplastic particles are present in surface water, sediments, and oceans all over the world. First reports of smaller plastic items were primarily focused on plastic pellets used in plastic productions. Plastic pellets were present in large quantities at beaches and coastline of for instance in New Zealand, the Lebanon, and Spain.[71-73] However, industrial plastic pellets only pose a small fraction of the numerous microscopic plastic fragments present in the ocean and other aquatic systems.[55] In the recent years, microplastic particles were detected in the form of spheres, fibers, and fragments in many coastal sediments or in the open ocean. For example, microplastics were determined at the Italian, Singapore, and Portuguese coast, at beaches of Hawaii and islands of the equatorial Western Atlantic as well as at shores of German and Greek islands.[45, 57, 74-78] Microplastics were quantified in concentrations in a range of four orders of magnitude, spanning 1.3 particles kg^{-1} (German island) over 13.5 particles kg^{-1} (equatorial western Atlantic) to 2175 particles kg^{-1} (Italy). In contrast to studies in the marine ecosystem, freshwater systems have attracted less attention. Only a few studies considered the investigation of the extent of the microplastic plastic pollution in inland waters such as lakes or rivers. A study of the river Danube revealed that the abundance of plastic particles exceeded the number of fish larvae, and that the river might transport high loads of plastic particles into the Black Sea.[79] Moreover, a study conducted with sediments of Lake Garda showed a high abundance of buoyant microplastic particles made from PE and PP, indicating the importance of buoyant microplastics for shore sediment. Nevertheless, less dense polymer particles, such as PVC and PET, were identified in the sediments, underlining the variety of microplastics present in shore sediments.[44]

Comparisons of the plastic abundance in dependence of the particle size indicated that the number of particles strongly increases with decreasing particle size, and therefore microplastics are much more abundant than macroplastics.[65, 70]

2.2.5 Environmental effects of microplastics

2.2.5.1 Effects on organisms

For microplastic particles different effects on the environment are expected than for macroplastic debris that were discussed in 2.1.2 (Figure 4). Microplastics possibly have a more serious and vital ecological role in the marine food-web. The small size of microplastics facilitates the uptake by organisms compared to larger particles. Microplastic ingestion has been reported for many different species, such as mussels, lugworms, crabs, seabirds, and fish.[80-83] As these smaller particles can be consumed by smaller organisms such as zooplanktons, isopoda, or mysid shrimps, which all are at the bottom of the food chain, biomagnification of microplastics is expected.[84-86] Furthermore, microplastics have been detected in mussels, which were cultured for human consumption.[87]

Since microplastics are of significantly smaller size compared to macroplastics, blocking of the gastro-intestinal system by these particles is less likely, and even small crustaceans such as isopods can excrete digested microplastics.[85] However, retention time of microplastics depends on the uptake route as well as the organism and might be long enough that ingested microplastics can be transferred to the next trophic level.[83] Adverse effects of microplastics to organisms have not shown any clear tendency yet. On the one hand-side microplastics did not seem to affect mortality of organisms such as isopods. This is likely related to the ability to excrete microplastics, as mentioned previously.[85] On the other hand, studies showed adverse effects of microplastic particles on juvenile and adult fish.[88, 89] Further studies showed that microplastics seem to affect the fitness of lugworms and are incorporated in mussel tissue and cells.[80, 81] A strong inflammatory response was the consequence of the uptake of microplastics in mussel tissue, as observed by von Moos *et al.* (2012). Noteworthy, the microplastic dosage was extremely high compared to environmental conditions (2.5 g L^{-1} of <80 µm PE particles).[80]

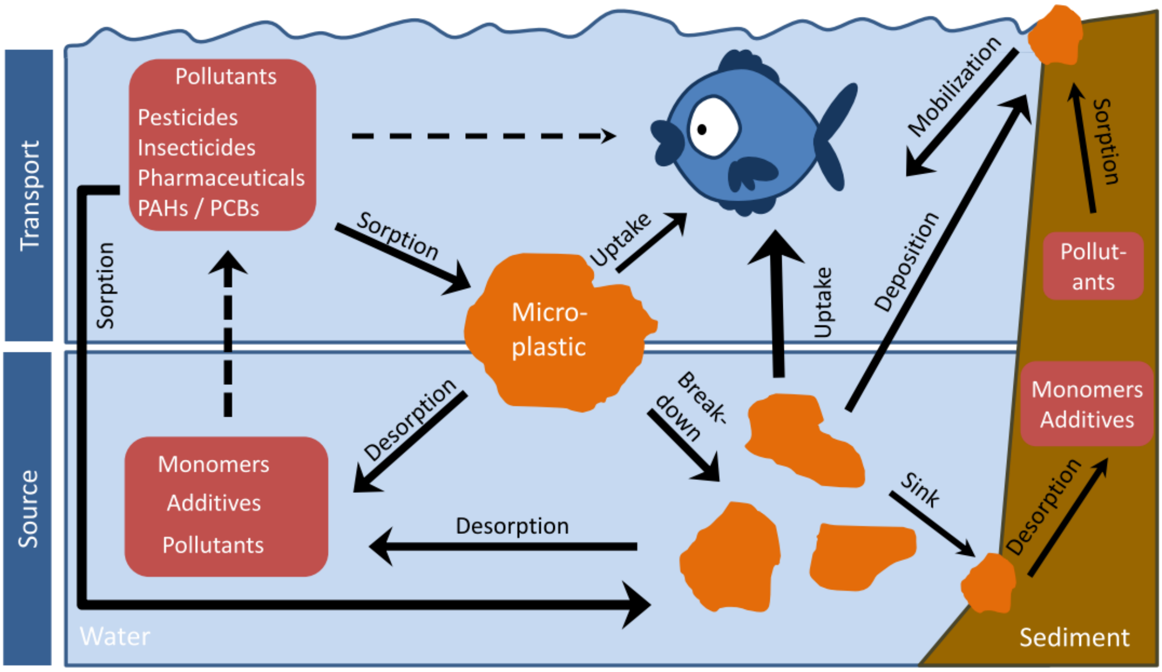

Figure 4: Possible impacts of microplastics on aquatic environments divided into microplastics acting as transporter or source. Impacts are shown for the water column as well as the sediment compartment. Dashed arrows show additional routes that do not necessarily involve microplastics.

2.2.5.2 Sorption and desorption of organic contaminants

Additionally to adverse effects of the plastic particle itself, microplastics can transport contaminants. These contaminants are on the one side present in the aqueous environment in form of pesticides, insecticides, pharmaceuticals, or other environmental pollutants, such as polycyclic aromatic hydrocarbons (PAHs) and polychlorinated biphenyls (PCBs).[90-93] Due to hydrophobic or polar interactions the contaminants can sorb to the microplastic particles from the aqueous phase and are enriched on the particles compared to the concentration of the surrounding water.[94] On the other hand, the polymer additives are environmental contaminants themselves, such as softeners and flame retardants. These additives are used to enhance to polymer material properties and are present in the polymer in relatively high concentrations. Furthermore, monomers used for the polymer production such as vinyl

chloride (used for PVC) or Bisphenol A (used for PC) pose an potential environmental risk and can be present in the final polymer as a result of an incomplete polymerization. [95, 96]
Persistent organic pollutants, such as PAHs and PCBs were detected in microplastics, which were separated from sediments all over the world.[97-100] Entering less polluted aqueous systems, microplastics loaded with contaminants can increase the aqueous concentrations of pollutants by desorption processes.[101] Thus, it is expected, that environmental pollutants can be carried into the ocean by plastic particles. Additionally, many microplastics are buoyant and travel in the sea surface microlayer. The sea surface microlayer describes a thin (1-1000 µm) layer on the top of the water surface, often summarized as a micro-habitat. Besides microorganisms the sea microlayer consists of surface active substances and organic compounds with low water solubility. According to their hydrophobicity, the concentration of many pollutants in the sea surface microlayer is distinctly higher than in the sea water.[102] Thus, higher amounts of contaminants can sorb faster on microplastics and possibly be transported to less polluted sediments by sinking or deposition processes.[103]
Moreover, it is possible that pollutants are transferred in organisms that consume the microplastic particles, although studies have not shown any clear trend yet. Thus, further studies on contaminant transport are necessary for an adequate estimation of contaminant leaching from microplastics in organisms. Laboratory studies on contaminant desorption under physiological conditions indicated elevated desorption rates of environmental contaminants from plastic particles.[104] Experiments with living organisms underlined the results of laboratory studies. Microplastics that were polluted with PAHs and fed to fish, seemed to have an increased adverse effect compared to clean microplastics.[88] Further, polystyrene microparticles transported PCBs into lugworms, even though the monitored effect was comparably small.[81] Contrary to these observations, models showed no significant transport of environmental contaminants PCB, bisphenol A, and nonylphenol into marine organisms.[105, 106]

2.3 Sorption

As discussed in the previous section, sorption of contaminants to the microplastics might be of paramount importance for the classification of the microplastic pollution. The term sorption describes the immobilization of substances at condensed phases from their surrounding area. It is a hypernym for different sorption processes and usually used, if no specific process can be defined. Therefore, the term sorption is used throughout this thesis, if a substance is immobilized on a solid. As the term sorption characterizes all processes of immobilization, it can be divided into the processes of adsorption, absorption, and ion exchange.[107] Depending on the sorbate/sorbent system one of these processes might superimpose the others, but under environmental conditions the adsorption of substances plays generally the most important role.[108] In this thesis, the sorption of non-charged environmental contaminants to different non-charged synthetic polymers is studied, thus the effects of ion exchange are likely to be of minor interest.

2.3.1 Adsorption

Adsorption describes the accumulation of a gas or solute at the surface interface of a liquid or solid phase, respectively (Figure 5).[109] As this thesis focuses on sorption processes between liquid and solid phases, the following considers only the processes occurring at liquid/solid interfaces. The accumulation of a solute on a solid phase at constant temperature and pressure is driven by a decrease of the surface free energy of an adsorbate-solution-solid interface.[110] The heat of adsorption of spontaneously proceeding adsorption reactions can be explained by regarding the changes of enthalpy and entropy of the adsorption. As the immobilization of the adsorbate usually leads to a decrease of disorder, the change of entropy is negative. Taking into account that the change of Gibbs free energy of spontaneous proceeding reactions is negative, the change of enthalpy must also be negative and exceed the absolute value of the change of entropy. Thus, adsorption processes are generally exothermal processes. The interactions causing the solute adsorption on the one-hand side can be a result of relatively weak physical forces, such as van-der-Waals forces. This process is also known as the so-called physisorption, which results in comparably low interaction or binding energies and thus in low reaction enthalpies.[111] On the other side, chemisorption that is characterized by analogy to a chemical reaction results in covalent bonds between the adsorbate and the sorbent and consequently in high reaction enthalpies. It needs to be mentioned, that there is no strict border between physisorption and chemisorption, and the boundaries between both mechanisms might be fluent.[111, 112]

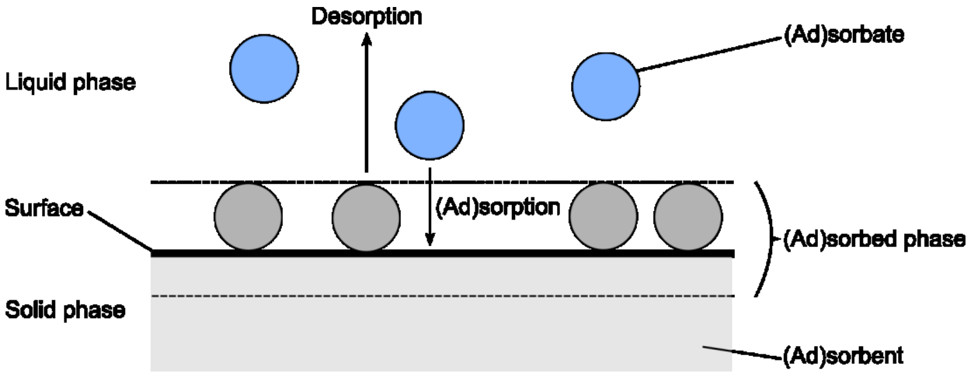

Figure 5: Basic terms of adsorption of molecules from a liquid phase to a solid surface. Worch (2012, modified).[110]

2.3.2 Sorption isotherms

Sorption of substances to different sorbents is usually characterized by sorption isotherms. These generally describe the relationship of the amount of sorbed phase per mass of sorbent and the equilibrium solute concentration at a constant temperature. The experimentally determined trend of the sorption isotherms is described by the application of different sorption models. Today, many different models for sorption isotherms are available as the applicability on experimental data is not always given for each model. Important models for sorption isotherms comprise the models of Henry, Freundlich, Langmuir, and the BET model (Figure 6).

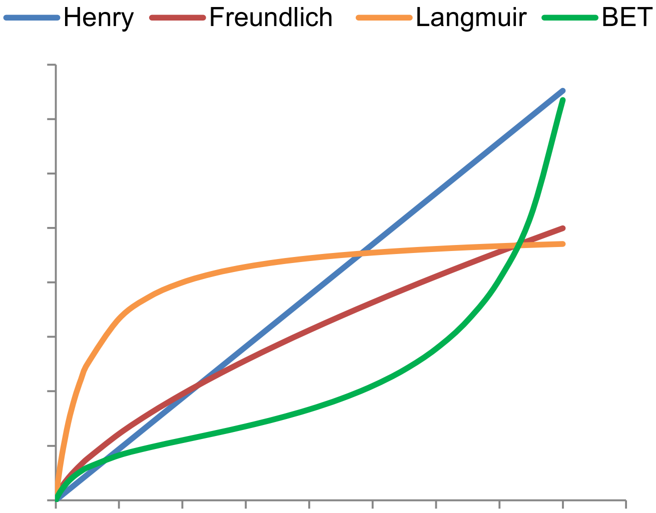

Figure 6: Scheme of the isotherm models which were are known as the Henry model, Freundlich model, Langmuir model, and the BET model.

2.3.2.1 Henry sorption model

The simplest of all sorption models is basically resembled by Henry's Law and based on a linear relation between the sorbed phase and the solute concentration at equilibrium.[113] Thus, the sorption of a substance at a given equilibrium concentration only depends on the distribution coefficient. Equation (1) shows the formula of the Henry model

$$q_{eq} = K_D C_{eq} \qquad \textbf{(1)}$$

where q_{eq} is the solid phase concentration, K_D is the distribution coefficient, and C_{eq} is the solute concentration at equilibrium.

Due to the simplicity of the model, its application might not be possible for large ranges of solute concentrations. Nevertheless, many sorption processes are characterized by this linear approach and distribution coefficients are available for a wide range of different sorbates such as environmental contaminant and sorbents such as soils or synthetic polymers.

2.3.2.2 Freundlich isotherm

One of the most used non-linear sorption isotherms is described by the Freundlich equation which is shown in equation (2)

$$q_{eq} = K_F C_{eq}^{\frac{1}{n}} \qquad \textbf{(2)}$$

where K_F is the Freundlich capacity factor, and 1/n is the Freundlich exponent.

In contrast to the Henry isotherm, the Freundlich isotherm takes into consideration the heterogeneity of the sorption sites at the surface of the sorbent. This heterogeneity is represented by the Freundlich exponent. For Freundlich exponents equal to 1 the Freundlich equation becomes equal to the Henry equation.

2.3.2.3 Langmuir isotherm

The models by Henry and Freundlich both assume that the sorbent provides unlimited sorption sites, and the sorbed concentration can rise *ad infinitum*. Like the Freundlich model, the Langmuir model yields in a non-linear sorption isotherm that describes the sorption in monolayers. Additionally, the Langmuir model takes into consideration that the surface of the sorbent can only provide limited and distinctly localized sorption sites. As a result the Langmuir sorption isotherm reaches a maximum loading of the sorbent for high solute equilibrium concentrations. Equation (3) shows the Langmuir model

$$q_{eq} = q_{max} \frac{K_L C_{eq}}{1 + K_L C_{eq}} \qquad \textbf{(3)}$$

where K_L is the Langmuir constant , and q_{max} is the maximum monolayer coverage capacity.

2.3.2.4 BET isotherm

The BET model was introduced in 1938 by Brunauer, Emmett, and Teller and is named by the initials of their last names.[114] All models described before only consider a sorption of the substances in a monolayer. However, under some circumstances sorption of the sorbate continues on the first monolayer. This could result in an increase of sorption to the polymer for high solute concentration after a plateau phase of the sorption isotherm close to the monolayer capacity. In contrast to the Henry, Freundlich, and Langmuir isotherm respectively, the BET model describes multilayer sorption which is usually indicated by an S-shaped curve of the sorption isotherm. The BET model is presented in equation (4)

$$q_{eq} = \frac{K_B q_m C_{eq}}{\left(C_s - C_{eq}\right)\left(1 + \frac{(K_B - 1)C_{eq}}{C_s}\right)} \tag{4}$$

where K_B is the partition coefficient, q_m is the concentration of a monolayer, and C_S the saturation concentration.

2.3.3 Kinetics of sorption processes

Besides the sorption capacity, the kinetic aspects of the sorption process are of great importance. Sorption kinetics is of high relevance in processes that are using sorption for the removal of substances, such as contaminants. The kinetics analysis of the sorption process allows or simplifies the dimensioning of pilot applications, as the time required for the completion of the sorption is an important factor.

The determination of sorption kinetics is not less significant for environmental investigations. The sorption kinetics gives insights into the uptake rate of the sorbate and is necessary to evaluate the relevance of sorption in dependence of the contact time of sorbent and sorbate. Thus, the residence time is a vital factor for the sorption process of environmental contaminants to microplastics that can act as a sorbent in aquatic systems.

To describe the kinetic of sorption processes, several mathematic models have been developed. These models can be divided in sorption reaction models and sorption diffusion models.

Sorption diffusion models assume that three steps are involved in the sorption process of substances to porous particles:[115]

1. Film diffusion of the sorbate from the bulk liquid to the external surface of the sorbent particle through the liquid film surrounding the particle.
2. Internal or intraparticle diffusion of the sorbate into the pores of the sorbent particle.
3. Reaction (sorption) of the sorbate at the sorption sites of the sorbent.

The rate limiting steps expected for sorption processes involving physisorption are the film diffusion and intraparticle diffusion, as mass action is a very fast process. Contrary, sorption reactions, which are based on chemisorption, can be limited by the reaction rate of the bond formation.

Sorption reaction models are based on the kinetic models of chemical reactions. They describe sorption as one whole process and are widely employed for studying sorption kinetics.[116-118] The first reaction model to characterize the sorption from a liquid phase to a solid was introduced by Lagergren (1898) and was used to describe the sorption of malonic acid to charcoal.[119] The model of Lagergren followed a first-order or pseudo-first order rate equation shown in equation (5)

$$\frac{\mathrm{dq_t}}{\mathrm{dt}} = \mathrm{k}\,(\mathrm{q_{eq}} - \mathrm{q_t}) \qquad \textbf{(5)}$$

where q_t is the concentration in the sorbent at time t, q_{eq} is the concentration in the sorbent at equilibrium, and k is the rate constant.

Integration of equation (5) with the boundary conditions t=0 to t=t and $q_t=0$ to $q_t=q_t$ gives equation (6).[120]

$$\mathrm{q_t} = \mathrm{q_{eq}}\,(1 - \mathrm{e}^{-\mathrm{kt}}) \qquad \textbf{(6)}$$

Pseudo-first order models were already used to characterize the sorption of organic environmental contaminants to glass state polymers such as PS.[121]

Besides the pseudo-first order reaction sorption models, pseudo-second order models are often applied for the characterization of the sorption of charged compounds such as metal ions.[122, 123] Equation (7) shows the nonlinear form of the pseudo-second order sorption model

$$\mathrm{q_t} = \frac{\mathrm{q_{eq}^2 k_2 t}}{1 + \mathrm{q_{eq} k_2 t}} \qquad \textbf{(7)}$$

where k_2 is the pseudo-second order rate constant.

However, sorption reaction models suffer in some cases in prediction accuracy and might not be adequate for the application of dimension e.g. fixed bed adsorbers. The reason for this inaccuracy might be found in the generalization of the sorption process to one single reaction. For environmental applications, such as the estimation of the sorption relevance of organic contaminants to polymer particles, the prediction using reaction sorption models might be accurate enough. Additionally, the environmentally present polymer particles are likely non-porous particles that possibly do not show diffusion into pores of the particle surface.

2.3.4 Glass transition temperature

One of the most important parameters characterizing a polymer besides the molecular mass and an important factor for the sorption to polymer particles is the so-called glass transition temperature. The glass transition temperature defines the temperature or the temperature range in which amorphous polymers or polymers with amorphous regions pass from a rubber-like elastic state into a hard elastic, relatively brittle state.

Most of the polymers consist of both crystalline and amorphous regions, in which molecules are freely flexible and form, according to their long molecule chains, tangles of lowest energetic state.

The elasticity of polymers can be divided into entropy-related elasticity and energy-related elasticity. The entropy-related elasticity describes the elasticity of polymers above their glass transition temperature. The polymer chains are able to rearrange from a tangle to straight polymer chains under the influence of external stress and consequently can reconfigure to a tangle after release of the external stress. Polymers in the glass state are not able to reconfigure the structure of the molecule chains and will thus break, if the stress exceeds the stability of the polymer.

The glass transition temperature is mainly affected by the structure of the polymer. Important for the glass transition temperature is on one hand the chemical compositions of the polymer backbone as it is known that e.g. aromatic groups increase the glass transition temperature.

On the other hand the substituents in the side chains of the polymer are of high significance for the glass transition temperature. The moieties of the side chain can increase or decrease the glass transition temperature depending on their effect on the chain flexibility. For example, the substitution of one hydrogen PE chain by either chlorine (PVC) or benzene (PS) results in an increase of the glass transition temperature. In contrast, an increase of the side chain length of acrylate-based polymers decreases the glass transition temperature.[124]

2.3.5 Analytical determination of sorption processes

The solute sorption from aqueous phases to solid phases can be determined by the application of different approaches. The sorption can be either monitored by the measurement of the remaining solute concentration in the aqueous phase or by the determination of the sorbed phase concentration in the solid phase. Both methods are applied in several studies, but mostly the determination of the remaining solute concentration is favored in laboratory experiments.

In both approaches the analysis of the sorbate or the sorbed phase is carried out with gas chromatographic (GC) or liquid chromatographic (LC) methods coupled to mass spectrometric (MS) or UV detectors (UV) after a suitable sample preparation was applied that solved the challenges of the different approaches.

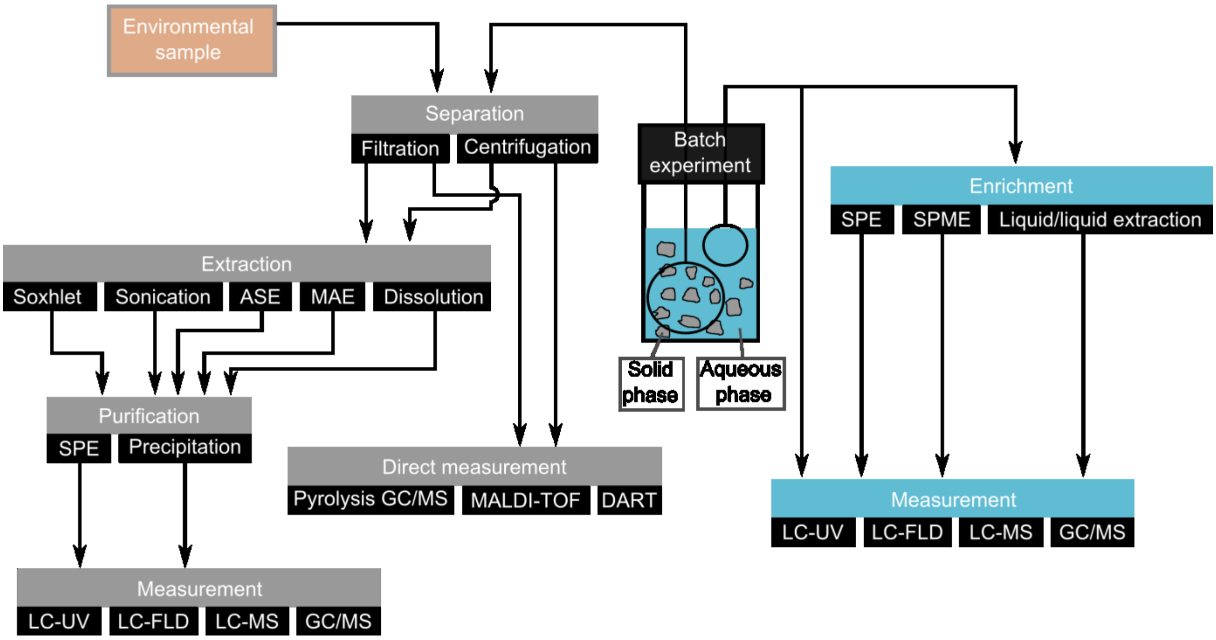

Figure 7: Different approaches to determine sorption in laboratory batch experiments or in environmental samples. Accelerated solvent extraction (ASE), microwave-assisted extraction (MAE), solid phase extraction (SPE), solid phase micro extraction (SPME), matrix-assisted laser desorption ionization-time of flight (MALDI-TOF), direct analysis in real time (DART), fluorescence detector (FLD).

Depending on the analyte properties and the concentration range of the sorption experiments, different sample preparation techniques are used to measure the solute concentration. If the solute concentration is high enough or sensitive detection methods are available, a direct measurement of the solute in the supernatant is possible.[125] Nevertheless, it is often necessary to enrich the analytes, as wide concentration ranges are studied for the determination of the sorption isotherms. Thus, sample preparation of the aqueous phase using solid phase extraction (SPE) with subsequent analysis via GC/MS, LC/MS, or LC/UV is often reported.[126, 127] In other studies passive samplers were used to enrich and extracted the analyte from the aqueous. For example, passive samplers made from polyoxymethylene were used to determine the sorption of phenanthrene to sediment.[128] Another study conducted solid phase micro extraction (SPME) using polydimethylsiloxane-divinylbenzene fibers for the detection of the solute concentration of different PAH congeners in batch sorption experiments with PE particles as sorbents.[94]

For the detection of sorbed substances in solid phases either a direct determination in the particles or a determination after the extraction of the solid phase is possible. A direct measurement to determine sorbed substances is often reported in literature by an analysis of the particles via pyrolysis-GC/MS or thermal desorption-GC/MS.[45, 129, 130] However, the methods might lack in reproducibility and quantitation is not straightforward.[131]

Therefore, an extraction of the solid particles is generally favored over a direct measurement. For the extraction of solid phases several different methods are reported in literature. To identify environmental contaminants in sediment particles such as PAHs or chlorinated alkanes, the application of Soxhlet extraction is described.[132, 133] Noteworthy, Soxhlet extraction is a time and solvent consuming technique, for this reason more effective extraction techniques were developed. For the determination of PCBs in Baltic Sea sediments, accelerated solvent extraction seemed as superior technique as the method is less time consuming than Soxhlet extraction.[134] However, the extraction of synthetic polymers might be troublesome with accelerated solvent extraction, as the polymers can partially dissolve in the solvents and block the connection tubing of the system.[135] Furthermore, methods using extraction procedures enhanced by sonication or microwave-assisted extraction are reported as fast and suitable alternative for Soxhlet extraction.[136] These techniques are used to extract environmental contaminants from synthetic polymers, e.g. sonication extraction was reported for the extraction of PE passive samplers.[137] Moreover, all of the above mentioned techniques were also used for the analysis of polymer additives, thus they seem to be appropriate for the analysis of sorbed organic substances.[138] Additionally, polymer additives were analyzed by dissolution of the polymer. This technique benefits from the complete extraction of the polymer particles, but requires a more complex sample clean-up prior to the measurement.[129] As described previously, for the measurements of the supernatants, the extracts are generally measured by LC or GC based methods.

3 Objectives

The first objective of this thesis was the determination of the extent of plastic pollution of inland waters to overcome the lack of data and estimating the abundance of microplastic in freshwater systems. Shore sediments of the river Rhine, Main, and the stream Schwarzbach appeared as appropriate environmental compartments to monitor the plastic pollution as buoyant and non-buoyant particles can be found. Furthermore, the rivers comprise one large European river (Rhine), a river with industrial influences (Main), and a small stream (Schwarzbach).

For a valid identification and determination of microplastic particles a suitable method should be established. Sampling of the sediments over a period of two years should show, if the abundances of plastic particles increased during this time interval. Detailed information gathered from spatial differences of the plastic pollution should help to identify direct sources or diffuse sources of plastic particles. Direct sources such as municipal waste water treatment plants or industrial areas, as well as different densely settled areas were comprised by the sampling area. Transport of plastic particles from river to river should be monitored by the sampling of tributary sediments.

The second objective of this thesis was the characterization of contaminant sorption to microplastic particles to estimate the relevance of this process. The characterization should be carried out by conducting batch sorption experiments in laboratory scale for polymers in the glass state. The focus of this thesis was set on the sorption of contaminants to polymers in the glass state, as previous studies focused on contaminant sorption to non-glassy polymers such as polyethylene and polypropylene. However, the sorption of contaminants to polyethylene is mainly driven by hydrophobic interactions, whereas other effects on the sorption process might be overlooked. Furthermore, it was expected that investigating contaminant sorption to polymers exclusively in the glassy state leads to a better comparability of the sorption process between the different polymer types.

To investigate sorption processes onto the polymers, on the one hand batch experiments should be conducted to study the sorption kinetics. Information about the kinetics of the sorption reaction might be one important factor to estimate the relevance of sorption in freshwater systems. On the other hand, sorption isotherms should be recorded in the batch experiments as another important indicator for relevance of sorption to the tested polymers.

Finally, the extraction of organic substances from microplastics that were separated from sediment samples should stress and confirm the relevance of sorption to microplastics under environment conditions.

4 Materials and Methods

4.1 Materials

4.1.1 Chemicals, solutions, consumables materials, and instruments

All chemicals utilized in this thesis were purchased from Merck (Darmstadt, Germany), Roth (Karlsruhe, Germany), Sigma Aldrich (Seelze, Germany) if not stated otherwise.
Ultrapure water was prepared by means of a Milipore Direct-Q3 system with a SmartPak® cartridge. If not stated otherwise, this ultrapure water was used for the preparation of solutions and dilutions. All solutions were made with ultrapure water if the term "water" is used. The preparation of the synthetic freshwater, the stock solution of reference materials, and the saturated sodium chloride solution is described in the annex (refer to 9.1.3.1, 9.1.3.2, and 9.1.4).
A detailed list of consumable materials used during this thesis including suppliers is provided in 9.1.1. All instruments used are listed in 9.1.2.

4.1.2 Polymers

All synthetic polymers for sorption experiments or for method validation experiments were supplied by Polymer Standards Services (PSS; Mainz, Germany) or BASF (Ludwigshafen, Germany) and listed in Table 2. Powders of synthetic polymers that were used for the sorption experiments were homogenized in a mortar to achieve comparable particle sizes. Particle size distributions of the polymers were measured by microscopy and are provided in annex.

Table 2: Polymers used in this work, including abbreviation used, glass transition temperature (T_g), formulation, molecular mass (M_W) with polydispersity index in parenthesis, and supplier.

Polymer name	Abbreviation	T_g [°C]	Formulation	M_W [g mol^{-1}]	Supplier
Polycarbonate	PC	145	powder	3690 (1.88)	PSS
Polyethylene, pellet	PE	-78	pellet	n/a	BASF
Polyethylene	PE	-78	powder	2190 (1.17)	PSS
Poly (methyl methacrylate)	PMMA	114	powder	3471 (1.09)	PSS
Polystyrene	PS	100	powder	3460 (1.06)	PSS
Polystyrene, expanded	EPS	100	Foam	256000 (2.89)	BASF
Polystyrene, pellet	PS168	100	pellet	271300 (3.09)	BASF
Polyvinyl chloride	PVC	85	powder	42400 (1.16)	PSS

4.2 Investigation of plastic particles in sediments

4.2.1 Area of investigation

The shore sediments were sampled in the Rhine-Main area of Germany at the river Rhine, the river Main, and the stream Schwarzbach (Figure 8). The sampling sites were chosen to represent different scenarios. All sampling sites represented varying population densities. Furthermore, sampling at sites in vicinity to the confluence of the river Main and the river Rhine (R1, R2, M2) was carried out to observe changes of the microplastic concentration of shore sediments by tributary influences. Two sampling sites were located in nature reserves (R5 and R7), where no direct sources which can influence the microplastic concentration are assumed. The stream Schwarzbach represents a small stream, where lower microplastic concentrations were expected (S1 and S2). Detailed coordinates of the sites are provided in the annex (Table 12).

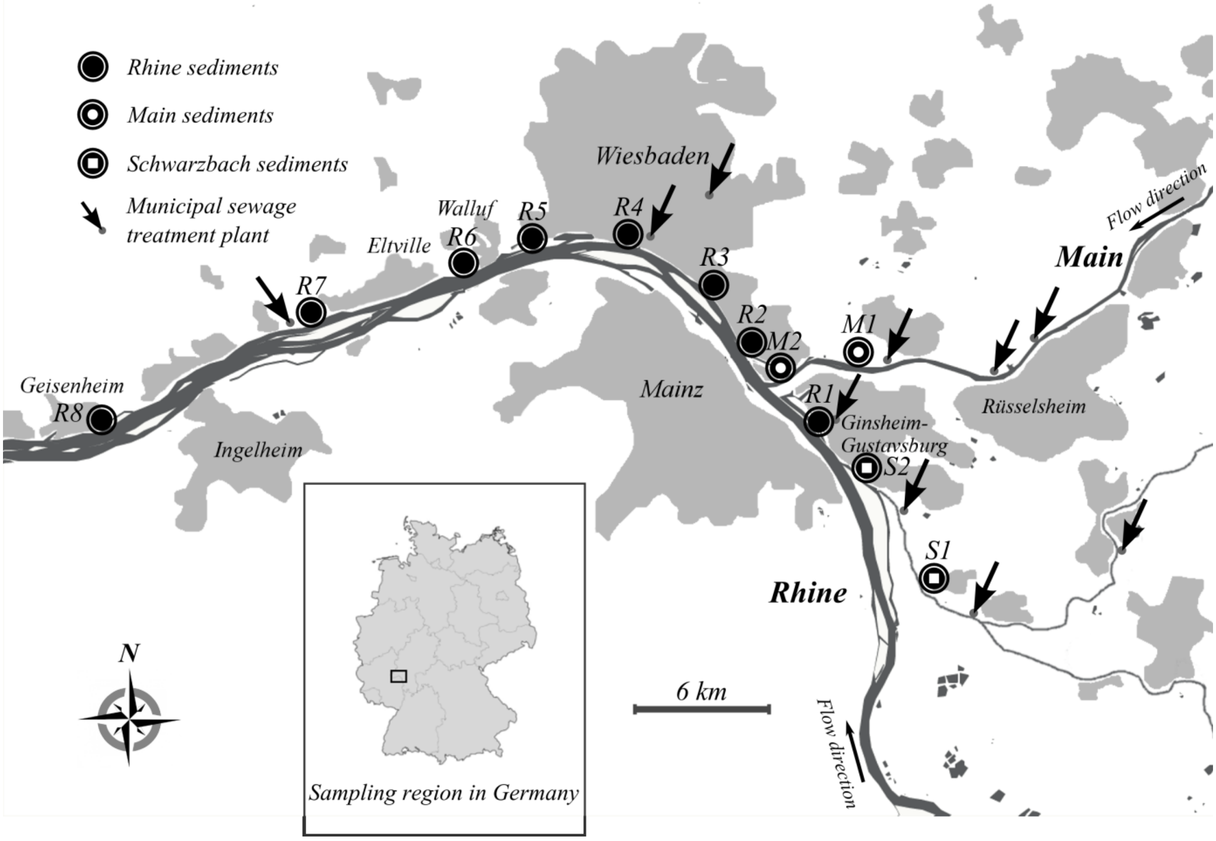

Figure 8: Detailed map of the sampling sites in the Rhine-Main area in Germany. Sampling sites are marked by circles; (S1) Astheim, (S2) Ginsheim-Gustavsburg Schwarzbach, (R1) Ginsheim-Gustavsburg, (M1) MZ-Kostheim 1, (M2) MZ-Kostheim 2, (R2) MZ-Kastel 1, (R3) MZ-Kastel 2, (R4) WI-Biebrich, (R5) WI-Schierstein, (R6) Walluf, (R7) Erbach, (R8) Geisenheim. Grey-shaped areas represent settled areas. Arrows mark the locations of municipal sewage treatment plants.

4.2.2 Sampling strategies

4.2.2.1 Sampling of Site R4 and R5 in May 2013

The sampling of the sediment at sites R4 and R5 in May 2013 was carried out by a zone sampling approach that is usually described in literature. At each site, a rectangular area (0.5 x 0.25 m) between the shoreline and the lowest flotsam line was selected. The sample was taken to a depth of 2-3 cm with a stainless steel spoon. The sampling was carried out in triplicates, and the sediments were stored in HDPE Rotilabo®-wide-neck-cans in dark at room temperature until further sample treatment.

4.2.2.2 Sampling of shore sediments from the river Rhine, river Main, and stream Schwarzbach from December 2013 until February 2015

The sampling of the sediment was conducted with a randomized sampling approach. Each sample was taken at the straight lengthy regions of the riverbank. The sediments were taken between the shoreline and the lowest flotsam line with a stainless steel spoon at 35-40 spots over a distance of 10-15m randomly, parallel to the shoreline of the rivers. Each spot had a size of approximately 30 cm². The distance between the flotsam line and the water line accounted 5-25 cm. Before taking the samples, plastics and natural fragments exceeding approximately 10 mm in size were removed. The sediment was sampled up to a depth of 2-3 cm, resulting in a total weight of 2-4 kg of wet sediment. The sediments were stored in HDPE Rotilabo®-wide-neck-cans in dark at room temperature.

At the sampling sites R4 and R8 three independent replicates were taken with this method to estimate the within-site variability. R4 and R8 were chosen to include a dense settled area with direct sources in vicinity as well as less dense populated areas. Each sample was taken as described previously, but sampling of exactly the same spot was avoided.

All sediment samples that were taken during December 2013 and February 2015 were sampled with this random sampling approach.

The sampled sediments are summarized in Table 3 including information on the different sampling dates and the different sample processing.

Table 3: Details of the sampling campaigns at the river Rhine, river Main, and stream Schwarzbach including dates of sampling, water levels of the rivers, and further processing. The processing includes sieving (S) ,density separation described by Thopmson *et al.* (2004) (DST), or vacuum-enhanced separation of plastic artefacts (VESPA), visual identification of plastic particles by microscopy (Mic), and FTIR (IR).

Date	Sites sampled	Water level [cm]	Sampling	Processing
May 2013	R4, R5	Rhine: 243	Zone	DST, Mic, IR
December 2013	R1-8, M1, M2, S1, S2	Rhine: 248 Main: 134 Schwarzbach: n/a	Random	S, VESPA, Mic, IR
September 2014	R4	Rhine: 263	Random	S, VESPA, Mic, IR
February 2015	R4	Rhine: 253	Random	S, VESPA, Mic, IR

4.2.3 Sieving

The wet sediments were placed in preweighed large glass Petri dishes and were dried at 50 °C in a drying cabinet for 3-7 days depending on the sediment moisture. The dried sediments were transferred in a sieving apparatus for further fractionation. The weight of the dry sediment was determined by difference weighing of the empty Petri dishes. The fractionation was carried out with three sieves containing mesh sizes of 63 µm, 200 µm, and 630 µm, respectively. The sieving apparatus was placed on an orbital shaker for 20 min at 200 rpm. Subsequently, the largest size fraction was examined by the naked eye, larger particles were measured, and particles exceeding 5 mm in diameter were removed. Particles smaller than 63 µm in size were discarded, because of blank issues. This procedure resulted in the size fractions: 63-200 µm, 200-630 µm, and 630-5000 µm. The total weight of each size fraction was determined before proceeding with the density separation.

4.2.4 Density separation

The separation of the plastic particles from sediment was carried out with two different methods. Sediments, which were treated by the method described by Thomson *et al.* (2004), were not fractionized by sieving.

4.2.4.1 Density separation by Thompson *et al.* (2004)

250 g of dried sediment was weighed in 1 L Erlenmeyer flasks and 500 mL saturated sodium chloride solution (refer to 9.1.3.1) was added. The mixture was stirred for 15 min with a magnetic stirrer, and the sediment was allowed to settle overnight. The buoyant particles

were carefully transferred with the supernatant solution to a glass fiber filter (4.7 mm) by decantation. The filter residues were subsequently washed with deionized water to remove residual sodium chloride solution. The filters and filter residues were transferred in preweighed hexagonal weighing pans and dried in a vacuum desiccator for three days.

Subsequently, particles exceeding 5 mm in size were removed with tweezers. Particles, which could be identified as natural debris were discarded, plastic particles were cleaned again with deionized water, dried in a vacuum desiccator for three days and analyzed by ATR-FTIR.

4.2.4.2 Vacuum-enhanced separation of plastic artefacts

During this thesis the vacuum-enhanced separation of plastics artefacts (VESPA) was developed.

The sediment fractions of 200-630 µm and 630-5000 µm, respectively, were filled in 500 mL filter flasks. If the weight of a size fraction did exceed 250 g, the density separation was done in two steps. Up to 400 mL of saturated sodium chloride solution was added depending on the volume of the sediment, and the suspension was stirred on a magnetic stirrer for 15 min. Fractions of 63-200 µm in size were filled in 250 mL filter flasks, and up to 150 mL of saturated sodium chloride solution was added, if the weight of this fraction did not exceed 75 g. Otherwise the separation was carried out according to the separation of the greater size fractions. The suspension was stirred for 15 min with a magnetic stirrer. All open mouths of the filter flasks were covered with aluminum foil to avoid contamination with dust particles. The sediment particles were allowed to settle overnight.

The filter flask was attached to a filtration unit with a clear vacuum tube (Figure 9). The vacuum filtration unit was covered by reaction vessel lid and sealed by an O-ring. Large buoyant particles of the size fraction 630-5000 µm were transferred to the glass fiber filter with the use of a spatula first to avoid clogging of vacuum tube or the nozzle of the filter flask. All other buoyant particles were transferred to the glass fiber filter in the vacuum filtration unit under vacuum by the addition of saturated sodium chloride solution to the separation flask. After the transfer of all buoyant particles from the density separation filter flask the vacuum tube was rinsed intensively with deionized water to transfer adherent particles to the glass fiber filter. Additionally, the filter residue was rinsed to remove residual sodium chloride. The filters and filter residues were transferred in hexagonal weighing pans and dried in a vacuum desiccator for one day.

Larger particles, natural or synthetic, from size fraction 630-5000 µm were removed with tweezers. Plastic particles, which could be identified by the naked eye, were cleaned again with deionized water and dried in glass Petri dishes in a vacuum desiccator. To destroy the accompanying natural debris the filter residues were treated with a mixture of hydrogen peroxide (30%) and sulfuric acid (98%) in ratio of 3:1 (v:v). The reaction mixture was gently stirred in an ice bath overnight. Subsequently, the reaction mixture was diluted with deionized water and filtered over a preweighed glass fiber filter. The filter residues were intensively rinsed with deionized water and dried in preweighed glass Petri dishes including the glass fiber filter in a vacuum desiccator for three days. Afterwards, the weight and the number of microplastics were determined, and plastic particles were visually identified by microscopy and analyzed by ATR-FTIR.

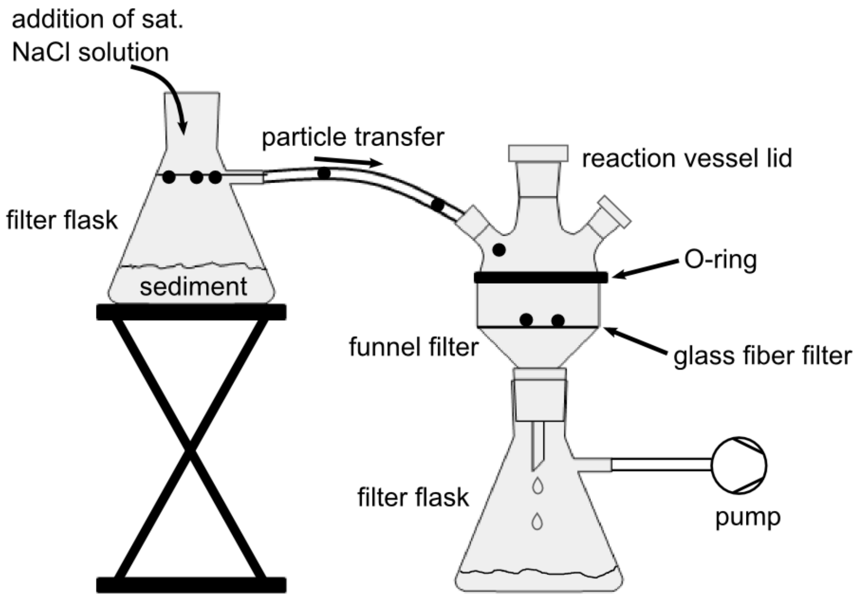

Figure 9: Schematic of the vacuum-enhanced density separation of plastic artefacts. Floating particles are transferred by addition of saturated sodium chloride solution by means of a vacuum directly to the glass fiber filter.

4.2.5 Analysis

4.2.5.1 Determination of weight and numerical abundance of plastic particles

The dry glass fiber filters were weight prior their use during the density separation or during the filtration after the destruction of natural debris. The plastic weight of each size fraction was determined by difference weighing of the dried filter residues. Particles greater than 630 µm were counted with the naked eye, plastic particles of smaller fractions were identified and counted using a binocular microscope.

4.2.5.2 Microscopic analysis

The microscope measurements were carried out with a binocular microscope using a magnification of x40-x100. All size fractions were examined carefully for remaining debris during the microscopic analysis. Obvious residual natural objects were removed with microforceps or dental explorer. Suspected natural debris or plastic particles were tested for hardness with the tip of the dental explorer. If natural or inorganic particles were identified by hardness tests, the determination of the particle weight was repeated.

Particles that were identified as microplastics were counted and were classified by their shape into the categories “pellet”, “sphere”, “fragment”, and “fiber”. Additionally, random particles were measured to check proper size fractionation. The measurement was carried out with the software Motic images plus (V 2.0). To calibrate the software, a calibration was performed with 0.1 mm and 0.6 mm dots of a calibration slide for microscopes. Pictures for the size analysis were taken with Moticam X in a resolution of 1200x800 pixels.

4.2.5.3 Fourier transform infrared spectroscopy

FTIR measurements of the polymers of size fraction 630-5000 µm and >5000 µm were performed by using a Perkin Elmer FTIR instrument. The FTIR instrument was equipped with a high ATR unit using a ZnSe crystal. If possible, a small slice was cut off the polymer particles with a scalpel to measure the IR spectra of a fresh polymer surface. The polymer particles were placed on the ZnSe crystal of the ATR unit with tweezers or a dissecting probe and covered by a stainless steel plate. Pressure was applied on the particles to maximize the contact surface with the ATR crystal. Ten scans per sample were acquired from 4000-700 nm, and a database search was carried out with Spectrum Search Plus (V3.00.05). The polymers were identified by means of an automatic comparison of the resulting spectra with spectra of a polymer library (Synthetic polymers ATR-library). For the accurate identification of the polymer, the match factor threshold was set to 0.70.

4.2.6 Method validation

4.2.6.1 Determination of blank values

All procedures involving plastic devices and sample preparation steps were checked for possible contamination with plastic particles.

4.2.6.1.1 Blank determination of the density separation

To estimate the blank values of the sediment sample preparation described in 4.2.3 and 4.2.4.2, three density separations were performed with 250 g commercially available clean sea sand. The sediments were processed as described in 4.2.3 and 4.2.4.2 and analyzed by microscopy (refer to 4.2.5.2).

4.2.6.1.2 Storage of sediment in HDPE wide neck cans

HDPE wide neck cans were used for the transport of the sediment samples. To exclude contamination of the sediment samples with plastic particles originating from the wide neck cans, 750 g of wet and clean sand was placed in two wide neck cans, and the closed cans were placed on an orbital shaker for one hour. Subsequently, the sediment was processed as described in 4.2.3 and 4.2.4.2. The identification of plastic particles was carried as described in 4.2.5.2.

4.2.6.1.3 Blank determination of the complete procedure

To estimate blank values of the entire sample preparation of sediment samples, blank values were determined for every set of analysis carried out by the procedure described in 4.2.3-4.2.5. The sieving and density separation was done with clean sea sand.

4.2.6.2 Recovery of the density separation

To assess the separation power of the method described by Thompson *et al.* (2004), recovery experiments with clean sand and polymer standards were performed. Powders of PMMA, PS, PC, and PVC were used to represent small microplastic particles. PE production pellets were used to estimate the recovery of larger microplastics. 10 mg of the polymer powders and 200 mg of the pellets respectively were mixed with 200 g of dry and clean sand. The density separation was carried out as described in 4.2.4.1 or 4.2.4.2 for each polymer in triplicates. The destruction of natural debris by the means of hydrogens peroxide and sulfuric acid (refer to 4.2.4.2) was skipped for better comparability.

4.2.6.3 Influence of hydrogen peroxide and sulfuric acid on natural debris and synthetic polymer particles

Powders of PMMA, PC, PS, and PVC were treated with hydrogen peroxide and sulfuric acid as described in 4.2.4.2. The weight of polymer particles was determined before and after the treatment by difference weighing. The reaction was carried out for 1 h, 3 h, and 24 h. The shape of the particles was analyzed by microscopy to observe any influence of the treatment as described in 4.2.5.2. Natural debris was obtained from sediment sampled at site R5. Natural debris of size fraction 630-5000 µm was used after polymer particles were removed. Plastic particles were removed prior weighing of the natural debris. The portion of natural debris was ground to additionally obtain fragments of smaller size.

The reaction for plastic particles and natural debris was carried out for 1 h, 3 h, and 24 h. For this experiment 10 mg of each polymer and 15 g of natural debris was used for each replicate.

4.3 Sorption experiments

4.3.1 Investigation of the sorption kinetics

For the investigation of sorption kinetics, synthetic freshwater (refer to 9.1.3.2) was mixed with the organic contaminants carbamazepine (CBZ), 17α-ethinylestradiol (EE2), β-hexachlorocyclohexane (β-HCH), γ-hexachlorocyclohexane (γ-HCH), chlorpyrifos, or o,p'-dichlorodiphenyltrichloroethane (DDT), respectively. The concentration of contaminant varied depending on their water solubility and the limit of quantification of the analytical method used for their determination. The final concentration, the logarithmic octanol-water partition coefficient (log K_{OW}), and the solubility in water of each contaminant are listed in Table 4.

Table 4: Contaminants used for sorption experiments, including log K_{OW} values, water solubility Concentration of the contaminants in synthetic freshwater used for the kinetic experiments. The references are provided in parentheses.

Contaminant	Log K_{OW}	Water solubility at 24 °C [ng mL^{-1}]	Concentration [ng mL^{-1}]
CBZ	2.45 (139)	17700 (139)	10
β-HCH	3.80 (140)	300 (141)	250
γ-HCH	3.20-3.72 (140, 142)	5000 (141)	1000
EE2	4.15 (143)	9200 (144)	25
Chlorpyrifos	4.70-5.27 (145)	2000 (146)	1000
DDT	4.90-6.90 (147)	5.5 (148)	2.5

The kinetic sorption experiments were carried out in duplicates in 22.5 mL glass vessels with screw caps and Teflon septa. Each batch contained 10 mL of a mixture of synthetic freshwater with a contaminant and 10 mg of PC, PE powder, PMMA, PS, EPS, or PVC respectively except for the mixture containing DDT. The sorption experiment of DDT was carried out in 100 mL brown glass bottles and 100 mL of solution was added to 100 mg of PC, PE powder, PMMA, PS, EPS, or PVC, respectively. The suspensions were mixed vigorously on a vortexer and covered with aluminum foil. The vessels were stored on an orbital shaker at 500 rpm for 30 days at 24 °C. Samples of the supernatant were taken periodically from each batch. 5 mL were sampled from the solution containing DDT and 100 µL from solutions containing CBZ, β-HCH, γ-HCH, EE2, or chlorpyrifos. The samples were stored in glass vials in a freezer at -18 °C until further processing. For all compounds samples without polymers were prepared as control samples. The control samples were treated exactly as the samples with polymer particles.

After 30 days, the suspensions were filtered through cellulose filters to separate the polymer powders from the solution. The filter residues were rinsed with 10 mL of water to wash out residual contaminant solution. The filters including the filter residues were dried in a vacuum desiccator for 3 days. Afterwards the polymer particles were transferred into glass vials and stored at 4-7 °C until the extraction of the polymer particles.

4.3.1.1 Sample preparation of the supernatant of CBZ and EE2 solutions

The supernatant samples of CBZ and EE2 were mixed with 50 µL of CBZ-D10 or Bisphenol A-D16 (BPA-D16) in methanol (CBZ-D10: β=1 ng/mL; BPA-D16: β=25 ng/mL), respectively, that was added to all samples as internal standard. The samples were mixed vigorously on a vortex mixer, filtered through syringe filters and filled in PP microvials for the measurement by LC-MS/MS.

4.3.1.2 Sample preparation of the supernatant from β-HCH, γ-HCH, chlorpyrifos, and DDT solutions

A liquid-liquid extraction with hexane was performed for all samples of β-HCH, γ-HCH, chlorpyrifos, and DDT solutions. 550 µL of atrazine in hexane (β=100 ng/mL) as internal standard was added to all samples in 1.5 mL Eppendorf cups. All samples were mixed carefully on a vortex mixer for 2 min in intervals of 5 s. The aqueous phase and the hexane phase were allowed to separate for 15 min. Subsequently, the samples were stored in a freezer at -18 °C for one hour. 500 µL of the hexane phase were transferred into 1.8 mL glass vials and evaporated to dryness at room temperature under a gentle stream of nitrogen. The dried residues were resolved in 40 µL hexane, transferred in glass microvials and measured by GC/MS.

4.3.1.3 Extraction of the polymer particles

The extraction of the polymer particles were done only for tetrahydrofuran (THF) soluble polymers (PC, PMMA, PS, and PVC). Polymer particles were dissolved in THF. For the extraction of CBZ, CBZ-D10 and for the extraction of EE2, BPA-D16 was added as internal standard. Atrazine was used as internal standard for the extraction of β-HCH, γ-HCH, chlorpyrifos, and DDT. The samples were filtered through syringe filters prior the manual injection into a GPC system. Each sample was injected threefold. The conditions of the separation on the GPC column and the fraction collection are stated in in the annex (Table 14). The fractions were collected in 4 mL test tubes. THF was evaporated to dryness under a gentle stream of nitrogen. For substances that were analyzed via GC/MS, the dried residues were dissolved in 200 µL hexane. The residues were dissolved in 100 µL methanol first with subsequent addition of 200 µL of water for substances that where analyzed by LC-MS/MS.

4.3.2 Acquisition of the sorption isotherms

Sorption isotherms were determined for the polymers PC, PMMA, PS, and PVC in combination with the contaminants CBZ, γ-HCH, and chlorpyrifos. Ten different solutions with concentrations ranging from 5-800 ng mL^{-1} were prepared in freshwater for each contaminant. The exact concentrations are provided in the annex (Table 13). 10 mL of synthetic freshwater and contaminant was added to 10 mg of the polymers. For all compounds, samples without polymers were prepared and treated exactly as the samples that contained polymer particles. The sample preparation of the sorption isotherm experiments were essentially carried out as the sample preparation of the sorption kinetic experiments (4.3.1), except the periodic sampling of the supernatant. After 30 days, a sample of the supernatant was taken according to 9.1.6 and prepared for the measurement on a LC-MS/MS system (CBZ) or a GC/MS system (γ-HCH, chlorpyrifos).

4.3.2.1 Sample preparation of CBZ for LC-MS/MS measurements

For the determination of CBZ by LC-MS/MS, 100 µL of CBZ-D10 in methanol at a concentration of 25 ng mL^{-1} was added to all samples as internal standard. Supernatant samples of volume of 100 µL were additionally mixed with 800 µL of water. All samples were mixed vigorously on a vortex mixer, filtered through syringe filters and filled in PP microvials for the measurement by LC-MS/MS.

4.3.2.2 Sample preparation of γ-HCH and chlorpyrifos for GC/MS measurements

Each supernatant sample of the sorption isotherm experiments that contained γ-HCH and chlorpyrifos was extracted by a liquid-liquid extraction with hexane. Atrazine was added as internal standard at a concentration of 100 ng mL^{-1}. 1.1 mL of hexane was added to each supernatant sample in a 15 mL falcon and mixed carefully by means of a vortex mixer for 2 min in intervals of 5 s. The phases were left to separate for 15 min, and the falcons were subsequently stored in a freezer at -18 °C for one hour. 1 mL of the hexane phase was transferred with an adjustable-volume pipette in a glass vial and was evaporated to dryness under a gentle stream of nitrogen. The dried residues were resolved in 200 µL hexane, transferred in glass microvials and measured by GC/MS.

4.4 LC-MS/MS and GC/MS analysis

The determination of the contaminant concentration was carried out using LC-MS/MS system consisting of an Agilent 1100 HPLC system coupled to an AB Sciex API 2000 mass spectrometer (CBZ, EE2) or on an Agilent 6890N GC system coupled to an Agilent MSD 5973 inert mass spectrometer (β-HCH, γ-HCH, chlorpyrifos, DDT).
All instrument parameters used for the analysis and details on the method development are provided in the annex (refer to 9.1.7.2.1 and 9.1.7.3.1).

4.4.1 Calibration

All measurements of the aqueous phase of CBZ and EE2 were quantified with an external calibration. Measurements of the hexane extracts of β-HCH γ-HCH, chlorpyrifos, and DDT were quantified with an internal calibration. Therefore, the standards containing the analyte were spiked into water and extracted as described in 4.3.1.2 and 4.3.2.2. Samples that were analyzed after the GPC clean-up were quantified with standards that did undergo the GPC clean-up as well.

4.4.2 Method validation

All steps involved in the sample preparation and analysis of the contaminants in the sorption experiments were carefully validated. Therefore, recovery experiments for all sample preparations were conducted by spiking known amounts of analyte prior the sample treatment. The recovery experiments were carried out close to the lowest concentration that was analyzed in the sorption experiments.
The GPC clean-up was developed with CBZ as a model substance and PS168 as polymer. Recovery of the clean-up for all substances was tested with PS168. Results of the determination of the fraction collection are provided in the annex.

4.5 Extraction of the polymer particles from sediment samples

4.5.1 Extraction of PS particles

PS particles were extracted with THF, sample clean-up was performed via GPC and extracts were prepared for GC/MS and LC-MS/MS as described in 4.3.1.3.

4.5.2 Extraction of PE particles

4.5.2.1 Extraction method

The extraction of PE particles was carried out with hexane. PE particles were placed in 22.5 mL vials and 10 mL of hexane was added. The vials were placed in an ultrasonic bath for 30 min. The hexane supernatants were subsequently separated with glass Pasteur pipettes in fresh 22.5 mL glass vials. The hexane was evaporated to approximately 1 mL under a gentle stream of nitrogen at room temperature and split in two approximately 500 µL fractions for GC/MS analysis or LC-MS/MS analysis, respectively.

4.5.2.2 Sample preparation for and measurement via LC-MS/MS

500 µL of the hexane extracts were transferred into 1.8 mL glass vials and evaporated to dryness under a gentle stream of nitrogen at room temperature. The residues were solved in 100 µL methanol and 200 µL of water was added. The methanol/water extracts were mixed vigorously on a vortex shaker, filtered through syringe filters and filled in PP microvials for the measurement by LC-MS/MS. The extract was analyzed in MRM mode for 34 priority pollutants. The instrument method is shown in the annex (refer to 9.1.7.2.2).

4.5.2.3 Sample preparation and measurement via GC/MS

The remaining 500 µL of the hexane extracts were transferred into 1.8 mL glass vials and evaporated to approximately 200 µL under a gentle stream of nitrogen at room temperature. The extracts were filtered through syringe filters and filled in glass microvials. The measurement of each extract was carried out with GC/MS in Scan mode and in SIM mode for 54 priority pollutants. The instrument methods used for the analysis are shown in the annex (refer to 9.1.7.3.2).

4.5.3 Blank preparations

To avoid false positive results, blank sample were prepared and treated as described for PE particles and PS particles, respectively. Blank samples were prepared in triplicates as described in 4.5.1 and 4.5.2, but without polymer particles. Intensities of substances presented in the results section were at least tenfold higher than in the blank samples.

4.6 Data analysis

4.6.1 Statistical analysis

If not stated otherwise all statistical analyses were carried out with the use of Microsoft Excel 2010. One-way analysis of variation (ANOVA) was carried out in Origin V6.0.

4.6.2 Modelling of isotherms and sorption kinetics

To model the sorption kinetics and the sorption isotherms it was necessary to calculate the sorption of the substances to the polymer. Sorption of the solute to the polymer was calculated by equation (8)

$$q = \left(1 - \frac{C_{aq}}{C_{aq\,0}}\right) C_{aq\,0} \frac{V}{m_{Sorbent}} \qquad \textbf{(8)}$$

where q is the concentration in the polymer in ng mg^{-1}, C_{aq} is the solute concentration in ng mL^{-1}, $C_{aq\ 0}$ is the initial solute concentration in ng mL^{-1}, V is the volume of the batch solution in mL, and $m_{Sorbent}$ is the mass of the polymer in the batch.

Modelling was performed with Origin V6.0 after drawing the concentration of the polymer against time for the sorption kinetics or after drawing equilibrium solid phase concentration against the equilibrium solute concentration for the sorption isotherms. Fitting of the model curves was conducted by a Levenberg-Marquardt algorithm that is following the least squares method. For the determination of the sorption kinetic model, the pseudo-first order reaction mode served as fitting functions (6). The models for the sorption isotherms were determined with by the application of the equations that are given by Henry (1), Freundlich (2), Langmuir (3), and the BET model (4).

4.6.3 Principle component analysis

Principle component analysis (PCA) was conducted with the software MYSTAT V12.02.00. For PCA, model variables for the polymers PC, PMMA, PS, and PVC were arranged in a single row. Model variables that were used for PCA were C/H ratios, O/C ratios, glass transition temperatures, and K_D values determined for CBZ, γ-HCH, and chlorpyrifos. The factor analysis was carried out with the principle component method using correlation for the matrix extraction.

5 Results

5.1 Microplastic particles in inland water sediments

Information about the pollution of inland waters with plastic particles was to the author's knowledge not available by 2010. This is why it was important to gather first data for an estimation of the importance of the microplastic pollution in inland water systems. Shore sediments seem to be a favorable sample compartment of freshwater systems because of various reasons. Firstly, shore sediments possibly contain buoyant as well as non-buoyant plastic particles. Buoyant microplastics are transported by the river current or by the movement of waves, whereas non-buoyant plastic particles are transported with the river sediment. Secondly, studies of marine habitats showed that concentrations of plastic particles were greater in shore sediment samples than sublittoral sediments in water surface samples. Higher concentrations yield in better reproducibility and less necessary sample volumes. Additionally, shore sediments are easy accessible for the sampling process.

5.1.1 Initial investigations on microplastic abundance in river sediments

To gather initial information on the abundance of microplastics in river shore sediment and establish a method for the microplastic analysis, shore sediment at two locations (R4 and R5) at the river Rhine was sampled. The sample preparation of the sediments was carried out according to a straightforward method described by Thompson *et al*. (2004).

The analysis of the sampling sites R4 and R5 revealed notable concentrations of larger microplastics in the size range of approximately 500-5000 µm (Figure 10).

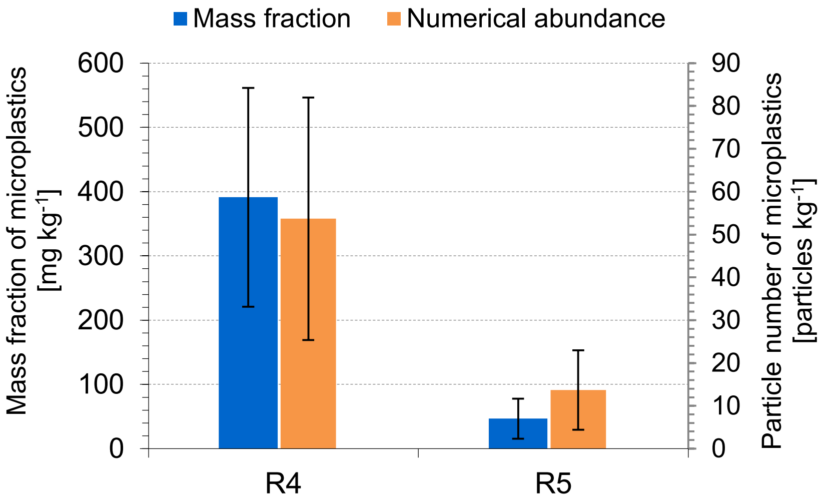

Figure 10: Analysis of river shore sediments sampled in May 2013. The mass fraction and particle numbers of microplastics separated from sediments from site R4 and site R5. The sampling was done in triplicates, and the density separation was carried out after Thompson *et al*. (2004).

The weight and the number of plastic particles, which could be separated from the sediments, strongly differed between both sampling sites. Additionally, both sampling sites showed a high within-site variability, which is reflected by the large deviation (relative standard deviation: 44-68%) of the triplicate analysis. This could likely be a result of the inhomogeneity of the sediment samples. On the other hand, the varying concentrations could as well indicate an insufficient sampling process or non-reproducible density separation. Possible plastic particles smaller than 500 µm were also detected by microscopy. However, these particles could not be identified unambiguously as plastic particles, even though if the shape of the particles was comparable to plastic microparticles because of the large abundance of natural debris aside the plastic particles. An identification of smaller particles would require further treatment of the sample for a better differentiation between natural and plastic debris.

The separated plastic particles were identified using ATR-FTIR spectroscopy. The abundance of each polymer type differs by the consideration of mass and number of the particles (Figure 11). With a proportion of 40% of the total plastic, PP is the most abundant polymer in terms of weight followed by PE (17.8%). In contrast to the low weight abundance of PS (3.3%), PS is the most abundant polymer in terms of particle numbers (41.2%). The large discrepancy of numerical and weight-related abundance of PS could be explained by the presence of mainly EPS in the sample.

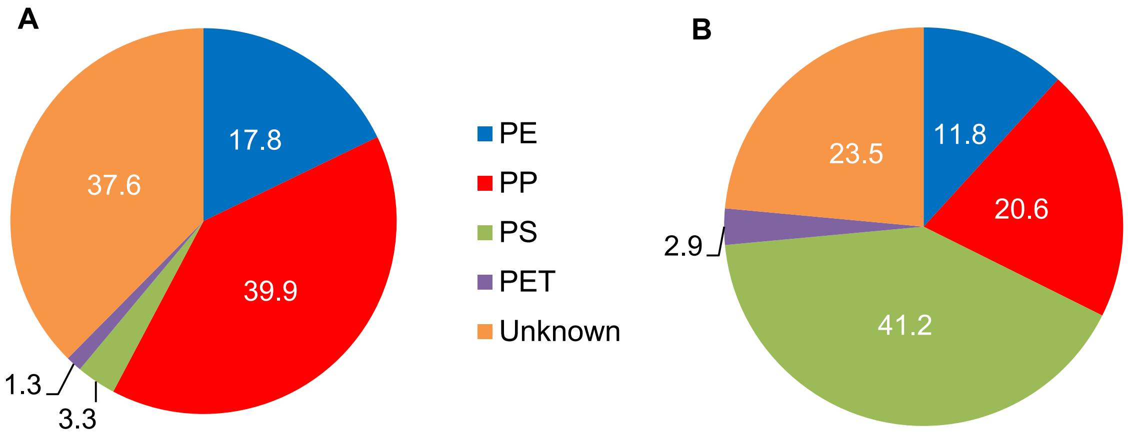

Figure 11: Abundance of polymer types by weight **(A)** and by number **(B)** in the sediment samples from R4 and R5. Identification of the polymer type was carried out by ATR-FTIR spectroscopy. Polymers identified were PE, PP, PS, and PET. Non-identified particles are marked as “unknown”.

5.1.2 Method development for the analysis of microplastics in sediments

The results obtained from the analysis of river Rhine shore sediments in 5.1.1 showed high within-site variability. It seems reasonable to assume that the main factor for the high variation of the microplastic concentration was a consequence of the inhomogeneity of the sediment samples. Furthermore, the sampling process did promote high within-site variability as only a small region of each site is sampled. Aside from the sampling process, a crucial step for reliable investigation of the plastic content of river sediments is the separation of plastic particles. The method used for the sample treatment showed several problems, especially the detection of smaller plastic particles needed improvements.

5.1.2.1 Improvement of the density separation

In a first step the density separation was validated and the further treatment of the plastic particles was tested. The method needed to be capable of separating most of the different synthetic polymers present in sediments in sizes below approximately 300 µm, combined with a good reproducibility. A straightforward method is the density separation with a solution of high density. To be capable of comparing microplastic concentrations in river sediments with former studies of marine habitats, the use of a density separation with saturated sodium chloride solution described by Thompson *et al.* (2004) is the method of choice, despite the poor separation of high density polymers e.g. polyethylene terephthalate (PET).

To assess the separation power of the method described by Thompson *et al.* (2004), recovery experiments with clean sand and polymer standards were performed.[55] Powders of PMMA, PC, PS, and PVC were used to simulate a microplastic portion of up to 500 µm in a sediment sample. Larger microplastic particles were simulated by PE pellets. Microscopic measurements of the polymer powders showed that the particle size did not exceed 200 µm in diameter (Figure 12B, C, and D). Measurements of the PE pellets resulted in a size of 1.1-1.9 mm (size of a square particle; Figure 12E).

The experiments showed excellent recoveries (100%) for PE pellets and consequently confirmed the reliability of the results obtained in 5.1.1 (Figure 12A, left-hand side). Thus, an influence of the density separation on the within-site variability can be excluded for larger particles. However, insufficient separation of the synthetic polymer powders was revealed by the experiments. The maximal recovery rate was achieved for PMMA (68%), recovery rates for PC, PS, and PVC varied between 28 and 52%. Poor separation of powders was very likely caused by adherence of the polymer particles to glass ware during decantation steps, what was visually observed by some particles remaining in the Erlenmeyer flasks. Further, the deviations between the single separations of more than 20-40% indicate a low repeatability of the density separation method.

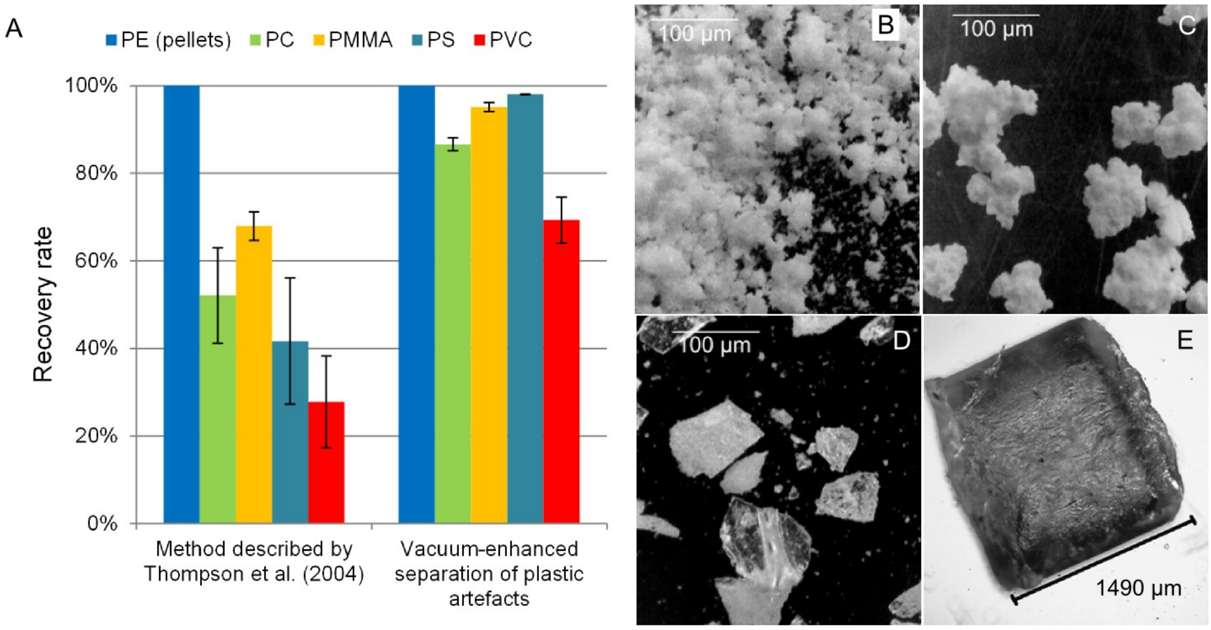

Figure 12: (A) Recovery rates of PE pellets, PC, PMMA, PS, and PVC separated from clean sand by two different density separation methods. Density separations were carried out in triplicates. Microscopic analysis of PC **(B)**, PVC **(C)**, PS **(D),** and PE **(E)** used for the recovery experiments.

To improve the recovery of the synthetic polymers and the repeatability of the separation, a new instrumental setup was developed that did not include decantation steps to transfer buoyant particles to the glass fiber filter during the separation steps. A scheme of the setup is provided in Figure 9. The recovery for all tested polymer powders was increased to 70-98% by the application of the new method. Furthermore, the transfer of the particles through the nozzle of the filter flasks by under-pressure showed excellent repeatability with standard deviations of 1-5% for all polymers tested.

5.1.2.2 Removal of natural debris in the filter residues

In addition to the polymer particles all buoyant natural fragments are separated from the sediment during the density separation. This natural debris complicates the visual identification of microplastics smaller than approximately 500 µm and prevents the correct determination of the plastic weight. For this reason, the destruction of the natural debris is an important step in the sample preparation procedure especially for the analysis of size fractions smaller than 630 µm.

A possible procedure to destroy natural debris was the treatment of the sample with a mixture of hydrogen peroxide and sulfuric acid. To assess the degree of removal dependent on the reaction time, natural debris was treated with hydrogen peroxide and sulfuric acid over a period of 24 h (Figure 13). Natural debris originated from site R5 and was obtained after sieving followed by a density separation of size fraction 630-5000 µm. Weight of the natural debris was determined after possible polymer particles were removed. Using this treatment, the mass of natural debris was decreased to 14.6% within 1 h. Further treatment of the natural debris with hydrogen peroxide/sulfuric acid resulted in a weight loss of 96.8% after 3 h and almost complete destruction of the natural debris after 24 h (0.9% residual natural debris).

As some polymer types are possibly not resistant to the sample preparation using hydrogen peroxide and sulfuric acid, the impact of this treatment needed to be tested on microplastics. Powders of PC, PMMA, PS, and PVC were used as model polymer particles and treated with the solution of hydrogen peroxide and sulfuric acid for 1 h, 3 h, and 24 h. During this reaction time, no influence could be observed on the tested polymers. The weight of the polymer recovered after each time period stayed constant within the measurement error and no visible modifications of the polymer surfaces by hydrogen peroxide/sulfuric acid were identified.

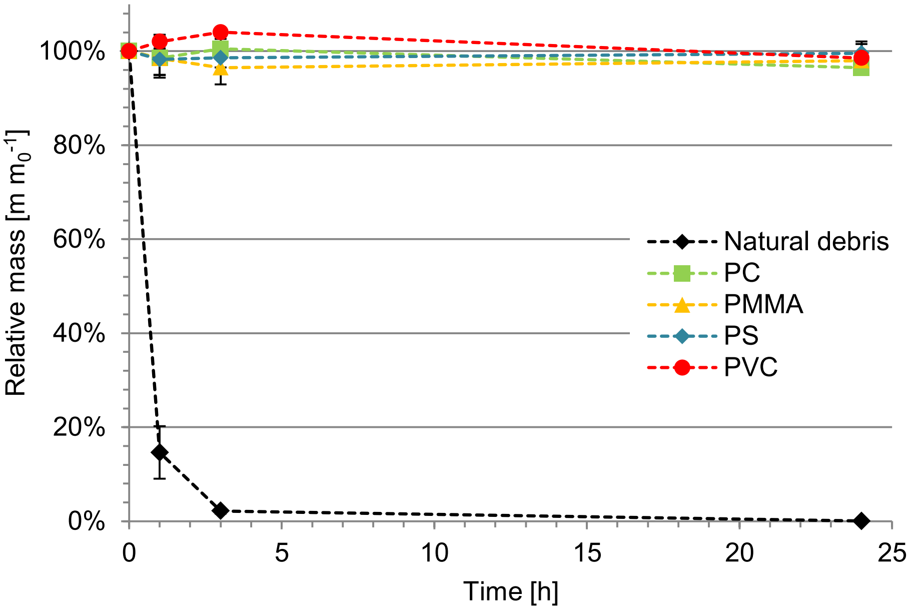

Figure 13: Influence of the treatment with hydrogen peroxide and sulfuric acid on the mass of natural debris (black diamonds) and on the polymers PC (red squares), PMMA (yellow triangles), PS (green diamonds), and PVC (cyan circles). The reaction was carried out over 24 h in duplicates.

5.1.2.3 FTIR measurements for the identification of plastic particles

The determination of the polymer type was performed by ATR-FTIR spectroscopy and a database comparison of the resulting IR spectra. An identification of the polymer particles from the sediment samples obtained in 5.1.1 was possible for most of the particles (62-74% of all particles). Particles, which were measured by ATR-FTIR were from the size fraction

630-5000 µm and did not undergo the hydrogen peroxide/sulfuric acid treatment. However, a significant amount of particles could not be identified and remains unknown, because of low match factors with the data base matching. Measurements of the polymer surfaces from unidentified samples often resulted in spectra with a visible C-H stretching vibration that was obtained in a ratio indicating the presence of a PE chain. However, broad and dominating absorption peaks between 1600-900 cm^{-1} prevented further identification. Thus, these particles were mainly matched to PE chlorosulfonated by the automatic database comparison resulting in match scores between 0.40 and 0.68. To improve the identification, the polymer particles were cut to obtain fresh polymer surfaces. Exemplary spectra of a weathered polymer surface compared to a fresh polymer surface are shown in Figure 14. Both spectra are similar in the range of 4000-1800 cm^{-1}, showing similar peaks for C-H stretching (3000 and 2800 cm^{-1}). However, they differ strongly in the important fingerprint area (1800-630 cm^{-1}), and only the fresh surface included signals indicating C=O stretching (1689 cm^{-1}), CH$_3$ bending (1390 cm^{-1}), and C-O-C stretching (1240 cm^{-1}). The comparison to database entries identified the polymer particle due to the spectrum of the fresh polymer surface as ethylene-vinyl acetate copolymer (match factor 0.897).

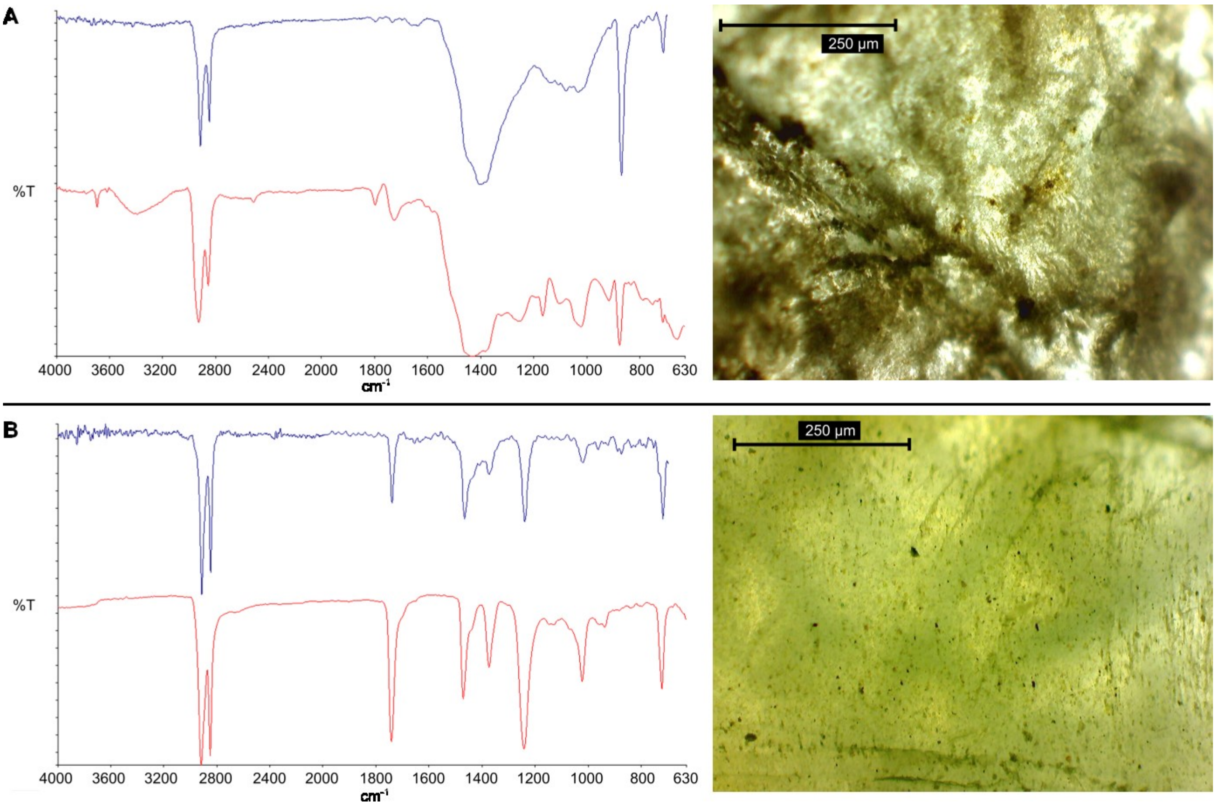

Figure 14: ATR-FTIR spectrum of a green polymer pellet scanning the aged polymer surface **(A)** and fresh polymer surface **(B)**. Blue lines represent measured spectra; red lines represent the respective database spectra with the best match factors. A microscopic image of the surface at a 40-old magnification is provided on the right hand-side.

5.1.2.4 Sampling method

To counteract the high within-site variability, the sampling method for sediment was changed. It was expected that microplastics might accumulate at specific areas at each site, thus the selection for distinct sampling zones would result in high within-site variability, visible in the high variation of the results obtained in 5.1.1. Further it was expected that the concentration of microplastics varies especially with greater distance perpendicular to the shoreline or between different flotsam lines. Therefore, instead of sampling distinct areas (e.g., 0.125 m²) one sediment sample consists of several small, randomly selected sediment portions, which were sampled at a small spot between the shoreline and the lowest flotsam line and were distributed over the complete sampling site (Figure 15).

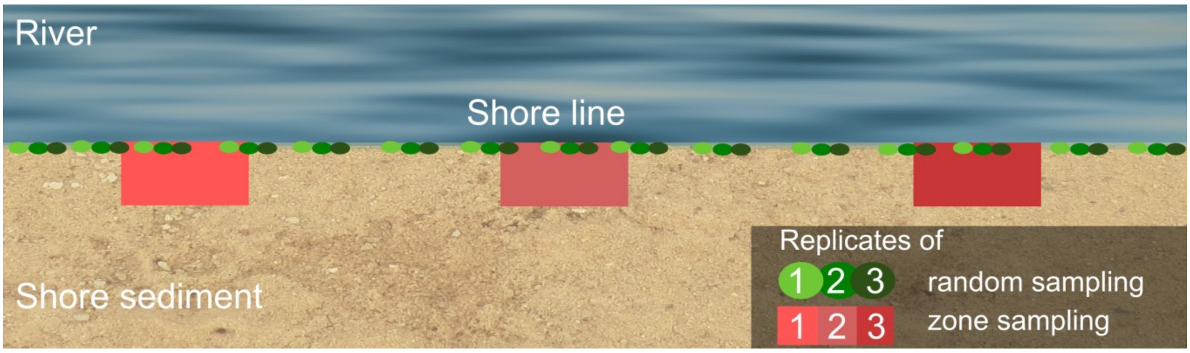

Figure 15: Design for the different sampling procedures of river shore sediment. Random, triplicate sampling of sediment along the sampling site is shown by green circles. Theoretical coverage of zone sampling of distinct areas (0.5 m x 0.25 m) is represented by red rectangles.

Random sampling of the sediments from sites R4 and R8 was done in triplicates to test for a decrease of the within-site variability by the application of the new sampling technique. R4 was chosen to represent a densely settled area, possible highly impacted by industrial activity and municipal sewage treatment plants. R8 should represent rural populated areas without direct industrial or sewage-related influences. Thus, the microplastic concentrations were expected to vary strongly in the sediments of both sites.

As the random sampling results in high sample volumes, further fractionation was required for a good sample handling. Processing of the complete sediment sample was necessary to take advantage of the sampling technique and avoid high deviations resulting from sample inhomogeneity. This is why a sieve fractionation was carried out resulting in sediment fractions 63-200 µm, 200-630 µm, 630-5000 µm, and >5000 µm.

Microplastic concentrations determined at both sites after random sampling, sieve analysis with subsequent density separation and sample clean-up with hydrogen peroxide/sulfuric acid showed significantly smaller in-site variability than samples of the sites R4 and R5 where zone sampling was applied (refer to 5.1.1). Using random sampling the relative standard deviation for all particles of the individual samples from site R4 amounted to 7.7%, and the relative standard deviation for total microplastic weight was 14.6% (Table 5). Microplastic concentrations of sediments from site R8 showed relative standard deviations of 17.5% for both, the total weight and numerical abundance of plastic particles. This result confirms the initial hypothesis of a within-site variability reduction by applying the random sampling technique.

Table 5: Mass fraction and item numbers of the triplicate analysis from sediment samples which were taken at the sampling sites R4 and R8 by random sampling. Data are shown as means and relative standard deviation in parentheses.

	Weight of plastic particles [mg kg^{-1}]		**Number of plastic particles [particles kg^{-1}]**	
Size fraction	**R4**	**R8**	**R4**	**R8**
630-5000 µm	268 (14)	100 (17)	65 (17)	15 (36)
200-630 µm	5 (47)	6 (28)	138 (10)	84 (28)
63-200 µm	2 (20)	2 (22)	412 (17)	223 (15)
Total	275 (15)	108 (18)	615 (8)	322 (17)

5.2 Microplastic abundance in shore sediments sampled in December 2013

Plastic particles were present in different shapes, sizes and colors in all sediments from sites R1-R8, M1, M2, S1, and S2 which were sampled on 5th December 2013. The mass fraction of microplastics varied between 22 mg kg^{-1} and 932 mg kg^{-1}, and the number of particles identified as plastic accounted for 228 particles kg^{-1} to 3763 particles kg^{-1} along the river Rhine (Figure 16). The sediments from the river Main contained a plastic fraction between 44 mg kg^{-1} and 459 mg kg^{-1} or 786 particles kg^{-1} and 1368 particles kg^{-1}, respectively. The lowest microplastic pollution was identified in a small stream (Schwarzbach) with concentrations between 18 mg kg^{-1} and 91 mg kg^{-1} or between 183 particles kg^{-1} and 307 particles kg^{-1}, respectively. The size fraction of 630-5000 µm was the most abundant fraction in terms of the total plastic weight. Particles larger than 5000 µm were only separated in sediments of R3, R4, R5, R6, and R8. However, the size fraction was neither included in the microplastic weight nor the microplastic numbers, since this size of those particles does not fulfill common microplastic definitions. As expected, the smaller size fractions (63-200 µm; 200-600 µm) contribute least to the total plastic weight of the sediments investigated. In contrast, most plastic particles in each sediment were identified in the smallest size fraction (63-200 µm) analyzed. The contribution of the largest size fraction to the total particle number is negligible (Figure 16).

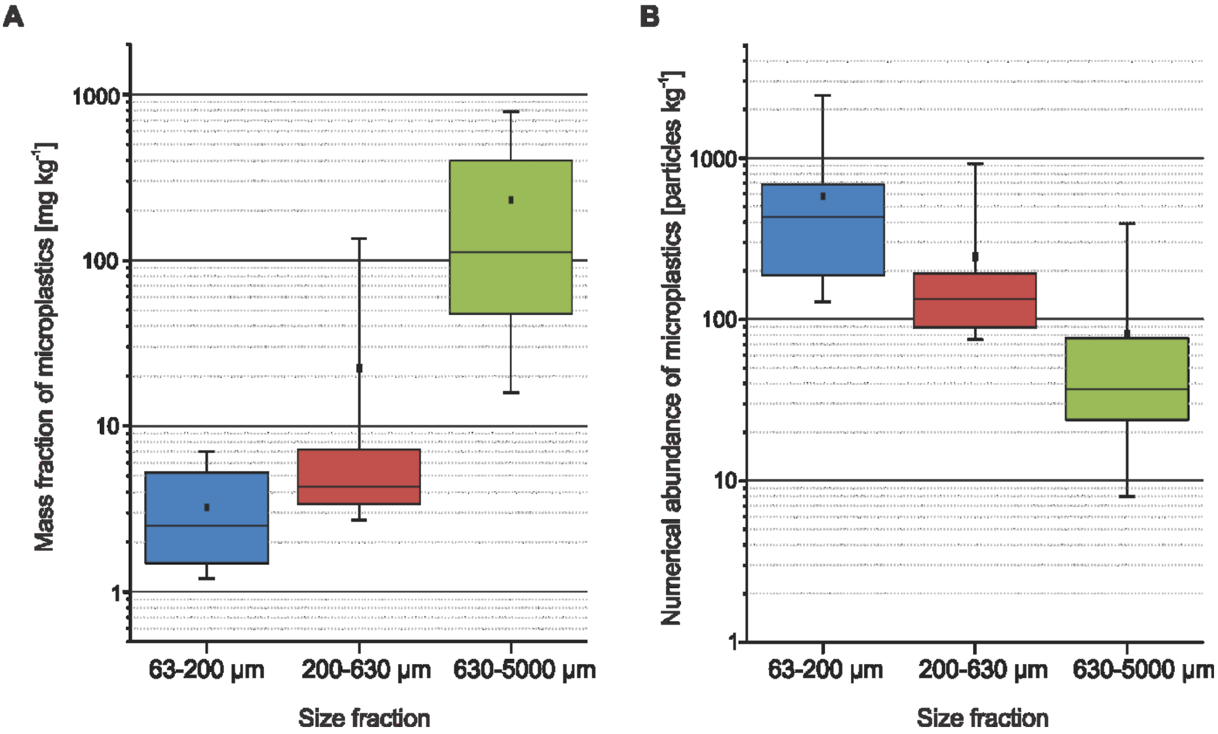

Figure 16: Weight abundance **(A)** and numerical abundance **(B)** of microplastic particles from twelve sediments (R1-R8, M1, M2, S1, S2) determined in the size fraction 63-200 µm, 200-630 µm and 630-5000 µm. Black rectangles represent the average of the data. Data is plotted in logarithmic scale (n=12).

5.2.1 Abundance of shapes

The microplastic particles of all size fractions were classified in categories fragments, fibers, and spheres. An exemplary classification of the particles into these shape categories is shown in Figure 17B. The category "pellet" was used for industrial preproduction pellets. Due to their large size, preproduction pellets were only detected in the size fraction 630-5000 µm with a relative abundance of 26% (Figure 17A). The averaged numerical abundance of fragments, fibers, and spheres was different in each of the microplastic size fractions. Thus, the abundance of spheres and fibers was higher in the smaller size fractions (50% and 13%, respectively) than in the size fraction 630-5000 µm (13% and 5%, respectively). In contrast, the relative frequency of fragments was the highest in the size fraction 630-5000 µm (56%). The abundance of fragments was slightly lower in the size fraction 200-630 µm (51%) and distinctly lower in the size fraction 63-200 µm (37%).

Noteworthy, all particles classified as spheres might be as well related to fragments which were polished to round form. Further, it seems reasonable to expect that fibers are possibly detected less frequently due to their small size in diameter and are lost during the size fractionation, as they are discarded with size fractions below 63 µm. This hypothesis is supported by the presence of larger, unevenly formed fragments where the edge lengths of one side exceeds the mesh size of the sieve (Figure 17B; e.g., F(413/153)).

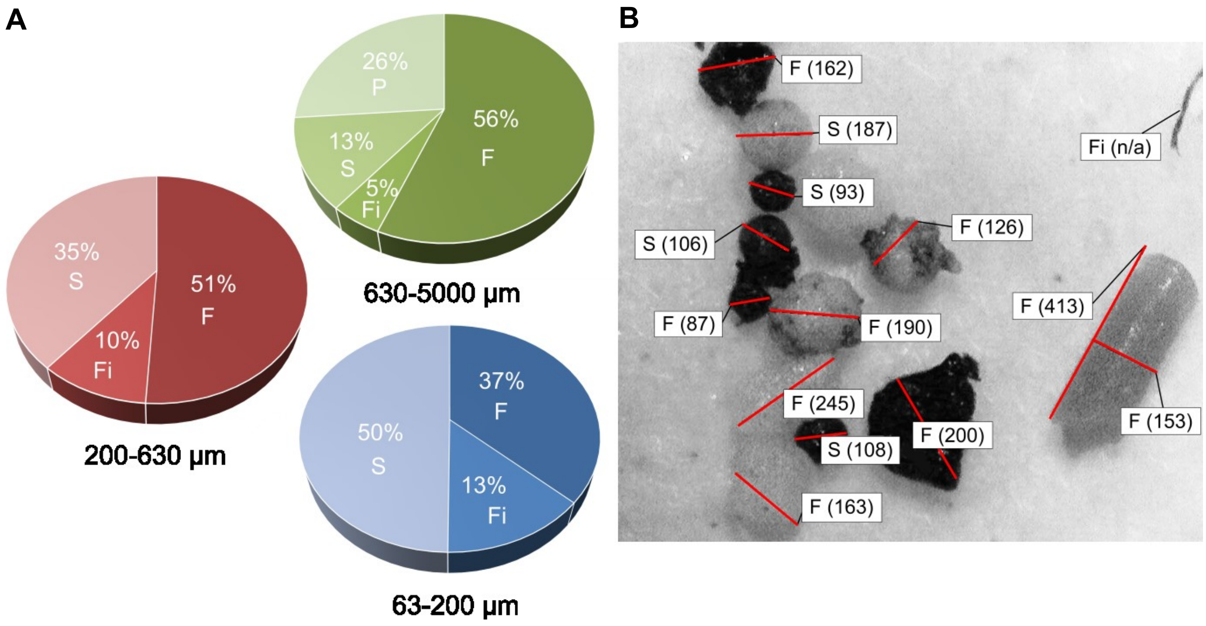

Figure 17: (A) Abundance of plastic pellets (P), fragments (F), spheres (S), and fibers (Fi) in the size fractions 63-200 µm (blue), 200-630 µm (red), and 630-5000 µm (green). **(B)** Microscopic image of the size fraction 63-200 µm at a magnification of 100-fold to show exemplarily the classification of the particle shape. Numbers in parenthesis represent the size of the particles in µm measured by the lengths of the red lines.

5.2.2 Spatial distribution of microplastics

The microplastic concentrations of the sediments showed substantial differences along the two rivers and the stream investigated (Figure 18). In sediments of the stream Schwarzbach and the river Main the mass fraction as well as the number of microplastics increased downstream of each river. In both cases, the increase of the mass fraction was distinctly stronger (mass: factor ≈5 (Schwarzbach) to 10 (Main), numbers: factor ≈2). Furthermore, sampling sites at the stream Schwarzbach (S1 and S2) showed the lowest mass and number of microplastics of all samples. At site S1 the weight fraction of the smaller size fractions (63-200 µm and 200-630 µm) was close to the limit of quantification, thus the mass fraction of this site could be lower. The number of microplastics at the sites S1 and S2 was similar to the microplastic numbers of less polluted Rhine sediments. The abundance of microplastics in Rhine sediments showed no continuous increase of microplastic particles in the flow direction of the river. Rather the microplastic concentration in the sediments from the site R1 to the site R3 increased strongly. Noteworthy, the sites R2 and R3 are located downstream of the confluence of the river Rhine and the river Main. The microplastic concentration of both rivers is in the same order of magnitude in the vicinity of the confluence with the river Main (sample M2 and R2). In contrast, the microplastic concentration before the confluence of the rivers Rhine and Main (R1) was considerably lower. The highest amount of plastic particles in terms of weight and number was separated from sediment of R3.

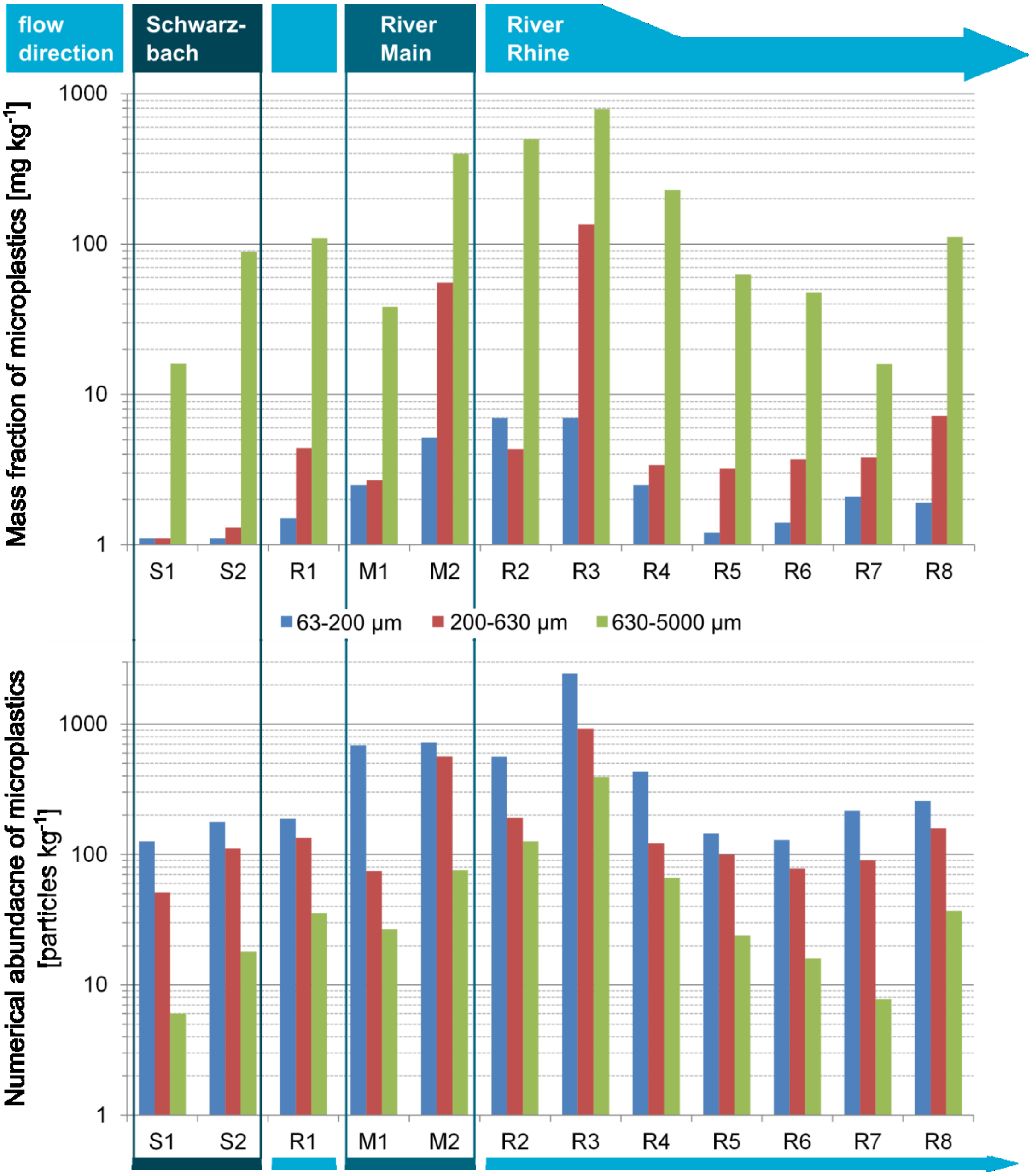

Figure 18: Spatial distribution of microplastics in terms of mass fraction and numerical abundance. Microplastics were separated from sediments of the stream Schwarzbach (S1, S2) the river Main (M1, M2), and the river Rhine (R1-R8), sampled on 3th December 2013. Data is shown for the size fractions 63-200 µm (blue bars), 200-630 µm (red bars), and 630-5000 µm (green bars) in logarithmic scale. The flow direction of the river is displayed by a blue arrow.

Very low mass fractions of plastic particles at the river Rhine were found in sediment samples close to nature reserves at R7 (21.8 mg kg^{-1}). Despite the low mass fractions of this sediment, the number of plastic particles found (R7: 314 particles kg^{-1}) was in the range of Rhine sediment samples, which were collected in less populated areas (R1, R5, R6, and R8). The numbers of plastic particles separated from Main sediments were comparably high and exceeded the average number of microplastics in sediments in the river Rhine. The amount of microplastic particles in the Main sediments differed not as strongly (approximately factor 2) as their highly dissimilar mass fractions (approximately factor 10).

5.2.2.1 Correlation of particle numbers and particle weight

As shown in Figure 16 and Figure 18, the contribution of each size fraction to the particle number or the plastic weight is inversely proportional. Nevertheless, the total particle numbers and the total plastic weight at each location show the same tendencies. To confirm the relationship of particle numbers and particle weight at each sampling site, the weight of all plastic items was plotted against the number of all plastic items. A good linear correlation (R^2: 0.85; $P<<0.05$) of the total plastic weight and the total plastic number underlined the same tendencies of weight and number of plastic particles (Figure 19). This result showed that the mass fraction and the numerical abundance can possibly be used interchangeable to describe the microplastic pollution in sediments.

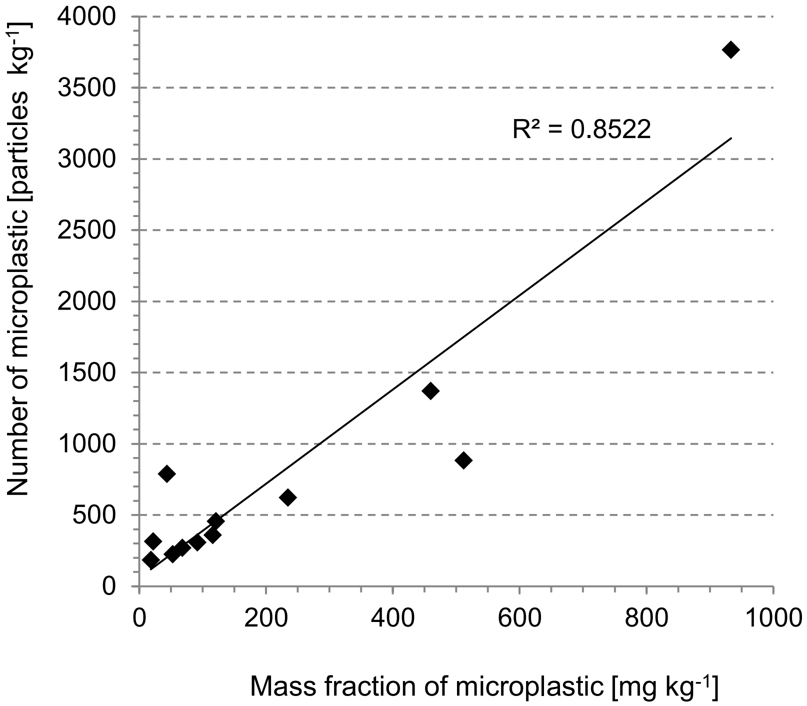

Figure 19: Correlation of total particle number and total particle weight at the sampling sites S1, S2, M1, M2, and R1-R8.

Further, the results implied that it might not be necessary to investigate all size fractions to estimate the microplastic pollution of a sediment sample, as the numerical abundance was mainly dependent on particles of the size fraction 63-200 µm whereas the mass fraction depended on microplastic particles in a size of 630-5000 µm (refer to Figure 16).

5.2.2.2 Correlation of population density and microplastics

A possible indicator for the microplastic pollution of sediments might be represented by the population density of the sampling sites, as the sampling sites comprised highly diverse settled areas. To investigate a possible relationship the population density and the abundance of microplastics at each sampling site, the inhabitants per km² among the sampling sites where correlated with the respective microplastic pollution. The data of the actual population density was obtained from the local registration office. The results did not show any correlation of the amount of inhabitant per km² with neither microplastic weight (R^2: 0.13; P>>0.05) nor the numerical abundance of microplastic particles (R^2: 0.06; P>>0.05).

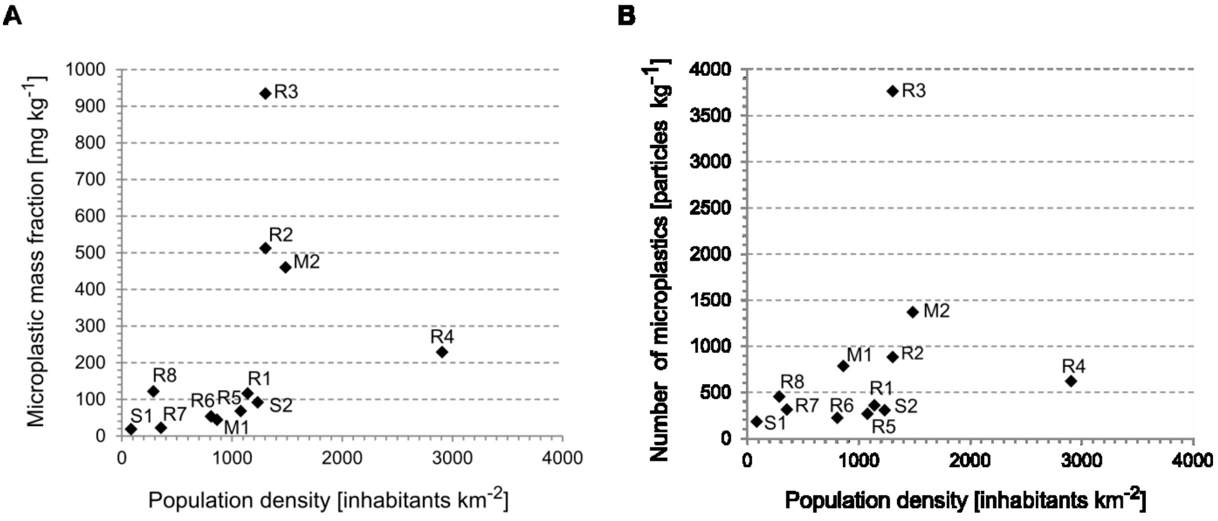

Figure 20: Correlation of population density with mass fraction of microplastics **(A)** and numerical abundance of microplastics **(B)**. Sampling sites are marked in the plots (S1, S2, R1-R8, M1, and M2).

5.2.3 Abundance of polymer types

To investigate a pattern of polymer types present in sediment samples and confirm the particles detected as synthetic polymers, ATR-FTIR analysis of the size fraction 630-5000 µm was performed.

The results of these measurements showed that almost 75% of the total plastic weight was contributed by PE and PP (Figure 21). PE posed in average 49% and PP in average 24% of the total plastic weight. The highest numerical abundance of polymer particles was represented by PS (mean: 54%). Almost all spherules found in size fraction 630-5000 µm consisted of PS, mainly in the form of EPS. This explains the great discrepancy between the high numerical abundance and the low weight abundance of PS particles. The polymers PE, PP, and PS together made up over 80% of all plastic particles in terms of weight and size identified in the sediments. The remaining proportion of plastics consisted of various types of plastics. In addition to the above-mentioned polymers, PET, PVC, ethylene vinyl acetate (EVA), ethylene propylene diene rubber (EPDM), PA, and acrylic-based polymers were identified.

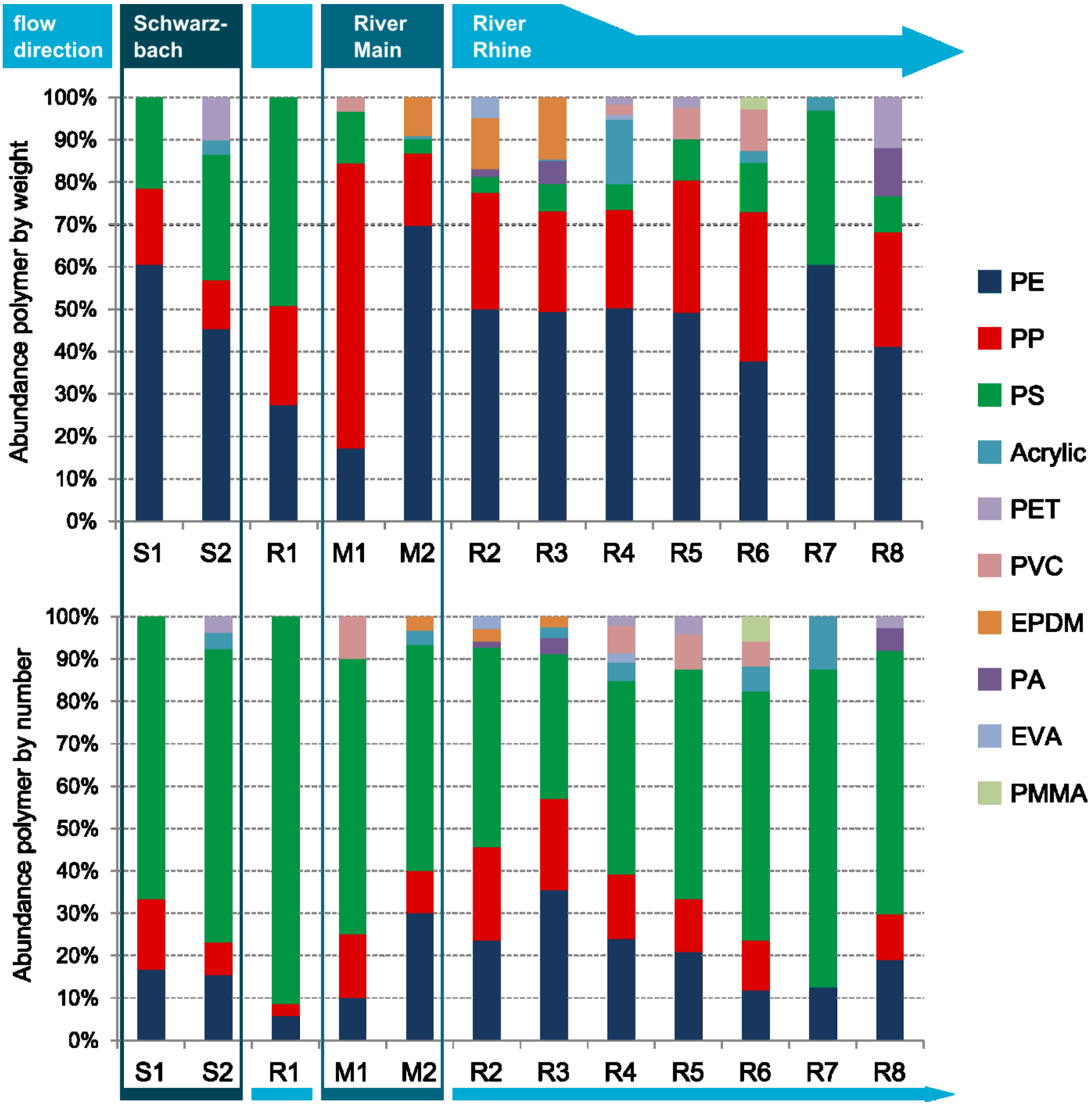

Figure 21: Relative abundance of each polymer type in terms of weight and numbers at the sampling sites from the stream Schwarzbach (S1, S2), the river Main (M1, M2), and river Rhine (R1-R8). The flow direction of the the river is shown by the blue arrow.

The compositions of the plastic particles identified at the single sampling sites showed several interesting patterns. PE and PS particles were found at all sites. From site R7, no PP particles could be detected. This could be related to the general low pollution with plastics of this site. Furthermore, the relative abundance of PE particles by weight is almost constant at the sites from R2 to R8 (mean: 49.5%; SD: 6.39%). In contrast, the composition of the polymer types by particle numbers changes strongly from sampling sites R2 to R8. The relative numerical abundance of PE and PP particles is proportional to the total plastic pollution of the respective sites. The abundance of PE exceeds the abundance of PP particles in terms of weight and numbers at all sites, except site M1 where the mass abundance of PP particles exceeded the abundance of PE. Noteworthy, the low mass fraction of site M2 might be a reason of the high relative abundance of PP particles.

Further, a change in the polymer pattern was observed at sampling sites downstream the confluence of the river Rhine and the river Main. On the one hand, the variety of different polymer types strongly increases. Additionally, PE and PP show an increasing tendency in particle numbers and weight in the sites R2 and R3, compared to R1.

The polymer composition of sites from the stream Schwarzbach was comparable to less polluted sites of the river Rhine (R5-R8) or, in terms of numerical abundance, to the river Main.

Additionally the ATR-FTIR analysis confirmed the presence of optical and chemical identical pellets in the river Rhine and in the Main mouth (Figure 22).

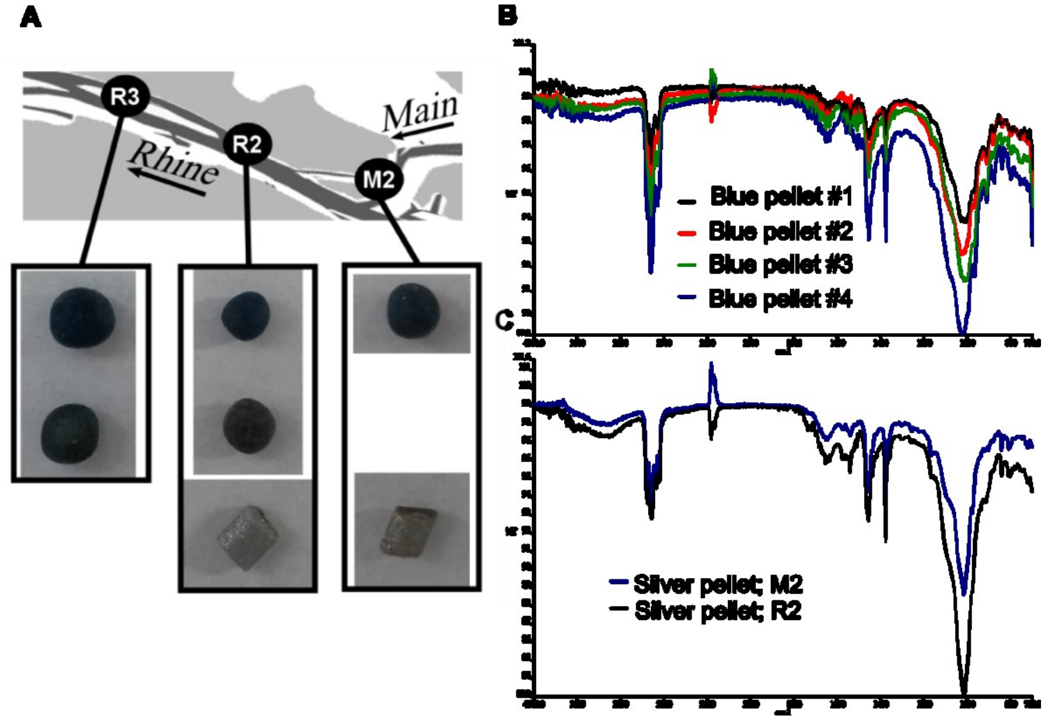

Figure 22: Identification of optical identical polymer pellets at sampling sites M2, R2, and R3 **(A)** as EPDM **(B)** and PP **(C)** by ATR-FTIR spectroscopy

These pellets where present at the consecutive sampling sites M2, R2, and R3. At M2 and R2 silver colored pellets were determined, which were both identified as PP. Moreover, blue EPDM pellets showed the same rubber-like consistency, resulting in reversible deformation under gentle pressure. The consecutive recovery of these pellets might indicate a transport from the river Main as both polymers where present in sediment of M2.

5.3 Annual variation of the microplastic concentration at site R4

During this study, sediment from site R4 was sampled in a period of two years. Samples in a distance of five to nine months resulted in concentrations between 200 and 390 mg kg^{-1} of microplastic particles during the monitored period (Figure 23). For all sampled dates, the results are comparable within the measurement error, and an one-way ANOVA showed no significant difference at a 5% significance level between the average microplastic concentrations of each sample date (F=2.45, p=0.138). Noteworthy, the data from 06/03/2013 is received from the initial sample preparation method. For a better comparability, only the mass fraction of larger microplastic particles (630-5000 µm) was analyzed for the samples of 15/09/2014 and 23/02/2015. As it was shown previously (5.2.2.1.), the mass fraction mainly depended on the size fraction 630-5000 µm and seems to be a sufficient indicator for the plastic pollution of a sampling site. The water level of the river Rhine was taken into account on all sampling dates to accomplish the sampling at a comparable height of the shore line.

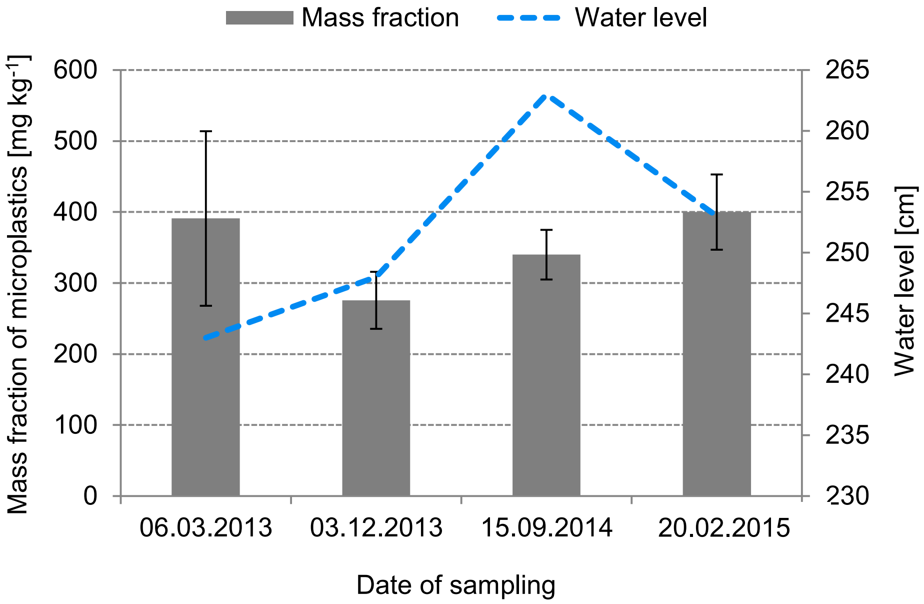

Figure 23: Mass fraction of microplastics separated from sediments of site R4 over a time period of approximately 2 years (grey bars, n=3). The water level of the river Rhine is shown by the blue dotted line (note that it does not represent the exact course of the the water level).

Due to this fact only small differences in the water level (243-263 cm) of the river Rhine are visible in Figure 23, and a relationship of the water level and the microplastic concentration was not monitored.

5.4 Sorption of contaminants to polymer particles in freshwater systems

Synthetic polymers, such as PE, are often used as passive sampler for the determination of organic contaminants in freshwater systems, because of their high sorption capacity. Furthermore synthetic polymers are one of the most significant pollutants in rivers, as shown in the previous section. For this reason, it could be expected that microplastic particles act like passive samplers and organic contaminants enrich on the polymer surface compared to the surrounding freshwater, like it was shown for the marine aquatic system.[149]

For a better understanding of the importance of sorption to synthetic polymers, batch sorption experiments were carried out in laboratory scale. The experiments were performed with different kinds of polymers to monitor additional effects such as polar dipol-dipol interactions as well as sorption to glass state polymers.

5.4.1 Determination of sorption kinetics of different organic contaminants to PE, PC, PMMA, PS, EPS, and PVC

Sorption kinetics were determined for the model substances CBZ, β-HCH, γ-HCH, EE2, chlorpyrifos, and DDT sorbed to the synthetic polymers PE, PC, PMMA, PS, EPS, and PVC. All investigated substances showed sorption to the polymers, and the concentration for the contaminants accumulated on or in the polymer particles. As expected, the concentrations of the sorbed contaminant generally increased with increasing K_{OW} of the contaminants.

To study sorption kinetics, the decrease of an initial aqueous concentration of contaminant was measured over time. Thus, the amount of contaminant sorbed to polymer was measured indirectly.

5.4.1.1 Carbamazepine

The batch sorption experiments of CBZ showed a low sorption to all tested polymers (Figure 24), and no sorption was determined in samples without polymer (Figure 41). The CBZ concentration decreased by approximately 10% compared to the initial concentration in samples containing PE and PMMA. The batch containing PE showed a continuous reduction of the CBZ concentration, nevertheless it did not reach equilibrium during the period of 30 days. For all tested glassy state polymers except PMMA the concentration CBZ decreased by up to 5% compared to the initial CBZ concentration. All polymers in the glassy state seem to reach equilibrium 5-12 days after the start of the experiment, depending on the polymer. Low sorption was observed for samples containing PC, PS, EPS, and PVC. Here the concentration of several samples did not significantly differ from the concentration of the control sample or the initial concentration. Albeit the samples of PC, PS, EPS, and PVC show comparable sorption after 30 days, the equilibrium is reached distinctly faster with PC and PVC particles (PC: 7 days; PS: 15 days; EPS: 12 days; PVC: 7 days). Due to the low sorption of CBZ, the deviation between the single replicates occurs to be relatively high. For this reason the sorption determined by the indirect measurement of the supernatant needs to be verified by the extraction of the polymers.

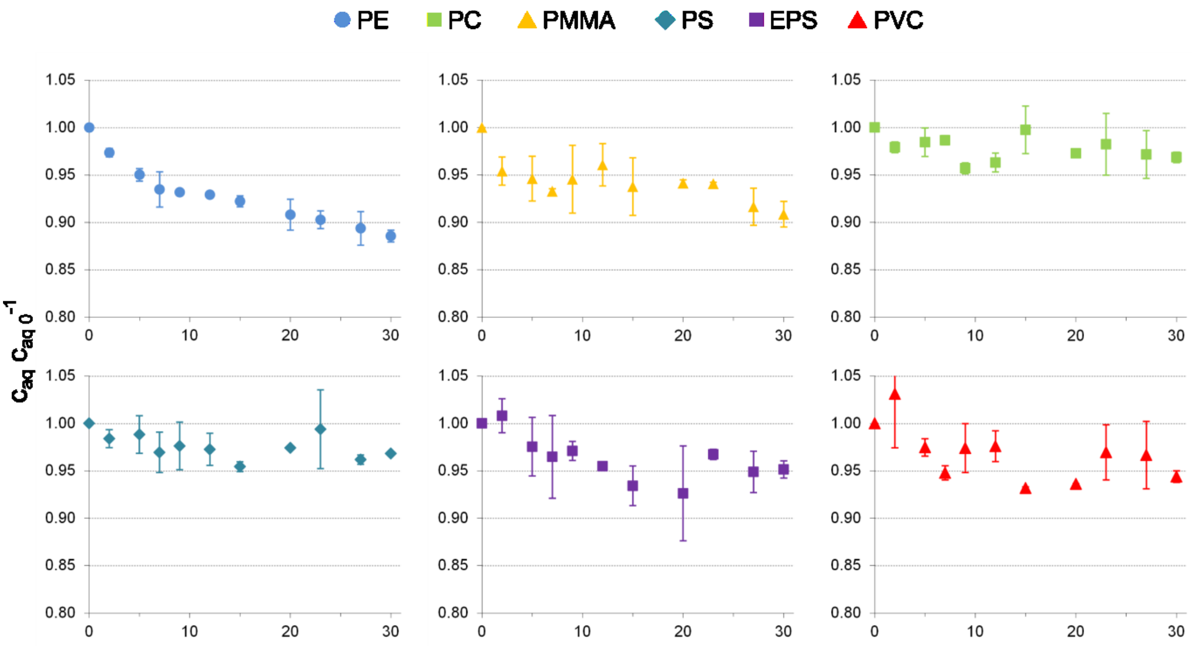

Figure 24: Sorption of CBZ to the polymers PE, PC, PMMA, PS, EPS, and PVC depending on time. The experiments were carried out in duplicates over 30 days. The decrease of CBZ is shown relatively to the initial concentration of CBZ.

5.4.1.2 β-HCH and γ-HCH

The sorption batch experiments of both HCH species showed very different results. The β-HCH concentration decreased significantly in the control batch without polymer after two days, whereas the concentration of γ-HCH in the control sample remained unchanged over the entire testing period of 30 days.

After two days the concentration of β-HCH dropped to approximately 20% of the initial concentration and then stayed constant until the end of the experiment (Figure 25). Samples containing PE particles showed the same decrease as the control sample after two days, but the concentration of β-HCH in the supernatant constantly decreased further to 10% of the initial concentration until the end of the experiment. Samples containing particles of glassy state polymers (PC, PMMA, EPS, PS, and PVC) showed a slower decrease of the β-HCH concentration after two days compared to samples containing PE particles. Furthermore the concentration of β-HCH in the supernatant increased again after an initial decrease in samples with PC and PMMA from day two to day five. Until 7 to 15 days the concentration of β-HCH in samples PC, PMMA, PS, EPS, and PVC dropped slightly below the concentration of the control sample. The concentration in the sample with glassy-state polymers seemed to reach equilibrium after 23-27 days.

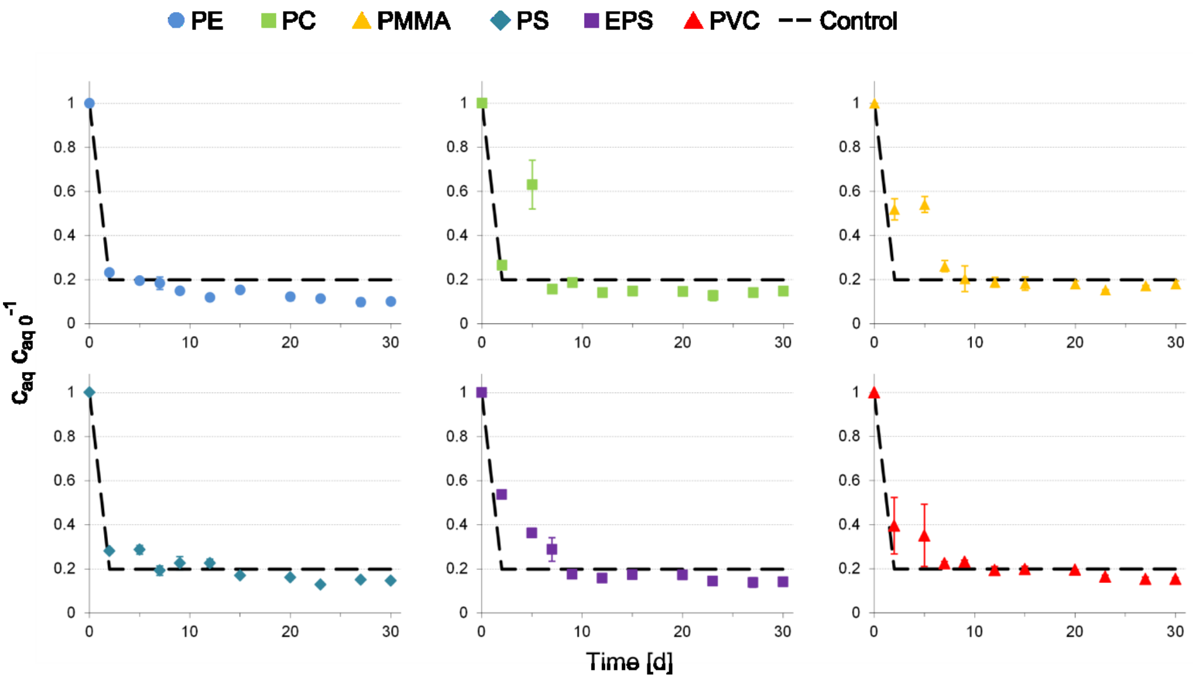

Figure 25: Sorption of β-HCH to the polymers PE, PC, PMMA, PS, EPS, and PVC in dependence on time. The experiments were carried out in duplicates over 30 days. The decrease of β-HCH is shown relatively to the initial concentration of β-HCH. Average concentration of the control sample after two days is shown as dashed line.

To investigate the effect of the slow sorption of β-HCH to glass state polymers, the experiment was repeated for PC, PMMA, PS, and PVC. For a better visualization of the effect of increasing β-HCH concentration in the supernatant the solution was allowed to equilibrate in the glass vials for 27 days without polymer (Figure 26). As shown in previous experiment, the concentration of β-HCH decreased to a level of 27-42% of the initial concentration. However, the concentration of β-HCH in the supernatant increased by subsequent addition of polymer particles within three days to a maximum of 65% of c_0 for PMMA particles. The lowest increase of β-HCH was measured in samples after the addition of PVC particles. The sample without particles did not change significantly in concentration. These results confirm the effect of different sorption kinetics of glass-state polymers that were observed in the previous sorption experiments with β-HCH depicted in Figure 25.

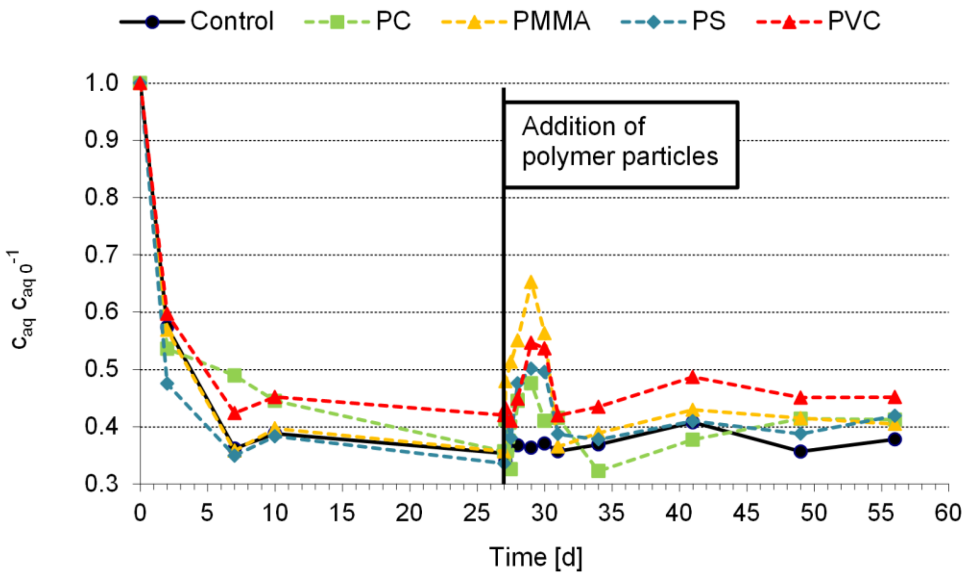

Figure 26: Concentration of β-HCH in the supernatant of five samples without polymer over 27 days. PC, PMMA, PS, or PVC particles, respectively, were added after 27 days to four samples.

In contrast to the sorption experiments with β-HCH, the concentration of γ-HCH stayed constant in the control sample at approximate 100% of the initial concentration (Figure 41). Samples containing polymers showed sorption to the polymer particles by the decreasing concentration of γ-HCH in the supernatant (Figure 27). Sorption of γ-HCH to PE particles did possibly not reach equilibrium during the period of 30 days, as visible by the continuously decreasing γ-HCH concentration, although the sorption rate decreased with proceeding time. Polymers in the glassy state reached equilibrium after approximately 5-15 days. The initial sorption rate of γ-HCH to PC was comparable to the sorption rate to PE. Lowest sorption of γ-HCH was observed for samples containing PS and EPS (sorption of PS: 15% of c_0; sorption of EPS: 11% of c_0). These samples reached equilibrium distinctly faster than samples with other polymers (within 5-7 days).

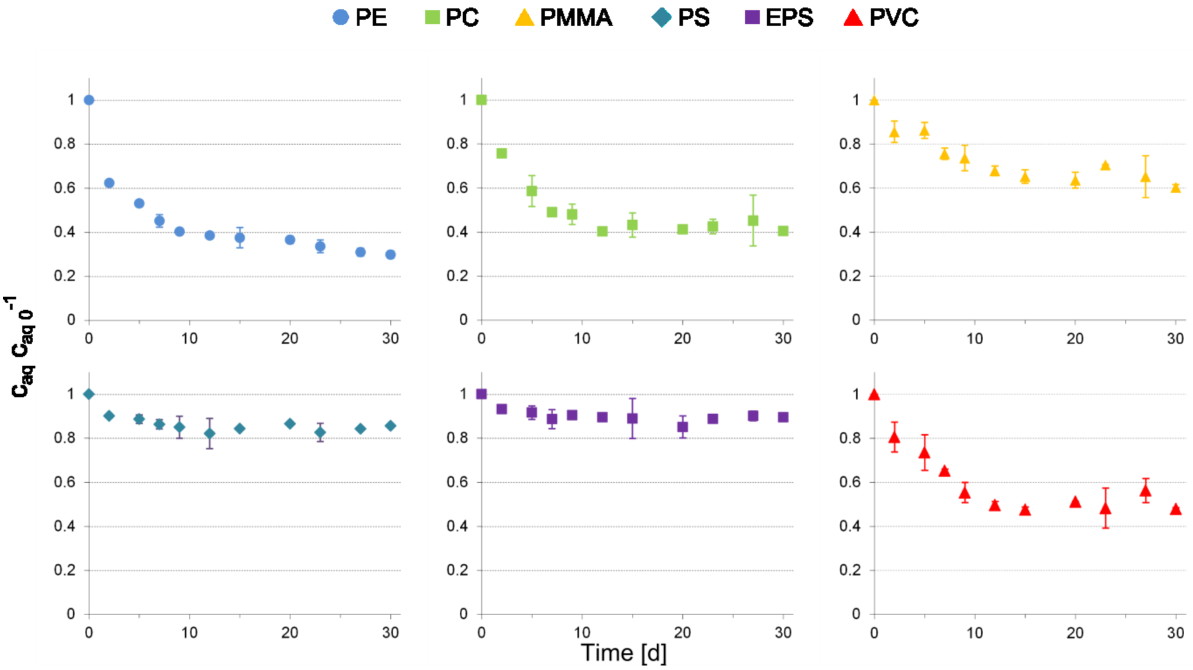

Figure 27: Sorption of γ-HCH to the polymers PE, PC, PMMA, PS, EPS, and PVC in dependence on time. The experiments were carried out in duplicates over 30 days. The decrease of γ-HCH is shown relatively to the initial concentration of γ-HCH.

5.4.1.3 Ethinylestradiol

EE2 showed sorption from synthetic freshwater to all polymers which were tested in this experiment (Figure 28). No sorption was detected in control samples (Figure 41). As shown for CBZ and HCH, samples containing PE particles did not reach equilibrium within 30 days, as EE2 concentration was constantly decreasing during the entire time interval of this experiment. Polymers in the glass state reached equilibrium after approximately 7 (PS and PVC), 12 (PC and PVC) and 15 (PMMA) days, respectively. It should be noted that EE2 measurements of the single replicates showed higher deviations, compared to other organic contaminants. Thus, the exact trend of EE2 sorption to the polymers remained uncertain. Comparable tendencies in terms of sorption kinetics are observed for the polymers PS and PVC, as well as for the polymers PC, PMMA, and EPS. PS and PVC reached equilibrium most rapidly and while showing the lowest sorption of EE2 (PS: 18% of c_0; sorption of EPS: 20% of c_0): The sorption curves of PC, PMMA and EPS show a relatively linear decrease of the EE2 concentration between day 0 and day 10, but EPS differs in the total sorption of EE2 (PC and PMMA: 39% of c_0; EPS: 28% of c_0).

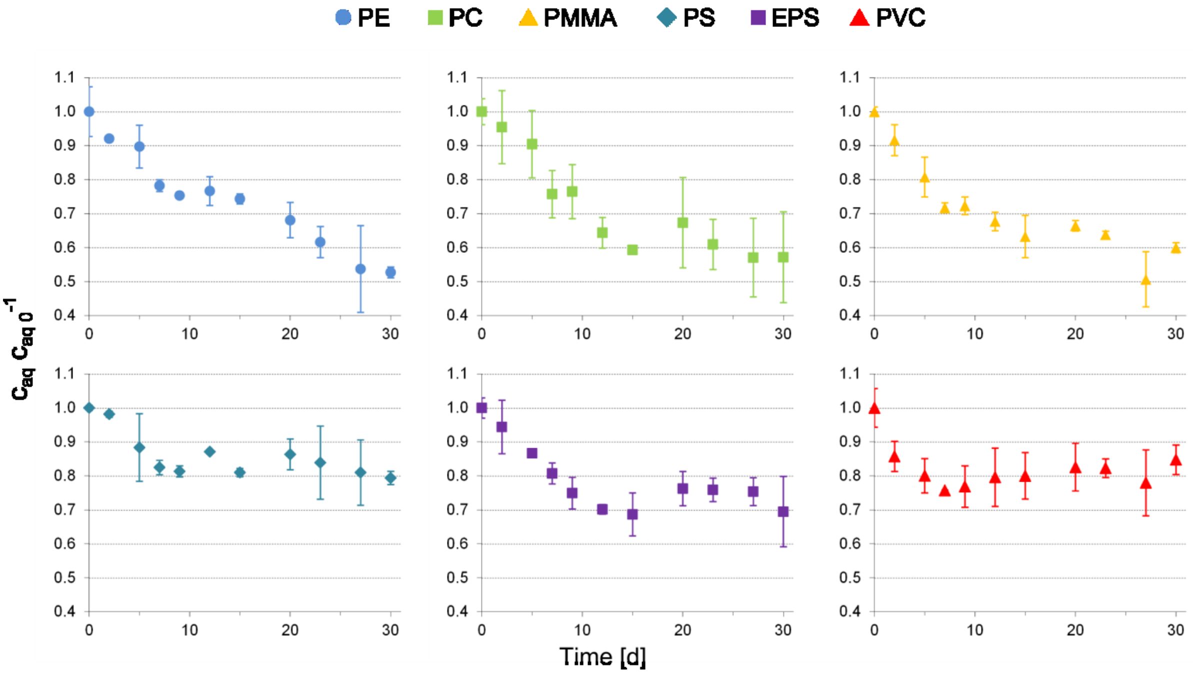

Figure 28: Sorption of EE2 to the polymers PE, PC, PMMA, PS, EPS and PVC in dependence on time. The experiments were carried out in duplicates over 30 days. The decrease of EE2 is shown relatively to the initial concentration of EE2.

5.4.1.4 Chlorpyrifos

Highest level of sorption to all polymers tested was determined for chlorpyrifos (Figure 29). This is likely related to the high K_{OW} of chlorpyrifos (log K_{OW}: 4.70-5.11). No sorption was detected in the control sample, despite the high initial concentration of chlorpyrifos (1 mg L^{-1}) and its high K_{OW} value. In contrast to experiments with CBZ, HCH, and EE2, sorption equilibrium was reached for all polymers within twelve days including PE. Due to the high sorption the determined concentration of chlorpyrifos in the sample was close to the limit of quantification of the method used.

The sorption rate of glassy state polymers was comparable to the sorption rate to PE except for PMMA. Nevertheless highest sorption was detected with PE particles (sorption of 92% of c_0). Sorption rate of chlorpyrifos to PMMA seemed distinctly slower between the days five to nine compared to other polymers in the glass state. Further, lowest sorption was detected for PMMA particles (sorption of 29% of c_0).

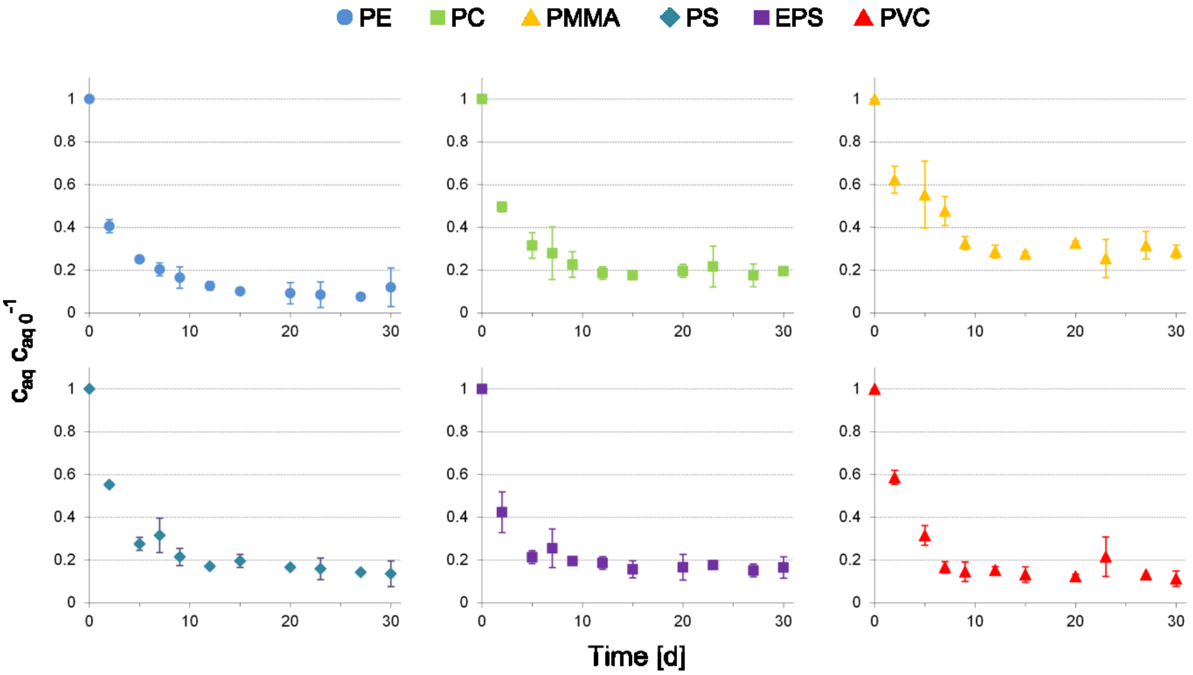

Figure 29: Sorption of chlorpyrifos to the polymers PE, PC, PMMA, PS, EPS, and PVC in dependence on time. The experiments were carried out in duplicates over 30 days. The decrease of chlorpyrifos is shown relatively to the initial concentration of chlorpyrifos.

5.4.1.5 DDT

As DDT was the model substance with the highest K_{OW}, the highest sorption was expected for this substance. However, a high loss of the aqueous concentration of DDT was detected in the control samples, as it was already observed for β-HCH. After two days, the DDT concentration in the control samples dropped to an average of 4.5% of the initial concentration (Figure 30). The concentration of DDT decreased also in samples containing polymer particles, but no significant difference between the control sample and the polymers were determined. Following the indirect sorption determination method, no accurate sorption to the polymer could be calculated. In contrast to experiments with β-HCH, the sorption rates in samples with glassy state polymers did not differ from the sorption rate of the control sample. To determine sorption kinetics of DDT the experimental setup used is not appropriate. Due to high sorption in the control samples that is probably related to the sorption to the glass surface the exact determination of sorption to the polymer surface was not possible.

To investigate the sorption of DDT to polymer particles the polymer particles themselves had to be analyzed (refer to 5.4.3).

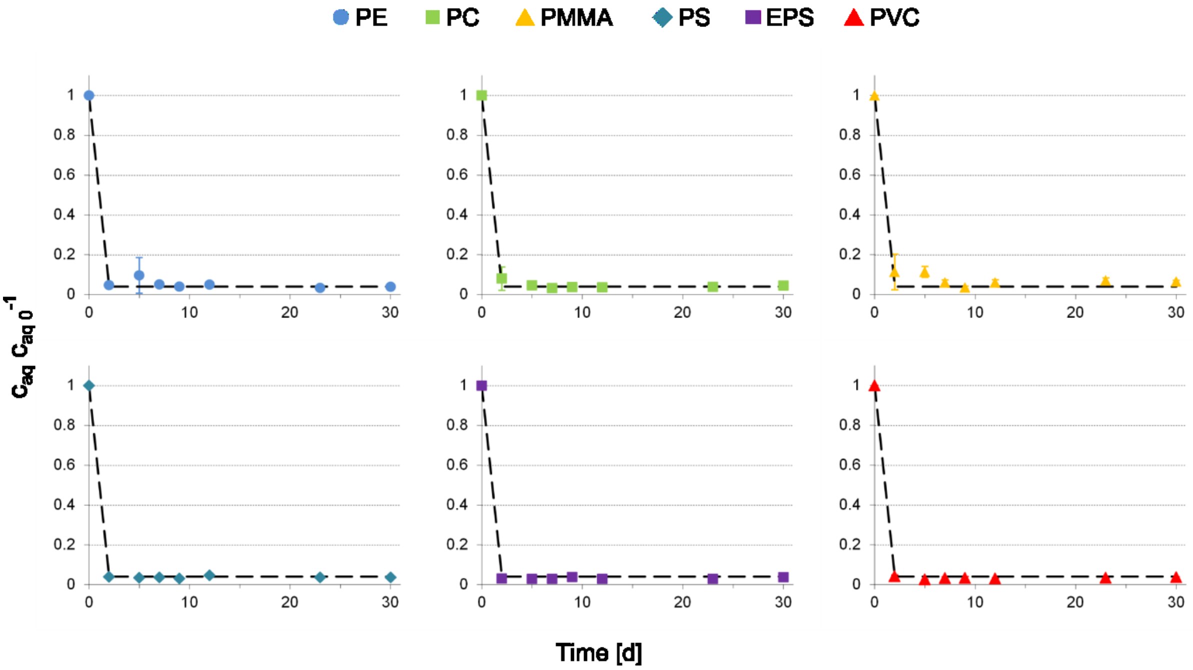

Figure 30: Decrease of DDT concentration in samples containing the polymers PE, PC, PMMA, PS, EPS, and PVC in dependence on time. The experiments were carried out in duplicates over 30 days. The decrease of DDT is shown relatively to the initial concentration of DDT. Average concentration of the control sample after two days is shown as dashed line.

5.4.2 Modelling sorption kinetics for CBZ, γ-HCH, EE2, and Chlorpyrifos

A pseudo-first-order rate law was applied to describe the contaminant sorption to polymers in the glass state. The model was only applied to contaminants of the sorption kinetic experiments that did not show sorption in the control samples.

The parameter calculated for the sorption models are shown in Table 6. Curve fits and the corresponding data are provided in the appendix (Figure 42-Figure 44). The rate constants that were determined for ranged from 0.004-0.029 h^{-1}. The rate constants of each polymer for the different contaminants were only comparable for the polymers PMMA and PS. The polymers PC, EPS, and PVC showed slightly different rate constants for each contaminant, possibly indicating a dependency of the sorption kinetic on the polymer used and contaminant that sorbs to the polymer. In average, the highest rate constants were determined for chlorpyrifos and the lowest for EE2. As already shown in the high decrease of the solute concentration highest sorption (q_{eq}) was calculated for chlorpyrifos. Sorption of γ-HCH and EE2 was comparable in terms of the respective initial concentration. It might be possible, that by increasing the EE2 concentration the sorption to polymer particles (q_{eq}) could increase and exceed the sorption of γ-HCH, as it would be expected based on the respective K_{OW} values. Equilibrium concentrations and rate constants for CBZ showed relatively high errors and low coefficients of variation. Low sorption of CBZ to the glass state polymer particles resulted in higher measurement errors of the aqueous concentrations (Figure 24), which were consequently transferred to the polymer loading. For this reason rate constants and equilibrium concentrations might only show tendencies. This can also be deduced from the high errors of the rate constants (58-134%).

Table 6: Parameters of a first order rate law for the sorbates CBZ, γ-HCH, EE2, and chlorpyrifos and sorbents PC, PMMA, PS , EPS, and PVC. q_{eq} is the equilibrium concetration in the polymer particle in ng mg^{-1}, k is the rate constant in h^{-1}, and $t_{1/2}$ is the half-life period in h. Errors of the parameters are shown in parantheses.

Sorbate	**Model parameter**			**Sorbent**		
		PC	**PMMA**	**PS**	**EPS**	**PVC**
CBZ	q_{eq}	0.245	0.630	0.290	0.563	0.512
		(0.043)	(0.046)	(0.049)	(0.106)	(0.162)
	k	0.025	0.024	0.011	0.005	0.005
		(0.034)	(0.014)	(0.009)	(0.003)	(0.005)
	$t_{1/2}$	28	28	63	136	138
	R^2	0.289	0.708	0.434	0.710	0.512
γ-HCH	q_{eq}	582.3	366.4	155.4	112.0	509.6
		(8.767)	(22.29)	(6.179)	(6.050)	(20.58)
	k	0.011	0.006	0.016	0.016	0.008
		(0.001)	(0.001)	(0.004)	(0.005)	(0.001)
	$t_{1/2}$	61	113	44	45	86
	R^2	0.990	0.922	0.911	0.850	0.950
EE2	q_{eq}	11.86	10.60	4.502	7.021	5.014
		(1.086)	(0.703)	(0.382)	(0.490)	(0.243)
	k	0.004	0.005	0.009	0.008	0.029
		(0.001)	(0.001)	(0.003)	(0.002)	(0.012)
	$t_{1/2}$	188	134	77	92	24
	R^2	(0.947)	0.935	0.818	0.887	0.843
Chlorpyrifos	q_{eq}	800.4	712.6	833.3	822.7	864.9
		(9.600)	(23.40)	(14.26)	(9.136)	(14.32)
	k	0.018	0.011	0.014	0.024	0.014
		(0.001)	(0.002)	(0.001)	(0.002)	(0.001)
	$t_{1/2}$	38	66	49	28	48
	R^2	0.991	0.953	0.984	0.991	0.985

5.4.3 Extraction of polymer particles

The concentration of contaminants sorbed to the polymer particles after the time interval of 30 days was calculated indirectly by the difference of the initial concentration and the aqueous concentration of the contaminant at equilibrium. To verify the correctness of the indirect sorption determination and to measure sorption of contaminants with loss in the control samples (β-HCH and DDT) an extraction of the polymers was carried out.

A new method was developed to ensure complete extraction of the polymers by dissolution in THF. This process excludes PE samples, as PE cannot be dissolved in THF. Obtaining a clean extract was a main goal for a robust and repeatable method to reach low limits of quantification for the single contaminants. Main matrix issues of the samples were expected by the polymers. Furthermore, the polymer matrix could possibly cause a re-sorption after evaporation of THF and solvent change that is necessary for LC-MS/MS analysis of CBZ and EE2.

GPC is routinely used for the characterization of polymers for the determination of their molecular weight. Furthermore, GPC is applied for the separation of substances by their molecular weight as sample clean-up in bioanalysis and food analysis. Based on this, the sample clean-up was carried out via GPC separations of the polymers and the contaminants. The application of GPC showed excellent separation of the contaminants from polymers used for the kinetic studies. The combination of GPC clean-up with following GC/MS or LC-MS/MS analysis yielded very good recoveries (93-101%) for all of the contaminants except DDT (52%). Recovery of DDT was improved by an internal calibration to 89%. All model contaminants were analyzed with very good repeatability resulting in low relative standard deviations of 5.7-6.4% for all substances.

The extraction of the polymer particles previously analyzed in the kinetic sorption experiments showed interesting tendencies (Figure 31). For all samples without loss in the control samples, the sorption to the polymers followed the same trend. Sorption of CBZ, γ-HCH, EE2, and chlorpyrifos showed very low deviation between the indirect determination of the sorption (measurement of the supernatant) and the direct sorption determination (extraction of the polymers). For these contaminants the results of the direct method were generally slightly lower. During the filtration of the polymers, which was carried out to separate them from synthetic freshwater of the sorption experiments, filter residues were rinsed with ultrapure water to remove adherent freshwater which contained dissolved contaminant. However, it is possible that contaminant which was sorbed to the polymer surface could also be removed during the rinsing step.

Samples of β-HCH and DDT showed tremendous differences between the indirect and the direct determination of the sorption after 30 days. For the sorption of β-HCH measurements of the supernatant showed concordant trends to the results of the polymers extraction but the concentration of β-HCH calculated by the indirect method was distinctly smaller. The concentrations determined by both methods differed between 170% and 270%. Even greater differences were observed for the sorption experiments with DDT. Due to the high loss in the control sample sorption between -0.06 and 0.02 ng mg^{-1} was calculated based on the measurement of the supernatant Extraction of the polymers revealed extremely higher sorption of DDT to the polymer particles. Over 1000 times higher concentrations of DDT were measured in the polymer particles after extraction (0.17-0.70 ng mg^{-1}).

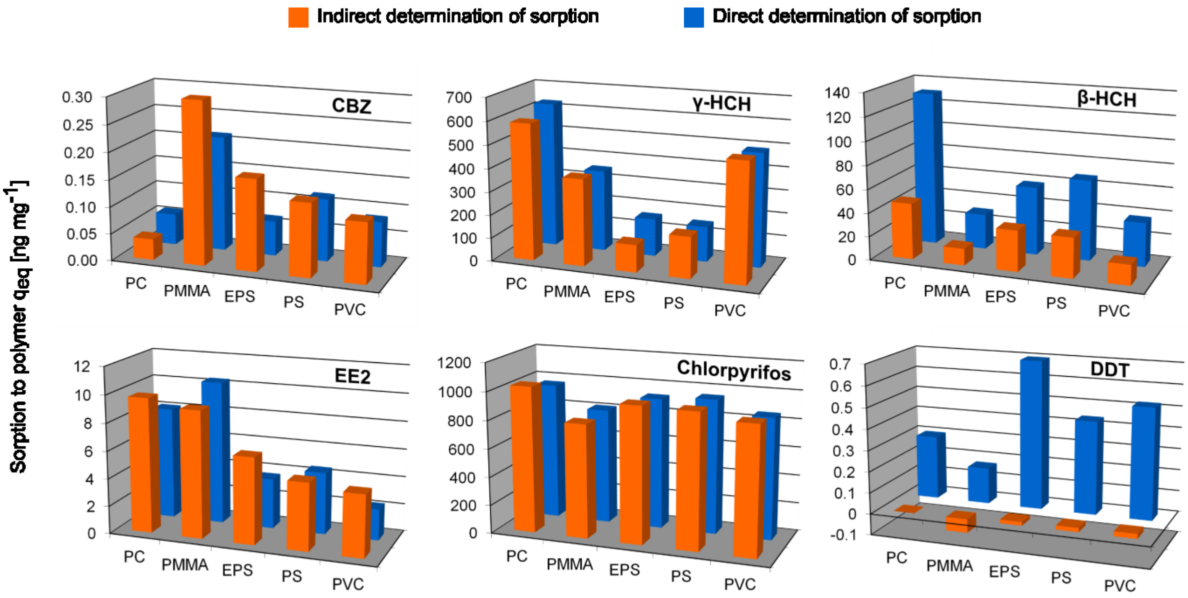

Figure 31: Concentration of the organic contaminants CBZ, HCH, HCH, EE2, chlorpyrifos, and DDT sorbed to the polymers PC, PMMA, EPS, PS, and PVC in 30 days. The amount of sorbed contaminant was determined by measurement of the supernatant (indirect method; orange bars) and by extraction of the polymer particles (direct method; blue bars).

For a better direct comparison of the sorption in dependence on the polymer, sorption of each substance was normalized to the maximum amount sorbed to a polymer (Figure 32). These data display should help to identify the influence of the sorbent on the contaminant sorption in terms of functional groups without the overlapping effect of absolute higher sorption due to higher partitioning coefficients.

The synthetic polymers differed in glass transition temperature and their structure. To address the structural differences, the polymers can be characterized by ratios of the elements C, H, and O. Polymer particles with higher O/C ratios (PC and PMMA) showed different sorption behavior than particles without ester groups. PC showed increased sorption efficiency for nonpolar substances with smaller size. Thus, both tested HCH species were detected with highest concentration in PC particles. However, sorption efficiency of PC seemed to decrease for substances with polar groups, such as amino groups (CBZ) or hydroxyl groups (EE2). In contrast PMMA showed the highest sorption efficiency for exactly these compounds (CBZ and EE2).

Substances with higher C/H ratios (PS or EPS) or without polar moieties (PVC) on the other hand showed better sorption efficiency of larger molecules with high K_{OW} values, as visible in the increasing sorption efficiency of chlorpyrifos and DDT. Noteworthy, all polymers showed relatively high sorption efficiency with chlorpyrifos.

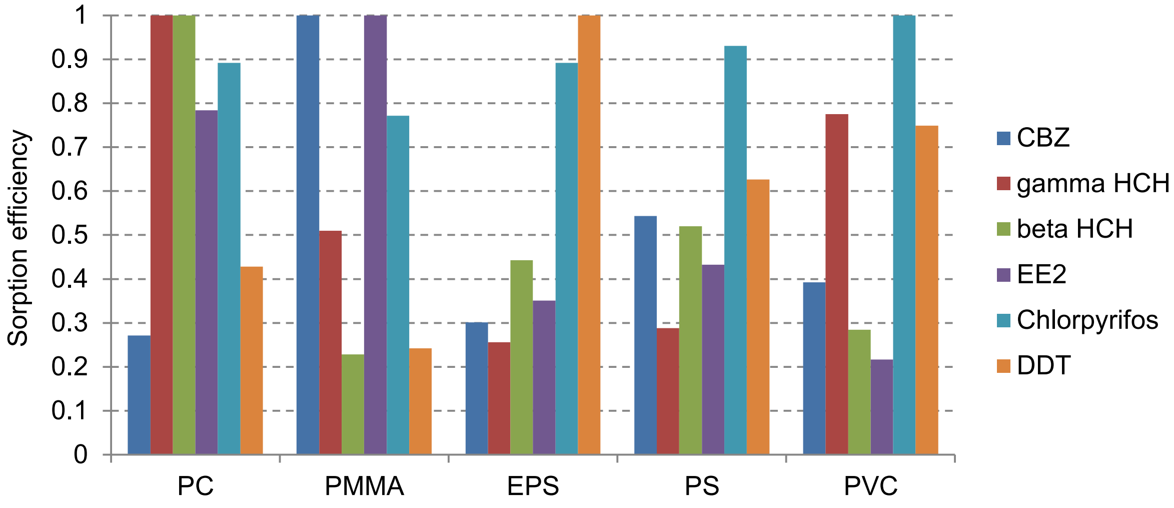

Figure 32: Sorption efficiency PC, PMMA, EPS, PS, and PVC in dependence to the contaminants CBZ, γ-HCH, β-HCH, EE2, chlorpyrifos, and DDT. Data is normalized to highest sorption of each contaminant. Contaminants are listed in order of increasing K_{OW}.

5.4.4 Sorption isotherms

Sorption isotherms of CBZ, γ-HCH, and chlorpyrifos were modeled for the polymers PC, PMMA, PS, and PVC. The kinetic experiments showed that these synthetic polymers reached equilibrium, or so-called “steady state”, within a time interval of 30 days. Further, the kinetic experiments revealed that the chosen contaminants showed measurable sorption at low concentrations for compounds with low K_{OW} values (CBZ) and further, substances with high K_{OW} values showed no sorption to glass surfaces (chlorpyrifos). No sorption isotherms were calculated for β-HCH and DTT due to the loss in the control samples and for EE2 due to high deviation between the single replicates of the kinetic sorption experiments.

The experimental data and the sorption isotherms calculated by different models for each of the four sorbents and three sorbates are shown in Figure 33.

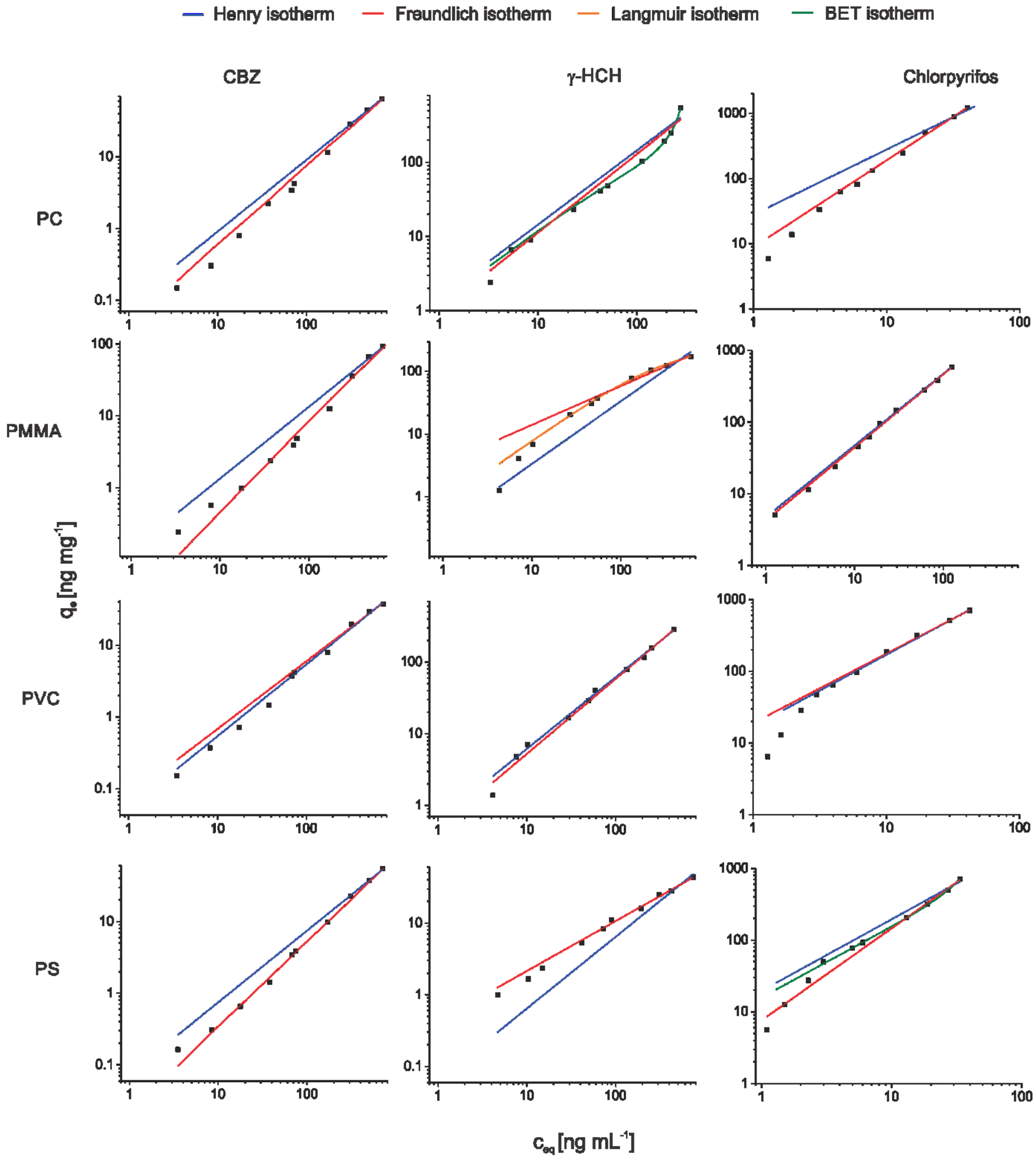

Figure 33: Sorption isotherms of CBZ, γ-HCH, and chlorpyrifos for the synthetic polymers PC, PMMA, PVC, and PS. Symbols represent experimental data and lines represent the best fit for the Henry model (blue), Freundlich model (red), Langmuir model (orange), and BET model (green). Only curves of models with reasonable fits are shown. Data are shown in double logarithmic scale.

All sorption isotherms were modeled using a linear partition model by Henry and the Freundlich model.

For most of the sorbate/sorbent combinations a good correlation (R^2>0.99) was achieved employing the Freundlich model. Generally, the correlation coefficient was higher by using the Freundlich model in contrast to the linear Henry model. Nevertheless, a relatively good correlation ($R^2>0.97$) was achieved with the linear model for all sorbate/sorbent combinations except for the combinations γ-HCH to PC and γ-HCH to PMMA. Furthermore, curves of the Freundlich fits for the sorbate γ-HCH and the sorbents PC and PMMA, respectively, showed relatively high deviations to the experimental data for low concentration of γ-HCH. This results in correlation coefficients of 0.965 and 0.985 for PC and PMMA, respectively for the Freundlich model fits. Reasons for the lower correlation compared to the other sorption isotherms are related to the high increase of sorbed γ-HCH to PC particles and on the other hand the decrease of γ-HCH sorption to PMMA particles in higher concentrations.

If no model could be applied with a coefficient of correlation of $R^2>0.99$ by either using Henry or Freundlich equations, models of Langmuir and Brunauer, Emmet and Teller (BET) were used to describe the sorption isotherms. The Langmuir model describes monolayer sorption as the Henry and Freundlich models, but with distinct localized sorption sites, resulting in a flattening of the isotherm curve at higher concentrations. BET isotherms are used to describe multilayer sorption of the molecules, resulting in an increase of the slope of the curve for high sorbate concentrations.

The model parameters of the linear Henry model, Freundlich model, Langmuir model, and BET model respectively are summarized in Table 7. As expected the distribution coefficients of the linear sorption model and the Freundlich model are increasing with an increasing K_{OW} of the sorbates. If the Freundlich coefficient is equal to 1, the Freundlich isotherm is identical to the linear Henry isotherm. However, a comparably low distribution coefficient was determined for the γ-HCH in combination with PS particles. This result is in concordance with the kinetic sorption studies where γ-HCH showed lowest sorption to PS and EPS particles, respectively. The trend of the experimental data of γ-HCH/PC and chlorpyrifos/PS implied multilayer sorption by exponentially increasing sorption at high concentrations, as confirmed by the good correlation to the BET model.

Table 7: Parameter of Henry, Freundlich, BET, and Langmuir model fits for CBZ, γ-HCH, and chlorpyrifos isotherms for PC, PMMA, PS, and PVC. K_D is the distribution coefficient in L g^{-1}, K_F is the Freundlich coefficient in (µg g^{-1})(µg L^{-1})$^{-1/n}$, n^{-1} is the Freundlich exponent, K_L is the Langmuir constant in L mg^{-1}, q_{max} is the maximum monolayer coverage capacity in mg g^{-1}, K_B is the BET sorption coefficient, q_m is the concentration of a monolayer, and C_s the saturation concentration. The quality of the model fit is represented by R². (N=10)

		CBZ				**γ-HCH**				**Chlorpyrifos**			
Sorbent	**Model**	**Parameter (Error)**			**R²**	**Parameter (Error)**			**R²**	**Parameter (Error)**			**R²**
PC	Henry	K_D	0.091	(0.002)	0.992	K_D	1.448	(0.152)	0.859	K_D	27.98	(1.291)	0.969
	Freundlich	K_F	0.046	(0.014)	0.998	K_F	0.0003	(0.001)	0.965	K_F	8.862	(1.329)	0.994
		n^{-1}	1.107	(0.041)		n^{-1}	2.574	(0.058)		n^{-1}	1.335	(0.243)	
	BET	K_B	n/a			K_B	4.442	(0.527)	1.000	K_B	n/a		
		q_m				q_m	95.04	(3.269)		q_m			
		C_S				C_S	333.2	(2.117)		C_S			
PMMA	Henry	K_D	0.134	(0.134)	0.978	K_D	0.331	(0.029)	0.865	K_D	4.703	(0.065)	0.997
	Freundlich	K_F	0.025	(0.011)	0.994	K_F	3.343	(0.792)	0.985	K_F	4.223	(0.439)	0.999
		n^{-1}	1.267	(0.045)		n^{-1}	0.621	(0.105)		n^{-1}	1.021	(0.022)	
	Langmuir	K_L	n/a			K_L	0.003	(0.0002)	0.998	K_L	n/a		
		q_{max}				q_{max}	264.3	(8.931)		q_{max}			
PS	Henry	K_D	0.075	(0.002)	0.994	K_D	0.065	(0.004)	0.934	K_D	19.55	(0.731)	0.980
	Freundlich	K_F	0.031	(0.005)	0.998	K_F	0.431	(0.061)	0.996	K_F	7.567	(1.729)	0.994
		n^{-1}	1.197	(0.020)		n^{-1}	0.697	(0.048)		n^{-1}	1.287	(0.042)	
	BET	K_B	n/a			K_B	n/a			K_B	2.359	(0.425)	0.999
		q_m				q_m				q_m	382.3	(63.57)	
		C_S				C_S				C_S	56.78	(3.837)	
PVC	Henry	K_D	0.054	(0.001)	0.989	K_D	0.616	(0.009)	0.997	K_D	16.98	(0.289)	0.995
	Freundlich	K_F	0.078	(0.029)	0.991	K_F	0.473	(0.085)	0.997	K_F	18.87	(2.102)	0.997
		n^{-1}	0.942	(0.067)		n^{-1}	1.046	(0.029)		n^{-1}	0.970	(0.034)	

5.4.5 Principle components analysis of contaminant sorption to polymer particles

To identify correlations between the polymers PC, PMMA, PS, and PVC and the respective sorption of contaminant, a PCA was carried out using parameters characteristic for the polymers and the K_D values obtained from the sorption isotherms. K_D values seemed to be an appropriate parameter to describe the sorption of the model substances to the polymer particles, although the regression coefficients of Henry model are lower than for other models used. However, the Henry model only results in one parameter describing sorption, what is suitable to perform PCA for possible polymer influences. Polymer parameters used for the PCA were, as already mentioned before, the C/H ratio and O/C ratio to describe the polarity and presence of aromatic groups in the polymer. Additionally, the glass transition temperature (T_g) of the polymers was used. The T_g is mainly affected by structural elements of the polymer and thus is a possible descriptor for sorption capacity of a polymer. A loading plot of Factor (1) and Factor (2) loadings and a scores plot for the principle component scores (1) and (2) is shown in Figure 34.

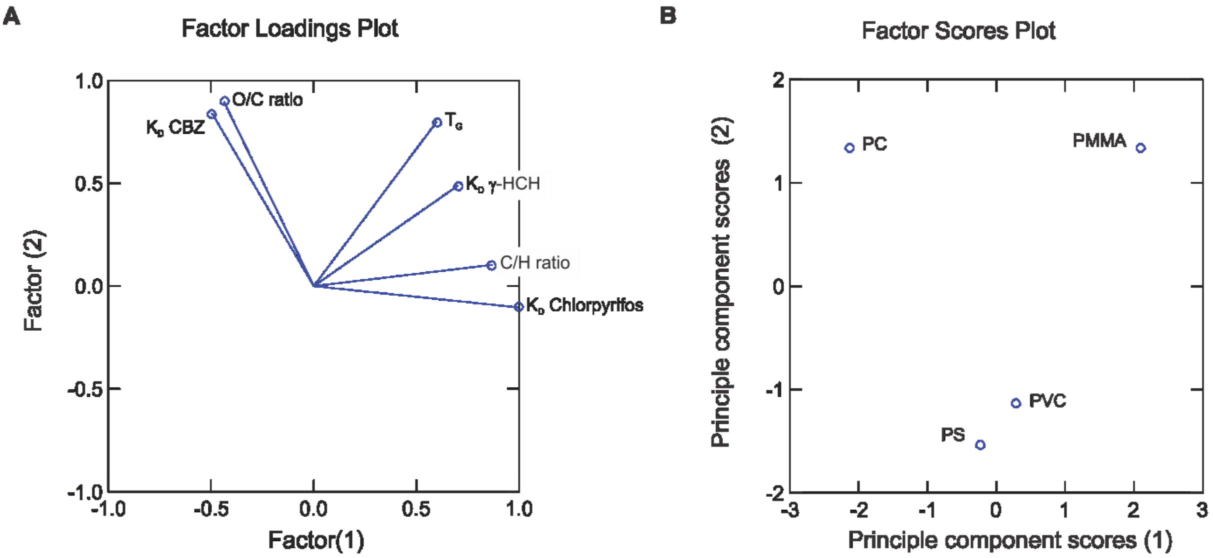

Figure 34: (A) Factor loading plot and **(B)** factor scores plot of the PCA with the K_D values of CBZ, γ-HCH, and chlorpyrifos as well as the polymer parameters T_g and the C/H and O/C ratios, respectively. Polymers used were PC, PMMA, PS and PVC.

The factor loading plot showed different dependencies of sorption on polymer parameters for the contaminants CBZ, γ-HCH, and chlorpyrifos. The sorption was represented by the K_D value of each polymer/solute combination. Factor scores suggested that a possible dependency between the O/C ratio and the K_D value for CBZ exists as both values pointing in the same direction of the plot. The C/H ratio and the K_D value of chlorpyrifos showed a similar direction and similar influences by Factor (1) loadings, whereas both were slightly different for Factor (2) loadings, as Factor (2) loadings differed by their algebraic signs. Nevertheless, C/H ratio seemed to have an influence on the sorption of highly nonpolar substances. For the sorption of small and nonpolar substances represented by γ-HCH neither the O/C ratio nor the C/H ratio of the polymers seemed to strongly affect sorption, as both are pointing in totally different directions. A dependency between the K_D value and the glass transition temperature might be possible.

The factor scores plot showed a grouping of the both polymers without ester bonds (PS and PVC). According to the factor scores plot PC and PMMA differed not in terms of Factor (1) scores, but were highly dissimilar in terms of factor (2) scores. Furthermore, PC and PMMA were separated from PS and PVC by factor (2) scores.

5.5 Extraction of PE and PS particles separated from sediments

The sorption experiments on laboratory scale showed that relevant sorption of substances such as insecticides with medium to high K_{OW} values occurs. To confirm the relevance of sorption of organic contaminants to microplastics in freshwater environments, polymer particles, which were separated from sediments during the investigation of the microplastic pollution in the Rhine-Main area, were extracted. To obtain first results, the extraction was focused on PE and PS particles respectively, as both were present in either high mass or high numerical abundance.

Via mass spectrometric measurements several organic contaminants were identified in the polymers. However, it is not possible to distinguish between contaminants that sorbed to the microplastics and between contaminants, used as additives or produced during the plastic processing.

5.5.1 Screening for contaminants using GC/MS and LC-MS/MS

All extracts of the pellets were analyzed with target analytical approaches using established screening methods first. For this reason, polymer extracts were analyzed using LC-MS/MS and GC/MS with multiple reaction monitoring (MRM) or single ion monitoring (SIM) modes, respectively.

No contaminants could be detected in the extracts using LC-MS/MS, which was used for the determination of polar to slightly non-polar priority pollutants such as pharmaceuticals or pesticides. Thus, no sorption of the model compound CBZ was observed under environmental conditions, neither with PE particles nor with PS particles.

In contrast, several different contaminants were observed after GC/MS analysis (Figure 35). Besides known polymer additives such as tris(2-chloroethyl) phosphate (TCEP) and triphenyl phosphate (TPP), different PAHs, γ-HCH, and chlorpyrifos were detected in some of the pellets. All analyses were only conducted qualitatively as no validated sample preparation methods were used for the extraction of the polymers. However TPP and TCEP were detected at high concentrations above the limit of quantification, yielding signal-to-noise ratios above 10:1.

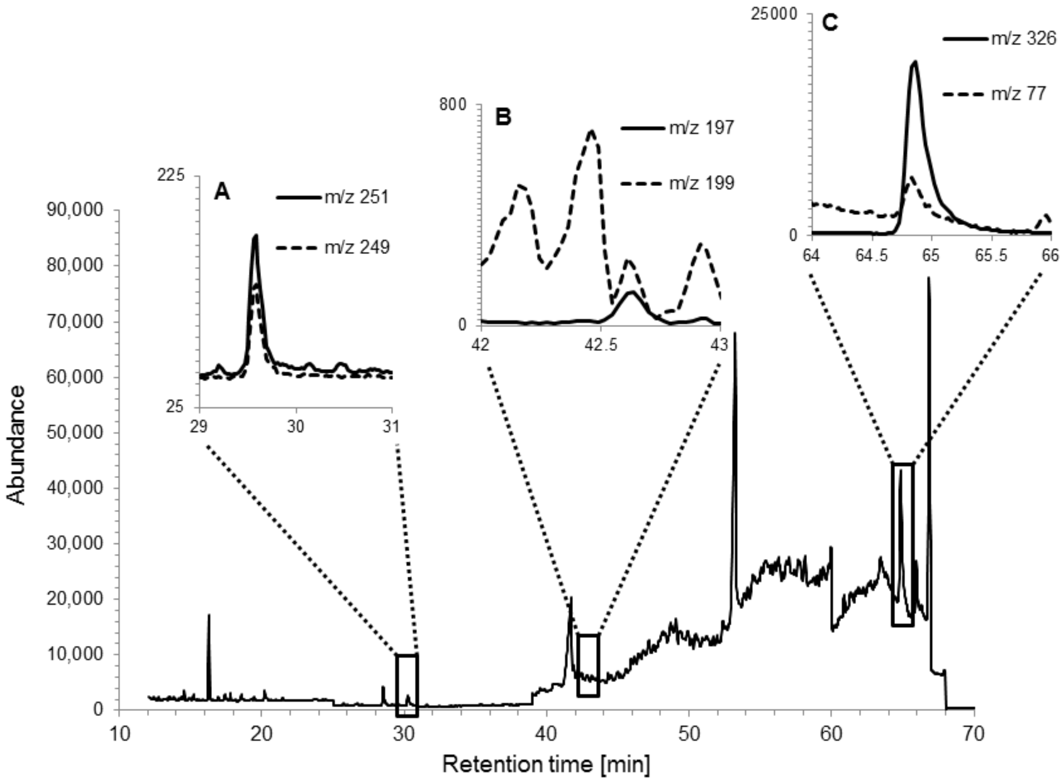

Figure 35: GC/MS total ion chromatogram of PE extract obtained in SIM mode. The details show exemplary extracted ion chromatograms of the detected substances TCEP (A), chlorpyrifos (B), and TPP (C).

5.5.2 Screening for contaminants by GC/MS measurements in Scan mode

To detect and identify substances that were not covered by the described screening methods, all extracts were measured with GC/MS in Scan mode. Mass spectra of the peaks obtained in the resulting chromatograms were compared to database mass spectra. In all chromatograms of PE and PS extracts, high peaks of long-chain carboxylic acids such as stearic acid or palmitic were identified, that are known polymer additives and used as e.g. plasticizers. However, these substances are not considered as emerging pollutants.

Aside these peaks with very large abundance, different phthalates, such as dibutylphthalate (DBP), di-n-pentylphthalate (DnPP), methyl-2-ethylhexylphthalate (M2EHP), or 1-butyl-2-isononylphthalat (B2INP) were identified in PE and PS pellets.

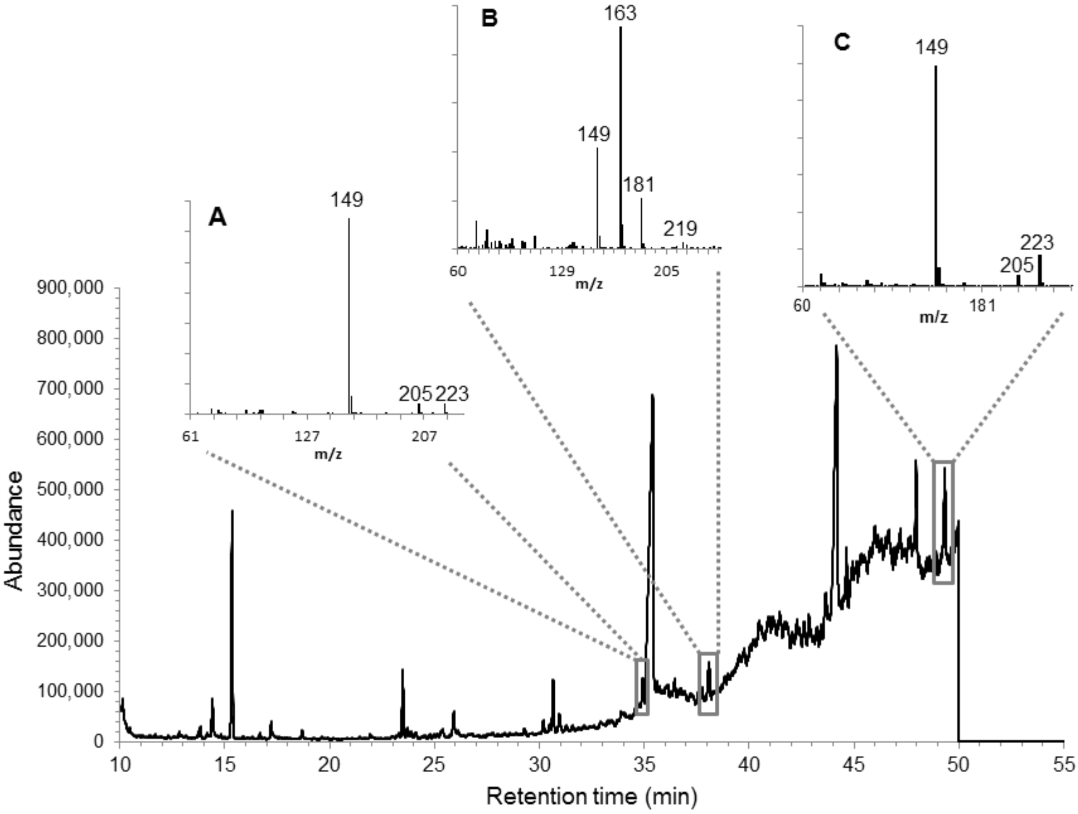

Figure 36: GC/MS total ion chromatogram of PE extract obtained in SCAN mode. Details show exemplary mass spectra of the substances DnPP (A), M2EHP (B), and B2INP (C), which were identified by database comparison with the highest match factors.

To summarize the results of the extraction of PE and PS particles from the river Rhine, Main, and the stream Schwarzbach all substances identified are listed in Table 8. Additionally to the above mentioned substances dinonylphthalate (DNP) and tris(2-chloroisopropyl) phosphate (TCPP) were identified. In all plastic particles different phthalates were identified.

Table 8: Summary of the substances identified in the extracted polymers listed by the origin of their sampling location.

Sampling river	PE	PS
Rhine	chlorpyrifos, phenanthrene, pyrene, TCEP, TPP, DBP, DnPP, M2EHP, B2NIP,	γ-HCH, chlorpyrifos, phenanthrene, pyrene, TCEP, TCPP, DBP, DNP
Main	pyrene, TCEP, DBP, DnPP,	phenanthrene, DBP
Schwarzbach	DBP, DnPP	γ-HCH, phenanthrene, DBP,

PAHs were identified in all PS particles. More substances were identified in polymer particles that originate from the river Rhine. This was likely a reason of the higher portion of plastic material that was available for extraction, as only few particles were separated in the Schwarzbach.

6 Discussion

6.1 Microplastics in freshwater sediments

The results obtained from sampling of river shore sediments revealed the presence of microplastics in inland waters. These results showed high concentrations of plastic particles (mass fraction: 392 mg kg^{-1}; numerical abundance: 57 particles kg^{-1}) in a sediment sampled in a dense populated area in proximity to industrial areas (R4). Approximately 75-90% less plastic particles were determined in sediment in proximity to a nature reserve (R5). These results disclosed problems regarding the microplastic analysis. First, a high deviation (RSD: 22-56%) of the microplastic concentration between single replicates was found, that was very likely caused by an inhomogeneity of the microplastic distribution at the sampling sites. This sampling site inhomogeneity is in concordance with deviations reported in other studies that addressed the microplastic concentrations in sediments.[39, 58, 150]

Second, a low numerical abundance of small plastic particles (< 1 mm) was determined for the shore sediments of the river Rhine compared to other investigations of sediment samples on microplastics.[65] This could possibly be attributed to the sample treatment since especially smaller particles did adhere to glass surfaces and could not be transferred to filters with larger particles. Further, high concentrations of natural debris prevented an accurate identification of small plastic particles.

6.1.1 Method development to improve microplastic separation

To overcome these problems new methodologies were needed to determine reliable results, applicable to particle sizes smaller than 500 µm. The aim was to develop a straightforward, cost-effective method based on a density separation with sodium chloride.

6.1.1.1 Sampling strategy

A great effect was expected by changing the sampling technique to obtain a homogenized sample representing the sampling location. Sampling of sediments usually was limited to small areas (e.g., 0.125 m²). Therefore, it appears to be unlikely to properly describe the average plastic pollution of a sampling site after this preselection.[45] In contrast to the method of zone sampling, very low deviations between the replicates were determined for the randomized sampling of small sediment portions over the complete sampling location during method validation (Table 5). Further, the standard deviation of the microplastic mass fractions at the sampling site R4 monitored over two years (Figure 23) decreased after March 2013, when randomized sampling was introduced. This underlines the good repeatability of randomized sampling compared to zone sampling. Drawbacks of the randomized sampling method are possible comparability issues with data acquired after zone sampling as the mass or numbers of microplastics determined via the zone sampling method are correlated to the sampled area.

This disadvantage can be overcome by an estimation of the sampled area, as the approximate depth and the approximate volume as given by the sampling vessels are known. Nevertheless, this calculation is only a rough estimation, as the sample depth slightly varied between 2 and 3 cm, resulting in an additional error of 33% for the plastic concentration per m². Besides, it cannot be excluded that the sampling vessel was entirely packed with sediment causing additional measurement errors. Despite these errors caused by unit conversion, the random sampling approach still seems to be advantageous over zone sampling as distinctly higher errors or deviations, which are probably resulting from the within-site variability, were reported in literature.[44, 45]

6.1.1.2 Sodium chloride for density separation

A straightforward technique for sediment treatment without the demand of highly technological instrumental setups is the density separation with sodium chloride. This method allows good comparability to previous sediment studies of marine habitats, although modifications to the methods described in literature might diminish this comparability. It needs to be addressed that the improvements made during method development were focused on separation and identification of plastic particles below 500 µm in size. For this reason, the results obtained by the new method are likely to be comparable to previous density separation-based methods, such as described by Thompson *et al.* (2004), as underlined by the recovery experiments with polyethylene pellets. Both methods were able to determine the mass and item number highly reproducibly for larger microplastics (Figure 12). Moreover, new and differing techniques are generally validated, allowing comparison to the results presented in this thesis.[43, 59]

However, different heavy liquids were used for the density separation in recent years. Earlier studies focused on a saturated sodium chloride solution that was also used in this thesis. Besides the comparability to former studies, sodium chloride solution has several advantages such as easy handling, unproblematic deposition of the non-toxic solution, and cost efficiency for the preparation of large volumes of a saturated solution. A drawback of the density separation with sodium chloride is the limited attainable density of the solution of approximately 1.2 g cm^{-3}. Thus, a separation of synthetic polymers such as polyoxymethylene (POM), PET, and PVC, which can exceed a density of 1.2 g cm^{-3}, might not be possible. Nevertheless, sodium chloride solution was favored over zinc chloride solutions because of the hazardous properties of zinc chloride. Using zinc chloride, it would be possible to prepare solutions with higher densities (>1.5 g cm^{-3}), which offer separation of polymers such as PVC, PET, or POM. For this reason, some studies focused on methods using a zinc chloride-based separation of the microplastics. Another suitable compound used for the preparation of a high density solution is sodium iodide. Yet, sodium iodide is only applied in small volumes, because of the high price (ten-fold the price of sodium chloride) and further sample pretreatments are necessary, counteracting the easy setup of a density separation.[56, 59] However, sodium chloride is recommended by the Joint Research Center of the European Commission to analyze microplastics implemented in the marine strategy framework directive.[151]

Recovery experiments of the VESPA showed that a sufficient separation can be achieved with sodium chloride, even for very small plastic particles. Further, the recovery experiments indicated that PVC particles can be separated with sodium chloride solution as well despite the limited density of 1.2 g cm^{-3}. Yet, it needs to be addressed that the density of industrially used PVC might be increased by the addition of polymer additives and recovery of PVC from environmental samples might be lower than in the laboratory experiments.[152]

6.1.1.3 Natural debris removal

The removal of natural debris with a mix of hydrogen peroxide and sulfuric acid has already been described by Imhof *et al.* (2013).[153] In contrast to the described treatment over three weeks, the results of this thesis showed a sufficient destruction (over 99%) of the natural debris after 24 h. Effects of the treatment on polymers, such as reduction in mass or change in shape were not monitored, even though acid-catalyzed hydrolysis is reported for some polymers.[154] However, the acid-catalyzed hydrolysis by Jung *et al.* (2006) was carried out over 24 days, whereas the destruction of natural debris was only conducted for 24 h. The advantage of acidic oxidation of the natural debris over an enzyme-based approach is the distinctly shorter reaction time, which is needed for a sufficient destruction of the natural organic material. Furthermore, the enzyme based approach is less efficient for the removal of wooden particles.[155]

6.1.1.4 Polymer analysis by FTIR

Aging of the polymer, dirtying, or fouling of the polymer surface prevented a correct identification of the polymer type. A treatment with hydrogen peroxide and sulfuric acid to clean larger particles could not be applied as a further investigation of contaminants sorbed to larger plastic particles was intended. The identification of larger plastic particles was clearly enhanced by the measurement of a fresh polymer surface, as broad absorption bands in the fingerprint area of the FTIR spectra were reduced and the database comparison yielded higher match factors.

6.1.2 Occurrence and spatial distribution of microplastics along the river Rhine, the river Main, and the stream Schwarzbach

6.1.2.1 Concentration of microplastics in the river shore sediments

The results of the sampling of river shore sediments between March 2013 and February 2015 revealed that the tested river systems are heavily polluted with microplastics. Plastic particles were determined in the range of 18.2-933 mg kg^{-1} (mean: 253 mg kg^{-1}; median: 120 mg kg^{-1}) or 183-3763 particles kg^{-1} (mean: 794 particles kg^{-1}; median: 406 particles kg^{-1}). These results lead to the conclusion that the extent of pollution of rivers with microplastics is in the same concentration range that has recently been reported for sediments of marine habitats. For example, plastic particles separated from sediments in the Venetian lagoon accounted for 672-2175 particles kg^{-1}.[57] Similar amounts of microplastics were separated from sediments of the East Frisian islands (678 particles kg^{-1}), although these results need to be treated with extreme care as no chemical or spectroscopic identification of plastic particles was performed.[58] Fewer microplastics were reported for sediments of Belgian harbors and the Belgian continental shelf.[39] All results of this thesis were significantly higher than number and mass of microplastics which were separated in the Belgian study by up to one (68-390 particles kg^{-1}) and two orders of magnitude (0.9-7.2 mg kg^{-1}), respectively.[39] A possible explanation might be differences in the methodological approaches, as Claessens *et al.* (2011) included only particles smaller than 1 mm in their study. This could explain the highly diverse mass fractions determined, since larger particles contribute most to the plastic weight. However, the different definition used for microplastic particles cannot explain the distinct differences in plastic particle numbers, as the main abundance of particles was found in the smallest size fraction. Very low abundance of microplastics was reported for sediment samples from the German island Norderney, where only 1.7-2.3 particles kg^{-1} were identified. The low amount of microplastics in Norderney sediments, compared to the results of this thesis might be related to the sources of the plastic particles. In the Rhine-Main area many sources are located, which possibly introduce microplastics in the rivers and consequently in the sediments, whereas at the island Norderney direct sources of microplastics are distinctly less present.

Comparison of the extent of the plastic pollution to the results from other studies is complicated, since no harmonized units are used to describe the amount of microplastic found. Due to application of the random sampling method, no distinct area could be sampled. Yet, it is possible to estimate the sampled area by the sample volume and depth of sediment taken from each location. This rough estimation yields approximately 140-7500 mg m^{-2} and 1400-30000 particles m^{-2} for the shore sediments, respectively (see Table 26). These results are within the range of concentrations reported in other sediment studies of the marine environment (0.21-77000 particles m^{-2}).[4] Although this range is rather high, the majority of studies reported plastic concentrations between 100 and 100000 particles m^{-2}, confirming the observation based on the microplastic concentrations per dry weight of sediment that were stated previously. Fewer microplastic concentrations were reported in sediment samples of the Lake Garda, amounting in 483-1108 particles m^{-2}.[44] The low abundance of microplastics in shore sediments of Lake Garda might be related to less industrial activity and population density compared to the sampling region in the Rhine-Main area, as already stated for the Norderney sediment samples before.

The mass fraction of the plastic particles decreased strongly with decreasing particle size in the shore sediments of the river Rhine, Main, and Schwarzbach. On the other hand, plastic particles are more abundant in number with smaller particle size. The trend of increasing particle numbers with decreasing size of microplastics in the river shore sediments is in agreement with the results for the abundance of different particle sizes of plastic debris in marine sediments. An investigation of Brown *et al*. (2010) described a similar increase of the numerical abundance of microplastics with decreasing particle size for estuarine shorelines.[65] Furthermore, a study of sediments collected at the Portuguese coast showed that the size fraction with particles larger than 5000 µm accounted for over 90% of the total plastic weight, but only 30% of all items were counted as macroplastics.[75] This leads to the assumption that the tendencies of microplastic size distribution in shore sediments of freshwater systems and marine systems are very likely to be comparable.

The abundance of particle weight and particle numbers showed a good correlation ($n=12$; $R^2=0.85$; $P<<0.05$) at all sites sampled in December 2013. This indicates that in general, either the particle weight or the numerical abundance of plastic particles can be used to describe the plastic pollution in a comparable way. Taking into account that the largest size fraction of microplastics contributes mainly to the microplastic weight, it is likely possible to estimate the plastic pollution of river shore sediments by an analysis of the largest size fraction only. The determination of microplastic concentrations would be dramatically simplified by this assumption, as the sample preparation for the largest size fraction is less time consuming, as the destruction of natural debris is usually not necessary. Comparability to other studies using either particle weight or numerical abundance to describe the plastic pollution and comparability to previous studies, which determined mostly larger microplastics, is also confirmed by this correlation. However, estimating microplastic pollution of sediments by the fraction of large microplastics only prevents the observation of shifts in micro particle occurrence and might result in an underestimation of plastic particles in the sediments. Thus, the selective analysis of large microplastics in sediments might be helpful for the general observation of trends of the plastic pollution, but does presumably not compensate for an entire analysis including small plastic particles in size fractions <630 µm. Future developments of plastic nanoparticle or microparticle usage might be overlooked by the analysis of large microplastics, and an identification of sources of these plastics might not be possible.

6.1.2.2 Particle shape of microplastics

The analysis of the particle shapes present in the sediments showed differences between the size fractions. The abundance of spheres in the size fractions 63-200 µm and 200-630 µm increased strongly. This could possibly be related to manufactured plastic microparticles that are used in cleansers and cosmetics and produced in this small size range. These microparticles might enter the aquatic environment more likely by sewage treatment plants rather than by improper waste disposal. Another indicator for sediments influenced by sewage are probably synthetic fibers that can be emitted through washing processes and are not completely removed by the sewage treatment.[54]. However, the abundance of fibers, especially in the smallest size fraction, was surprisingly low. If the sediment is severely influenced by sewage water as indicated by the large abundance of microparticles, a higher abundance of fibers would have been expected. This discrepancy could be explained by two reasons. On the one hand, it is possible that fibers could not be determined accurately as their size or diameter is smaller than 63 µm and thus fibers are lost during the sieving step of the sample preparation. On the other hand, it cannot be excluded that fragments, which were polished to a round form by physical forces contribute to the number of spheres. Fragments were the most abundant class of microplastic particles in the size fractions 200-630 µm and 630-5000 µm, respectively. The large abundance of fragments is presumably an indication for the proceeding degradation of larger plastic items classified as mesoplastics or macroplastics. The degradation to smaller fragments is time dependent as many polymers provide a good mechanical stability. However, aging of the polymer under environmental conditions increases brittleness.[156] For this reason, the great number of fragments present in the sediments possibly indicates that plastic items spent a long time in river systems or the terrestrial environment. Moreover, the large abundance of fragments is possibly explained by tire wear particles. All sampling sites except site S1 are located in vicinity to frequented roads. Hence, it is likely that polymer particles resulting from tire wear can be recovered in the sediments. Several black and pressure resistant particles were determined in the size fractions 63-200 µm and 200-630 µm that could not be identified via FTIR according to their small size and the black color. Thus, these particles could not be associated explicitly to tire material such as styrene-butadiene copolymers. Noteworthy, high input of tire wear particles is expected and very probably exceeds the discharge of other polymeric synthetic microparticles by several orders of magnitude.[157]

In contrast to the results of this thesis, no spheres or round particles were identified in the lagoon of Venice, whereas the same amount of fibers (11%) in relation to the total amount of particles was found.[57] This might indicate a possible ambiguity error between spheres and fragments as discussed before, though it is not clear if Vianello *et al.* (2013) differentiated between spheres and fragments.

6.1.2.3 Polymer types in the sediments

Polymers separated from the sediments were mainly identified as PE and PP in terms of weight or as PS particles in terms of numbers. This result is not very surprising because of various reasons. On one hand, the high level of industrial relevance of PE, PP, and PS is a reason for their high abundance, as they cover 53.7% of the European plastic demand.[158] The polymers recovered from the sediment did not match the European plastic demand exactly, but the distribution of polymers found follows the same tendency. However, especially the low density polymers PE, PP, and PS (in the form of EPS) are identified with large abundance in shore sediments (84.2% of all polymers) compared to the corresponding plastic demand of 53.7%. Further, the abundance of high density polymers such as PVC and PET is distinctly smaller in the shore sediments. This could be explained by different transport mechanisms in water systems. The low specific densities of PE and PP and the floating ability of expanded PS allow a widespread distribution of these polymers in aqueous systems. They can easily be transported by rain water or rivers and accumulate in shore sediments due to wave movement and currents. Consequently, these three polymers are also the most frequently identified polymers in studies of marine sediments.[4] The transport of non-buoyant particles like PVC and PET needs to be compared to the transport of sediment, thus they are possibly present in higher abundance in river bed sediments than in shore sediments. PVC and PET are also high-production volume polymers, but their high density complicates the separation with sodium chloride solution. Hence, an underestimation of both, PVC and PET, is possible. The low abundance of other polymers such as PA or acrylic polymers can be explained due to less frequent usage.[3]

6.1.2.4 Spatial distribution of microplastics

To identify possible sources or indicators for the plastic pollution of the river shore sediments from the river Rhine, Main, and Schwarzbach, a detailed analysis of the spatial variation of microplastics is necessary.

Sediments of sampling sites located at or in vicinity to the confluence of the river Rhine and the river Main showed an extraordinarily high amount of microplastics compared to other sampling sites at the river Rhine. There are several possible reasons, which could explain this high abundance of plastic particles at the sampling sites M2, R2, R3, and R4. At a first glance, it is noticeable that all four sites are located in densely populated areas (1305-2907 inhabitants km^{-2}). However, there is no significant correlation of the population density and the masses and numbers of microplastics separated at each sample location (microplastic weight $n=12$, $R^2= 0.13$, $P>>0.05$; microplastic number $n=12$, $R^2=0.06$, $P>>0.05$; Figure 20). The correlation could be improved when the sampling site with the highest population density but lower microplastic pollution (R4) was excluded from the correlation, though the less populated regions do not show any clear relation between the microplastic concentration and the population density. This indicates that there is no direct or diffuse source of the microplastic concentration of river shore sediments which could be represented by the population density.

The lack of correlation of microplastics pollution and population density is in concordance with the result of an earlier study of shore sediments.[54] Though, it is contrary to results of recent surface water studies of the Laurentian Great Lakes and estuaries in the Chesapeake Bay.[60, 69] These contradictory observations might be explained by the comparatively high resolution of sampling sites in a relatively small sampling area with highly diverse population densities considered in this study.

It is important to notice that the population density does not represent other point sources like industrial activity or sewage treatment plants. Sewage treatment plants for example are known sources of small plastic particles and fibers, which could explain the high abundance of particles in the size range from 63-200 µm in the sediment samples. Especially sediments of sites R2 and R3 were severely polluted, but there are no municipal sewage treatment plants located in proximity to these sites. Moreover, sampling sites which are located near municipal sewage treatment plants (R1, R4, S1, and S2) did not show a distinctly higher abundance of particles in the size range between 63 µm and 630 µm. Further, all sewage treatment plants in the area of investigation consisted of similar treatment stages (mechanical stage, biological stage, and nutrient removal), but sediment microplastic concentration varied strongly, what underlines that there is possibly no direct influence of sewage treatment plants on shore sediments that were monitored in this thesis.

Additionally, the very high concentration of microplastics at the sampling sites R2 and R3 cannot be explained by a direct emission from industrial areas. The analysis of sediments downstream of a plastic processing industrial area, that is located between sampling sites R3 and R4, did neither show a direct (site R4) nor an indirect (R5-R8) increase of microplastic concentrations. High abundances of industrial pellets were determined in shore sediments from site R2 and R3 as well. For these reasons, neither the population density nor sewage treatment plant locations nor industrial activities seem to be good indicators for microplastic pollution of the river shore sediments in the monitored area. There exist different possible explanations for this finding. On the one hand, the spatial resolution of the sampling sites might be too high to show a distinct relationship between the above mentioned indicators and the microplastic concentrations. This is underlined by comparison of the average pollution of the sampled area (6400 particles m^{-2} or 222 particles kg^{-1}) to less populated areas like the subalpine Lake Garda or the island Norderney, located in the North Sea. In both cases lower (Lake Garda: 795 particles m^{-2}) or extremely low (Norderney: 1.8 particles kg^{-1}) microplastic concentrations were measured in the shore sediments. Comparing the microplastic pollution of this larger area with indicators such as population density, industrial activity, and sewage treatment plant density, a correlation is probably possible. On the other hand, the spatial resolution might not be high enough to discover influences such as run-off of industrial facilities or sewage treatment plant as the location of the sediment possibly was not close enough to the mentioned sources.

Another possible reason for the missing correlation between the microplastic concentration on the one-hand side and expected indicators on the other side might be that these factors are superimposed by hydrodynamic effects. These influences affect the mobilization or immobilization of sediments and riverine plastic transport, such as channel currents, channel geometry, stagnant water zones or flood events. Indicators for this hypothesis are on the one hand the impact of the river Main, which is potentially visible at the sampling sites M2 and R2 close to the Main mouth. The concentration of microplastic particles was in the same range at both locations, whereas the concentration of microplastic particles in river Rhine sediment is increased twofold from site R1 to site R2. Furthermore, the theoretical sediment movement as given by the channel geometry of the confluence of both rivers indicates that the sediment from R2 is probably influenced by the river Main.[159] The polymer composition of the sampling sites underlines the influence of the river Main on the pollution of Rhine sediments. A difference in the polymer composition is obviously visible behind the confluence of the river Main, where the variety of different polymer types strongly increases compared to the composition of R1. Additionally, the tendency of increasing numbers of PE and PP particles was clearly visible at the sampling sites behind the confluence of both rivers. Further indicators for the influence of the river Main on plastic pollution of the river Rhine is the presence of equally colored EPDM pellets (blue) and PP pellets (silver). These pellets were detected in the Main mouth (M2) as well as downstream of the confluence of the rivers Rhine and Main (R2 and R3). None of these pellets could be detected in the sediment from R1, which was sampled at the river Rhine before the confluence of both rivers or in sediments of the Schwarzbach. FTIR spectra of both pellet species were identical. Generally, colored pellets are clearly found less frequently than non-colored or white pellets. Absence of silver pellets in other sediments and the rubber-like consistency of the blue EPDM pellets are further indicators of a similar origin for both pellet types along the river Main. The occurrence of these specific pellets shows the traceable influence of the Main plastic burden on the river Rhine. Consequently, it can be expected that transport of microplastics from tributaries to main streams is an important transport route for plastic microparticles. Sewage treatment plants and industrial areas are not always located on larger streams, and the results showed that it is very likely, that sediments are not only polluted locally.

Moreover, great influence of the river currents and channel geometry might be visible in the huge concentrations of microplastics from R3 sediment. Since no direct source such as sewage treatments plants or industrial areas were identified in proximity to site R3, a current-based formation of sinks for plastic debris might be indicated by this result. The site R3 is zoned by a 2.6 km long river island from the shipping channel of the river Rhine. Thus, less wave movement and a lower flow rate can be expected in this area. As the tip of the river island is located 2 km downstream of the confluence of the river Main and the river Rhine, the right shoreline of the Rhine is likely influenced strongly by the river Main and could explain the high concentration of microplastics. Noteworthy, the hypothesis of rivers as sinks and transporting vectors for plastic litter is not self-contradictory. It needs to be addressed that rivers are dynamic systems with fast changing water levels and that all sampling site were located in the floodplain of the river Rhine. For this reason, all sinks are very likely temporal sinks that can be depleted during flood events and increase the amount of plastic litter in the river.[21] Nevertheless, further studies on plastic sink formations along rivers have to be carried out.

The results of sediment samples from less populated areas and nature reserves (R5 and R7) confirm the river-based distribution by a diffuse ubiquitous occurrence of smaller microplastics. This resulted in a high baseline contamination of all samples with smaller plastic particles.

The composition of the plastic particles identified at the single sampling sites showed several interesting patterns. Despite the distinctly different microplastic concentrations at all sites, particles of PE and PS were present in all sediments. PP was detected at all sites except the sediment sample from R7. This could be related to the general low pollution with plastics of this sample location. Furthermore, the relative abundance of PE particles by weight is almost constant at the river Rhine sites R2- R8 (mean: 49.5%; SD: 6.39%). In contrast to the particle weight, the composition of the polymer types by particle numbers changes strongly from sampling sites R2 to R8. However, the relative abundance of PE and PP particles is proportional to the total plastic pollution of these sites. This difference in the pattern of abundance by weight and abundance by particle number can be explained besides an influence of the river Main by the different forms of appearance of PE, PP, and PS. Whereas PE and PP were present in the form of pellets, foils and fragments, PS was mainly observed in the form of expanded PS. Due to the low density of expanded PS, the contribution to the total weight is almost negligible. Thus, a change in the relative abundance of PS is illustrated more clearly by the composition of the particle number.

6.1.3 Consistency of the microplastic pollution

Microplastic particles of the size fraction 630-5000 µm were monitored in sediment of R4 over a period of two years. The results showed only little variation between all samples and statistical analysis confirmed similar concentration of microplastics at this sampling site over two years. High influence on the microplastic concentration was expected by the water level of the river Rhine. As the water level affects the position of the shoreline, sediment samples were taken at comparable water levels. However, the tendency of the water level (increasing or decreasing water level) might impact microplastic concentration, as buoyant microplastic could be drained from sediments during flood periods. Thus, measurements after decreasing water levels might result in lower microplastic concentrations. This effect could not be clearly monitored via repetitive analysis of sediment samples of site R4. Therefore, the stable microplastic concentration at site R4 suggests a constant pollution of the river Rhine with microplastic over two years. Contrary to the constant concentration of microplastics in Rhine shore sediments, a study of the river Danube showed distinctly different concentrations of microplastics between 2010 and 2012.[79]

6.2 Sorption of contaminants to polymer particles

6.2.1 Sorption in dependence on K_{OW} values

Sorption of three different contaminants from synthetic freshwater to the polymers PE, PC, PMMA, PS, and PVC was investigated in laboratory scale experiments. All chemicals showed sorption to the polymer particles that generally was higher with increasing K_{OW} values of the contaminants. The time necessary to reach equilibrium or steady state varied depending on the polymer and maximum sorption of the contaminant to the particles. With increasing K_{OW} values of the contaminants generally faster solute sorption to the polymer was observed.

A dependence between sorption and K_{OW} values was already shown for the sorption of PAHs on PE by Fries *et al.* (2012).[94] Sorption of PAHs with higher K_{OW} values to PE lead to a higher sorption on the particles and also a faster decrease of the aqueous solute concentration. Furthermore, Fries *et al.* could not reach sorption equilibrium for PAH in PE pellets. This is in concordance with the results presented in this thesis.

Sorption equilibrium was not reached for PE particles and all contaminants within the time interval of the batch experiments of this thesis except chlorpyrifos and DDT. This is possibly related to diffusion of the contaminants into the PE particles, as the sorption experiments were carried out above the PE glass transition temperature. In contrast, no diffusion or only very slow diffusion of substances into the particles is expected for polymers in the glass state.[160, 161] The sorption experiments with the glass state polymers PC, PMMA, PS, and PVC reached equilibrium within the duration of the sorption experiment. This likely supports the hypothesis of almost no diffusion into the particle interior, as it is expected to be a slow and time-consuming step.[160] The low diffusion likely affected sorption efficiency of the glassy polymers. Due to low diffusion into PMMA, PC, PS, and PVC particles respectively, sorption of the contaminants to PE particles seemed to be higher. Nevertheless, sorption experiments are focused glass state polymers. As higher sorption was expected to PE particles, PE was used as positive control sample.

6.2.2 Sorption isotherms and sorption kinetics of CBZ

Sorption kinetics experiments and sorption isotherms of CBZ revealed relatively low sorption of CBZ to polymer particles. Nevertheless, CBZ was enriched on the polymer particles by a factor of 63 compared to CBZ in the same mass of water. Kinetics models of CBZ sorption to the glass state polymers followed a pseudo-first-order rate law. Solute sorption to polymers was already described by a first-order reaction models for PAHs and polychlorinated biphenyls.[121, 162]

This approach was followed to determine the sorption kinetics of CBZ. However, the model parameters determined for the kinetics of the CBZ sorption showed high error values, resulting from high measurement errors of CBZ sorption to glassy state polymers. Generally, the sorption kinetics implied a fast sorption of CBZ to the polymer surface and, after all free binding sites were occupied, sorption reached equilibrium. The rate constants for the sorption of CBZ to PS, EPS, and PVC were distinctly lower than the rate constants for the CBZ sorption to PC and PMMA. These observations are likely attributed to the fact that the kinetic model is lacking initial data points that describe the sorption kinetics, and only the final loading of the polymer was measured because of a too fast sorption of CBZ. For this reason, the sorption kinetics of CBZ is only a weak indicator for the sorption behavior of CBZ as the indirect determination of CBZ sorption at low solute concentration resulted in high errors of the applied model, and the parameters were not determined accurately.

Sorption isotherms of CBZ underlined the low sorption of CBZ to glassy state polymers. Sorption isotherms of CBZ were almost linear, resulting in n^{-1} exponents of 0.79-1.06. This indicated that sorption sites at the polymer surface are not highly heterogeneous.

The K_F values determined via the Freundlich fits were greater than K_F values stated in literature for sandy sediments. Scheytt *et al.* (2005) reported K_F values for the sorption of CBZ to sandy sediments that ranged from 0.00013-0.00534 ($\mu g^{1-1/n}$ $L^{1/n}$ g^{-1}) depending on the sediment. Freundlich exponents were close to 1, resulting in comparable K_F and K_D values. K_D values for the sorption of CBZ to sandy sediments determined by Scheytt *et al.* were ranging between 0.00021-0.00530 L g^{-1}.[163] K_D and K_F values that were obtained for the polymers in this thesis were 20-fold to 600-fold higher than K_D and K_F values determined by Scheytt *et al.* (2005) for sediments consisting of fine-grained alluvial sand and containing low amounts of organic carbon. The lower K_D and K_F values in literature might be possibly explained by the low content of organic carbon of the sediments that strongly seemed to affect the sorption of contaminants. Although, sediments offer several sorption mechanisms such as sorption to natural organic matter, interactions with polar or charged species and interactions with mineral surfaces.[164] Because of possible polar interactions between CBZ and polar moieties of the sediment higher sorption of CBZ might be expected for sediments. However, ionic interactions between charged CBZ and the sorbent play a minor role because of the high pKa of CBZ that is far beyond the experimental conditions. The pH-dependency of CBZ sorption to polymers can be neglected as neither protonation nor deprotonation can affect the polymeric sorbent, as it was shown for sediments.[165] Nevertheless, the role of polar interactions between CBZ and polymers is underscored by the high sorption efficiency of PMMA for CBZ compared to the other glassy polymers. High sorption of CBZ might be explained by polar interactions between CBZ and PMMA, as PMMA is the polymer with the highest O/C ratio of glassy polymers used for sorption experiments.

Distinctly greater Freundlich coefficients were reported by Ternes *et al.* (2002) for the sorption of CBZ to activated carbon from ultrapure water and groundwater (K_F: 90-141 mg g^{-1} $[(mg\ L^{-1})^{-1}]^n$).[166] Contrary to sorption isotherms of the polymers in this thesis, Freundlich exponents were of the sorption isotherms to activated carbon were distinctly smaller than 1 (n: 0.19-0.22). Reasons for the different sorption of CBZ to activated carbon are possibly the high internal surface area of activated carbon with easily accessible micropores and highly heterogeneous sorption sites. Glassy polymers do neither offer the same amount of micropores nor relevant diffusion into the particles. Thus, CBZ sorption to glassy polymers is, as expected, not comparable to a technically used sorbent such as activated carbon.

6.2.3 Sorption kinetics and sorption isotherms of γ-HCH

The kinetic models for γ-HCH sorption to glassy polymers showed that the sorption rate is close to the range of rate constants reported for the γ-HCH sorption to aquifer materials.[167] Rate constants for a first-order model to aquifer materials varied between 0.018-0.049 h^{-1} depending on the sands. [167] The lower end of the rate constants is close to the rate constants of the glassy polymers from this thesis (0.006-0.016 h^{-1}). However, the sorption isotherms and the parameters obtained differed strongly from literature values. K_D and K_F values were greater for the sorption to polymers. Highly non-linear sorption isotherms of γ-HCH were obtained for the polymers PC, PMMA, resulting in lower regression coefficients for the linear Henry model (R^2_{PC}: 0.86 R^2_{PMMA}: 0.87). The isotherm data for the sorption to PC suggested multilayer sorption of γ-HCH and was best characterized by a BET isotherm. In contrast, no multilayer sorption was described for the aquifer material by Weber *et al.* (1988). Multilayer sorption of γ-HCH could explain the high sorption to PC for both HCH species, as the sorption efficiency for β-HCH and γ-HCH was obviously the highest with PC. On the other hand multilayer sorption of γ-HCH to PC poses the question why no evidence for multilayer sorption to PC particles was monitored for the substances CBZ and chlorpyrifos.

Sorption isotherms of γ-HCH for all glassy polymers showed particularly higher K_D or K_F values than reported for lindane sorption to natural zeolite except for PS. Due to low sorption of γ-HCH to PS, K_D and K_F values were in the range of natural zeolite.[168]

Sorption of γ-HCH to activated carbon was, as already discussed for CBZ, greater than γ-HCH sorption to glassy polymers.[169] Also the rate constants for sorption of γ-HCH to activated carbon were distinctly higher than the rate constants for sorption to glassy polymers. This is not very surprising, as, activated carbon is a technically used sorbent offering a high internal surface area that facilitates the high sorption of contaminants, as mentioned previously.

6.2.4 Sorption kinetics and sorption isotherms of chlorpyrifos

Sorption of chlorpyrifos was already monitored for PE films that are used as agricultural soil covers by Nerin *et al* (1996).[170] Sorption kinetics to the polymer film was in the same range as obtained for the sorption of chlorpyrifos to the polymer particles in this thesis. The concentration of chlorpyrifos increased in PE foils over 15 days. This result is comparable to the sorption kinetic experiments performed in this thesis.

Sorption isotherms of chlorpyrifos were nearly linear (Freundlich exponents n^{-1}=0.97-1.34) and could be described by the linear model resulting in regression coefficients between 0.969-0.999. Sorption of chlorpyrifos to the glassy polymers seemed to slightly better follow Freundlich isotherms as regression coefficients were improved for all polymers ($R^2_{Freundlich}$:≥ 0.994). This indicates that sorption sites at the sorbent surface seemed to be relatively homogenous for chlorpyrifos sorption. Only for PC particles seemed to provide a more heterogeneous surface for chlorpyrifos sorption (R^2_{Henry}=0.97; Freundlich exponent n^{-1}=1.33). The good linearity of chlorpyrifos sorption isotherms is in concordance to observations reported for the sorption of chlorpyrifos to different soils, where n^{-1} values between 1.05-1.12 indicate linear isotherms.[171] However, sorption to soils, represented by the K_F values (K_F: 332-1028 mg kg^{-1} [(mg $L^{-1})^{-1}]^n$; note the unit of the sorbent mass is kg), was lower than sorption to glassy polymer. This might be related to the short equilibration time of 24 h in the experiments carried out by Yu *et al.* (2006). The sorption kinetic investigations with chlorpyrifos and the different polymers in this thesis revealed that all samples need several days to reach sorption equilibrium (Figure 29).

6.2.5 Sorption kinetics of β-HCH and DDT and losses in control samples

The kinetic sorption experiments of β-HCH and DDT showed high sorption to glass surfaces, as the aqueous concentration of both compounds decreased strongly in the blank samples. Losses of DDT to glass vessels in laboratory studies were described already by Picer *et al.* (1977).[172] The pronounced and unexpected loss of both substances was possibly caused by the increased ionic strength of synthetic freshwater used during sorption experiments compared to deionized water that is usually used for the determination of the water solubility.[173] This could cause salting-out-like effects reducing the solubility of β-HCH and DDT and thus promoting interactions of glass and the substance.[174] By the addition of ions to the aqueous solution, more organized water structures are formed and might increase cavity energy which is required for the dissolution of β-HCH and DDT. It needs to be addressed, that these salting-out effects are usually described for ionic strength higher than the ionic strength of freshwater. However, it is known that sorption of PAH to glass surfaces increases with increasing calcium chloride concentrations, and the largest effect on sorption for highly non-polar substance such as pyrene was obtained after the addition of 1 mM calcium chloride to ultrapure water.[175] Concentrations of β-HCH and DDT, used in the sorption experiments, were close to the maximal solubility of both substances. These concentrations were necessary to maintain comparable experimental design of the sorption batch experiments and manage the determination of β-HCH and DDT, but possibly resulted in high losses of both compounds in control samples.

6.2.6 Possible mobilization of sorbed β-HCH by microplastics

Sorption kinetics of β-HCH showed a slower decrease of β-HCH concentration in samples containing polymer particles in the glass state. Different sorption kinetics of polymer and control samples could be explained by different sorption behavior between the glass surface and the polymer particles. Sorption of β-HCH on glass surfaces was monitored by the decrease of the aqueous β-HCH concentration. No further decrease of the concentration showed that after an initial sorption β-HCH, no diffusion into pores of the glass surface occurred. Samples containing polymer particles showed different sorption, as diffusion of β-HCH into the polymer particle is very likely possible. However, sorption of substances to polymer particles below their glass transition temperature is distinctly slower and follows a more complex mechanism.[160] Thus, sorption in samples containing PMMA, PC, PS, EPS, and PVC respectively, to the polymer surface or glass surface initially follows the same principle as in control samples with occupancy of free sorption sites. After all surface positions are occupied, the time-dependent diffusion from the surface into pores or cavities of glass state polymers might clear sorption sites on the polymer surface. Assuming that the polymer surface is the more suitable sorbent for β-HCH, an increase of the aqueous concentration is caused by a shift of the equilibrium, which induces desorption of β-HCH from the glass surface. When all low energy cavities and surface positions are occupied, the concentration of β-HCH in the supernatant drops below the concentration in the control sample, because of the additional sorption of β-HCH to polymer particles. Further diffusion of β-HCH into the particles was not determined or could not be measured in the time interval of the experiment as β-HCH concentration reached equilibrium for PMMA, PC, PS, EPS, and PVC. The hypothesis suggests a mobilization of β-HCH by polymer particles that were sorbed to glass or glass-like particles. Mobilization of β-HCH sorbed to soils by DOM has already been monitored by Kalbitz *et al.* (1997).[176] The hypothesis of β-HCH mobilization could be confirmed by the addition of plastic particles to control samples in equilibrium. In this experiment an increase of the aqueous β-HCH concentration after the addition of polymer particles was monitored (Figure 37).

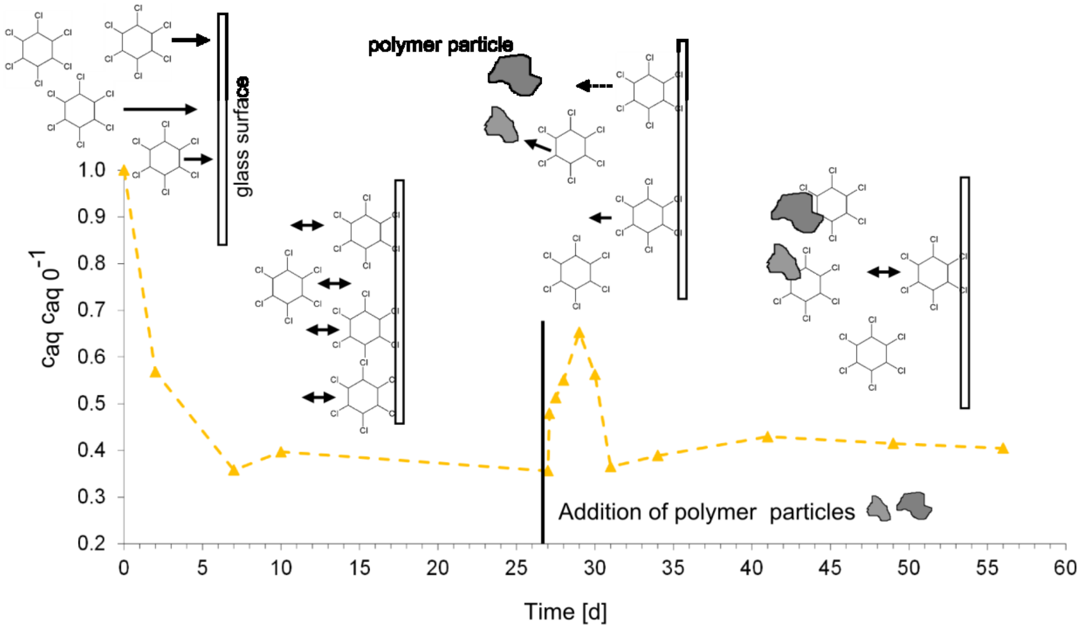

Figure 37: Proposed mobilization of β-HCH sorbed to glass in an initial step by the addition of polymer particles (data of PMMA shown).

6.2.7 Determination of contaminant sorption via a direct and an indirect method – A comparison via polymer extraction

The polymer extraction after the 30 days sorption kinetic experiments showed low deviations between the indirect and the direct method for three out of six contaminants. Higher deviations were obtained for CBZ and the contaminant with losses in the control samples, namely, β-HCH and DDT. Deviations within the CBZ sorption determination by the direct and the indirect method can possibly be explained by the rinsing of the filtered polymer particles. As CBZ is the most polar compound used in the sorption experiments, interactions between CBZ and the polymer surface might be not as strong as for the other model substances used. Hence, rinsing the polymer particles with ultrapure water probably led to desorption of CBZ. For this reason, the CBZ concentration on the polymer particles determined by the indirect measurement exceeds the concentration of the polymer extraction. The loss of CBZ during the rinsing step seemed to be comparable for all polymers as the trend of the sorption to each polymer remained the same for both methods of sorption determination.

Concentrations of β-HCH and DDT showed a different behavior as CBZ and higher concentrations were determined with the direct method. This was very likely attributed to the high sorption in the control samples. Extraction of the polymer particles showed that sorption of DDT to glass was also affected by the presence of the sorbent and not only by the glass surface in the reaction vessels as high concentrations of DDT were extracted from the polymer particles. Thus, solute interactions with the polymer particles are possibly prompted by salting-out effects as described for the control samples. If polymer particles were present, sorption of DDT to the polymer particles could exceed the sorption to the glass surface. This indicates that the polymer particles are the favored sorbent in the ternary system (water - glass surface - polymer particle). This hypothesis is underlined by the results of the extraction of the emptied glass vessels that were employed for the sorption kinetic experiments. The concentrations of DDT that were extracted were below the limit of detection except for PMMA and PC.

For substances with high K_{OW} values, low water solubility and no losses in control samples (γ-HCH, EE2, and chlorpyrifos) both, the direct and the indirect determination of sorption are suitable. Losses of sorbed solute by rinsing of the polymer particles seemed to be insignificant with these compounds, as the deviation between the indirect and the direct methods were very low.

Sorption of organic contaminants becomes more relevant with increasing K_{OW} values of the contaminants. Sorption of more polar organic compounds such as pharmaceuticals to microplastic particles might not play an important role especially with regards to microplastics as carrier for these contaminants. Even though CBZ was enriched on plastic particles, nowadays concentrations of pharmaceuticals in the environment might be too low to allow reasonable sorption to microplastics. The same assumption is probably valid for EE2. Despite the higher K_{OW} of EE2, environmental concentrations are very likely too low to enrich high amounts of EE2 in microplastic particles in freshwater systems. This might be different for marine habitats, especially for the water surface. Since microplastics made from PE and PP are buoyant, they interact with most contaminants in the so-called sea surface microlayer. In this organic-rich layer, hydrophobic organic compounds are present in distinctly higher concentrations than in the subjacent water column. Kinetic studies of EE2 showed that even at low concentrations, serious amounts of EE2 sorbed to all polymer particles.

Hydrophobic insecticides such as HCH, chlorpyrifos, or DDT are of more serious concern. These substances showed very high sorption even at very low concentrations. Further, sorption kinetics showed that these compounds can sorb in a short time in very large scale to microplastics. Sorption kinetics of β-HCH suggested a relocation of the sorbed phase. This could cause a mobilization of contaminants by microplastics, if the polymer is the more favorable sorbent.

Aside the characteristics of the sorbates (K_{OW}, solubility), the polymeric sorbent seemed to have a strong influence on the sorption. On one side, T_g is an important factor for the sorption of contaminants, as polymers above their glass transition temperature such as PE showed higher sorption of contaminants in the kinetic experiments of this thesis. On the other side, structural elements of the polymers such as the presence of phenyl moieties or ester bonds affect their sorption efficiency. This is underlined by the results of the sorption isotherms and the results of the PCA of the glass state polymers. As all the polymers PC, PMMA, PS, and PVC were employed as sorbents below their T_g, the sorption behavior should be comparable (unlike to PE).

Furthermore, the kinetic studies showed a relatively fast sorption of the contaminants within a few days. Thus, microplastics, which are immobilized at shore sediments until the next flood event in e.g. agricultural used regions, can possibly sorb high amounts of hydrophobic insecticides and pesticides. If and in which concentration range environmental contaminants are mobilized from sediments, as it was possibly observed for the glass surface in the laboratory scale experiments of β-HCH, needs to be addressed in future studies. But it is very likely that this relocation of the sorbed phase from sediments to the polymer depends on the type of sediment.

6.3 Environmental contaminants in microplastics from sediments of the river Rhine, river Main, and stream Schwarzbach

As expected from the results of the sorption experiments in a laboratory scale, environmental contaminants were detected in the microplastic particles that were separated from sediments. Although the abundance of substances that were identified as environmental contaminants is relatively low, their presence in the pellets is detectable.

In several polymer particles, substances were detected that are used as polymer additives. Contrary to expectations, di(2-ethylhexyl)phthalate was not identified in the polymer samples, even though is widely used in the polymer production.[177] However, different other phthalates, such as DnPP and DBP, were identified in the PE, PP, and PS pellets. Furthermore, heterogenic phthalates were determined. It is expected that these substances originate from the polymer particles themselves and desorb from the plastic to the surrounding aqueous phase. Phthalates are of serious concern as they are likely able to inhibit enzymes or act as endocrine disruptors.[178, 179]

The detection of γ-HCH and chlorpyrifos showed the high relevance of insecticide sorption to the polymer particles. Both substances sorbed already in high concentrations to the polymer particles in the laboratory experiments.

The presence of PAHs in the polymer pellets is not very surprising. PAHs are ubiquitously distributed nonpolar substances, thus several studies reported their presence in rivers and due to their hydrophobicity especially in river sediments.[180-182] Moreover, studies of plastic pellets detected PAHs already in PE, PP, and PS particles and laboratory experiments of Fries *et al.* (2012) proved high affinity of PAHs towards plastic particles.[94, 100, 183] The detection of PAHs in the plastic particles is on the one-hand side very likely attributed to the sorption of PAHs from the surrounding water or air. On the other hand, it cannot be excluded that PAHs were already present in the preproduction pellet or the final plastic product. Since the production of monomers for plastics such as PS includes educts such as crude oil, benzene, and ethyl benzene the formation of PAHs under heat can be assumed.[184] PAHs could be formed as well during the polymerization of the final product as the formation of PAHs from styrene containing polymers might occur already at relatively low temperatures.[185]

The results of the extractions confirmed that microplastic can act as a sink for hydrophobic organic contaminants. For environmental contaminants, which did not sorb to the polymer particles from river water, it is possible, that microplastics act as a source for hazardous chemicals which desorb from the plastic particles and increase the concentration of contaminants in less polluted sediments.

6.4 Conclusion

The results of this study reveal that inland river systems are severely polluted with microplastic particles. Synthetic polymers were determined in all of the tested shore sediments from the rivers Rhine, Main, and the stream Schwarzbach in Germany. Large abundance of buoyant, high production plastic particles (PE, PP, and PS), and the presence of many spherical microparticles showed the importance for regulation on plastic products. Furthermore, the results of the thesis highlight the significance to identify direct sources of microplastics to mitigate the environmental pollution with plastic particles. This is underlined by the continuous input of plastics, resulting in a constant pollution of river shore sediments. Further, an identification of direct microplastic sources located at inland river systems might diminish the discharge of microplastics into the oceans dramatically, as the results proved riverine transport of microplastics that will likely end up in the ocean. These results can only provide a snapshot of the microplastic pollution in a limited research area. However, the results strongly promote further monitoring of microplastics, especially as the research area was located in an industrial country with a well-developed waste management system. Thus, the global problem of the pollution of aqueous systems with plastics might be significantly higher.

The importance of further studies on the effects of the microplastic pollution is underscored by the sorption experiments conducted in this thesis. The enrichment of nonpolar contaminants on the synthetic polymers promotes the hypothesis that microplastics act as sinks for organic contaminants. Plastic particles loaded with organic contaminant can enter unpolluted systems or organisms where the microplastics possibly act as a source by desorption of the organic contaminants. Additionally, microplastics are a source for various plastic additives. These additives were identified with large abundance in plastic particles originating from environmental samples. Some of these additives have already been detected in freshwater systems, are regulated by REACH, and are known emerging pollutants. Thus, the results of this thesis indicate that mitigation of plastic release into the environment might reduce also the environmental concentrations of non-volatile plastic additives.

The research conducted provides new insights in the plastic pollution of river shore sediments and contains evidence that sorption of organic contaminants to microplastics is a relevant process in freshwater systems. These results underline the urgency for further systematic monitoring studies of inland waters. Additional desorption experiments of plastics loaded with different contaminants need to be conducted for the final classification of the importance of contaminant sorption. Thus, it is not known, if and how fast contaminants desorb from microplastics, as studies on contaminant transfer are rare and contradictory. The uptake of microplastics by surface-feeding organisms and possible resulting contaminant transfer might be a relevant process, although effects that were monitored in laboratory studies with different organisms and contaminated microplastics reported in literature were relatively low. Transport and contaminant sorption processes of microplastics and sediments could open up new transport routes for hydrophobic contaminants, as indicated by the mobilization of contaminants in the sorption experiments conducted. Additionally, investigations on competitive sorption of contaminants to polymers and other naturally occurring colloidal material, such as humic acids or natural organic matter, are necessary to fully explain the relevance of microplastic contaminants sorption.

Nevertheless, the results of this work strongly promote that regulations of plastic products is inevitable as unknown side effects of the popular but anthropogenic material plastic can intervene environmental processes.

7 Perspectives

The results of this thesis highlight the great importance of microplastics for freshwater ecosystems. The occurrence of the plastic particles and the consistency of the pollution in river shore sediments stress the relevance for further monitoring studies. Attention should be focused on a harmonized nomenclature of microplastic particles with official guidelines for microplastic studies. Therefore future studies should integrate additional units to describe the microplastic pollution in their investigations to establish a better comparison of the different environmental compartments. Moreover, an integral step of future investigations should be a sufficient validation of the microplastic analysis, as different technological approaches might be used, or future technological improvements will be implemented for the determination of microplastics. Such a validation process would also allow a comparison of the results between the different microplastic studies. The method development performed in this thesis showed the potential of the straightforward density separation. Future improvements can be focused on the identification of the plastic particles. The hardness test of polymer particles, as carried out in this study, is a time consuming process that is not suitable for routine analysis and might be substituted by techniques such as Raman or FTIR microscopy. Furthermore, techniques such as MALDI-TOF or pyrolysis-GC/MS have great potential for the analysis of synthetic polymers. Additionally, the development and use of internal standards for the accurate quantitation of microplastics would lead to more valid and comparable results. In any case, systematic investigations that are accomplishing international comparable results should be the aim of future studies. Currently, studies are lacking comparability because of to many different approaches that were followed for the microplastic determination, as mentioned previously.

Furthermore, the determination of suitable indicator substances for the presence of microplastics or the investigation of the extent of the plastic pollution could simplify the analysis and help to harmonize the international research in the field of microplastics.

The high abundance of microplastics at distinct sampling sites determined in this thesis is an indicator for plastic sink formation along river shores. However, only little is known about plastic movement in rivers. Estimations of riverine transport of plastic particles would benefit from detailed studies of the floating behavior of plastics in large rivers. Further, detailed plastic movement might help to determine possibilities to mitigate the discharge into oceans by installing adequate restraint systems. Additionally, point sources need to be identified to intervene in the direct discharge of plastic material into the environment with appropriate actions. The generally high pollution of the sediments with microplastics stresses the urgency for further mitigation of plastic discharge into the environment. Sustainable alternatives for synthetic polymers, reduction of plastic usage, and the sensitization of the population could help to decrease the production of plastic waste and decrease the discharge by diffuse sources of plastic litter such as improper waste disposal.

Even though if there are first estimations of plastic waste input from land-based sources into the ocean, mass fluxes of plastics in river systems need to be part of future investigations. There is too little knowledge about the amount of plastics that are transported from the inland into the oceans.

Sorption of environmental contaminants from freshwater to synthetic polymers was determined for all plastic particles tested. This suggests that sorption is relevant for microplastic particles in freshwater systems. However, these results were determined neglecting the presence of other particular material such as natural organic matter. Further sorption experiments combining e.g. humic acids with polymer particles as sorbents in environmental relevant ratios are necessary to estimate the entire importance of contaminant sorption in freshwater systems. If sorption is investigated in a system with different sorbents available such as natural organic matter and polymer particles, the extraction of the separated particles is necessary for each individual sorbent. This is underlined by the results of the DDT sorption presented in this thesis. Here no indirect sorption calculation was possible because of different sorption affinities of DDT to the glass surface or the polymer particles, respectively.

The investigation of desorption rates of contaminants from microplastic particles is of high significance to estimate the final impact of sorption as mentioned previously. On one side high amounts of additives were identified in environmental microplastics, one the other side sorption experiments as well as the extraction of environmental microplastics revealed sorption of pesticides. Thus, investigations on leaching in freshwater and salt water environments could enlighten the importance of microplastics acting as carriers for these substances.

Dozens of commodity polymers are used in everyday life and substantial amounts of plastic waste are expected to be generated by packaging. A substitution of synthetic polymers by more ecofriendly alternatives and a sensitization of the public consumers on plastic waste handling are likely promising possibilities to reduce the discharge of plastics into the environment. Therefore, future developments should focus on both, the improvement of biodegradable polymers or the usage of conservative materials, as well as to arouse public awareness regarding the end-of-life handling of plastic products.

8 Summary

The present thesis aimed to investigate the occurrence of microplastics and the sorption of contaminants to microplastics in freshwater systems.

Therefore shore sediments of the river Rhine were sampled in an initial investigation to estimate the relevance of microplastics for inland water systems. Sampling and sample preparation were performed by methods described in literature. In this initial investigation microplastics were determined in high mass fractions of up to 400 mg kg^{-1} or up to 100 particles kg^{-1}, confirming the high significance of microplastics in inland waters. However, the method used for sampling and sample preparation exhibited several disadvantages resulting in high standard deviations, poor separation and identification of particles <500 µm, and misidentifications using FTIR spectroscopy. For this reason, the sampling strategy of the shore sediments was improved, a new instrumental setup was developed for the density separation of the plastic particles and a sample clean-up procedure was established. The newly developed sampling strategy resulted in low within-site variability of the sampling sites (8-18%), and the improved density separation lead to good recoveries of small plastic particles (70-98%). The application of sieve fractionation as sample pretreatment and acidic oxidation as sample treatment after the density preparation enabled the determination of particles <500 µm.

For the detailed analysis of the microplastic pollution of riverine freshwater systems, shore sediments of the river Rhine, the river Main, and the stream Schwarzbach were sampled and prepared applying the newly established methods. High amounts of microplastics were determined in the shore sediments yielding concentrations of up to 1 g kg^{-1} or 4000 particles kg^{-1}. The largest mass fractions and particle numbers were identified in the river Rhine, the lowest amount of plastic particles were determined in sediment samples of the small stream Schwarzbach. Most abundant polymers in the sediments were PE, PP, and PS, covering over 75% of all polymers identified.

Distinctly larger amounts of microplastics were detected in sediments of the Main mouth and in Rhine sediments in vicinity and downstream of the confluence of the river Main, suggesting a direct influence of the river Main on the pollution with microplastics in the river Rhine. This influence was underlined by identification of identical pellets in sediments of the Main mouth and the river Rhine as well as by the increasing diversity of polymer types present in the sediments in vicinity to the confluence of both rivers. No correlation was observed for the population density and the microplastic concentration in the sediments. Furthermore, the microplastic concentration could not be explained exclusively by industrial or sewage-related influences. Those might be superimposed by hydrodynamic effects such as channel currents or stagnant water zones.

Sorption of contaminants to microplastics was investigated in batch experiments to determine sorption kinetics and sorption isotherms for four different polymers (PC, PMMA, PS, and PVC) and six different contaminants (CBZ, β-HCH, γ-HCH, EE2, chlorpyrifos, and DDT). All tested contaminants showed sorption to the polymer particles. However, neither sorption kinetics nor sorption isotherms could be calculated for β-HCH or DDT, because of strong sorption in the control samples. Sorption of the contaminants was determined for all polymers after 30 days by measurement of the aqueous phase and by extraction of the polymer particles. Substantial differences were detected between the determination of sorption via measurement of the aqueous phase and via the polymer extraction, if losses in the control samples had been observed. Sorption kinetics of all other polymer/contaminant combinations were modelled using a pseudo-first order reaction model, and rate constants determined were generally slightly lower than rate constants reported for sediments. Sorption isotherms were modelled using the Henry model, Freundlich model, the Langmuir model, and the BET model. Most of the sorption isotherms were almost linear resulting in Freundlich exponents close to 1 for all model substances and polymers, except the sorption of γ-HCH to the polymers PC, PMMA, and PS. Thus, linear isotherms resulted in good correlation coefficients and K_D values determined were used to analyze relationships between contaminant sorption and polymer parameters via PCA. A correlation of the sorption of substances to polymers was observed from sorption experiments and PCA, if both contained polar moieties offering the possibility for polar interactions. Moreover, strongly hydrophobic substances seemed to favor sorption to polymers with nonpolar moieties.

The extraction of the microplastic particles from sediments of the river Rhine showed low abundance of pesticides and environmental contaminants such as PAHs. More polar substances such as pharmaceuticals were not detected and might therefore not be relevant for sorption processes in freshwater systems. In contrast, high concentrations of polymer additives, such as flame retardants or phthalates were detected in the polymers, stressing the importance of microplastics as source for these chemicals of serious concern.

This thesis provides new aspects in the field of microplastics proving their large abundance in freshwater system and that microplastics are a possible relevant source and sink for organic contaminants.

9 Annex

9.1 Materials and Methods

9.1.1 Consumable materials

A detailed list of consumable materials that were used for sediment sampling, sorption experiments and the sample analysis is provided in Table 9.

Table 9: Consumable materials used in this work.

Material	Supplier
Aluminum foil	Carl Roth, Karlsruhe, Germany
Cellulose filter, MN610, 70 mm	Carl Roth, Karlsruhe, Germany
Glass micro fiber filters GF/A 47 mm	Whatman, Maidstone, UK
Glass micro vial (0.3 mL) with cap	AZ Analytik, Langen, Germany
Glass petri dish (large; diameter)	Carl Roth, Karlsruhe, Germany
Glass petri dish (small; diameter)	Carl Roth, Karlsruhe, Germany
Glass vial (1.8 mL) with cap	AZ Analytik, Langen, Germany
Glass vial with thread (1.8 mL) with cap	AZ Analytik, Langen, Germany
Glass vials with threat (22.5 mL) with cap and Teflon septa	AZ Analytik, Langen, Germany
PP micro vial with cap	AZ Analytik, Langen, Germany
PP syringe Omnifix-F, 1 mL	Carl Roth, Karlsruhe, Germany
PP wide-neck-cans, 2.5 L	Carl Roth, Karlsruhe, Germany
Syringe filters regenerated cellulose (0.45 µm, 13 mm)	Carl Roth, Karlsruhe, Germany

9.1.2 Instruments

All instruments that were used in this thesis are shown in Table 10.

Table 10: Instruments used in this work.

Instrument	Manufacturer
Orbital shaker KL2	Edmund Bühler GmbH, Hechingen, Germany
Vortex shaker Genius 3	IKA, Staufen, Germany
Stainless steel test sieves (mesh size 63 µm, 200 µm, 630 µm)	Haver & Boecker OHG, Oelde, Gemany
Drying Cabinet Memmert UM-500	Memmert, Schwabach, Germany

Instrument	Manufacturer
Microscope BA310E with Moticam X	Motic, Hongkong, China
Analytical balance Kern ARS 120-4	Kern & Sohn, Balingen, Germany
Analytical balance Scout Pro SPU6000	Ohaus Corporation, Pinebrooks, USA
FTIR instrument Spectrum BX with ATR-unit	Perkin Elmer, Waltham, USA
Ultrasonic bath USC 200T	VWR International, Radnor, USA
GPC system: Degasser ERC-3322, Bischoff HPLC Compact Pump 2250, PSS RI-71 refractive index detector, and Gilson FC 203B fraction collector	ERC, Riemerling, Germany Bischoff, Leonberg, Germany Polymer Standard Services, Mainz, Germany
LC-MS/MS system: Agilent 1100 (Degasser G1379A, Binary pump G1312A, Auto sampler G1367A, DAD detector G1315A), and AB Sciex API 2000 mass spectrometer with ESI source.	Agilent, Santa Clara, USA AB Sciex, USA
GC/MS system: Agilent 6890N with 5973 inert MSD	Agilent, Santa Clara, USA
Membrane nitrogen generator NGM-22-LC/MS coupled to SF 4 FF oil-free orbiting scroll compressor	CMC, Eschborn, Germany Atlas Corpo, Stockholm, Sweden

9.1.3 Solutions

9.1.3.1 Saturated sodium chloride solution

360 g of sodium chloride was added to 900 mL of deionized water and stirred for 30 min at room temperature. Subsequently, the solution was filtered through glass fiber filters and stored in brown glass bottles until usage.

9.1.3.2 Synthetic freshwater

Synthetic freshwater was prepared based on Smith *et al.* (2002).[186] 10 mg magnesium chloride hexahydrate, 20 mg calcium chloride, 16 mg sodium sulfate, 5 mg potassium bicarbonate and 15 mg sodium bicarbonate were mixed with ultrapure water in a 1000 mL volumetric flask and stirred for 30 min. The solution was stored in dark at 4-7 °C until usage.

9.1.4 Reference materials and stock solutions

A stock solution of 1 mg/mL in methanol or acetone was prepared for each reference material listed in Table 11, except BPA-D16 and CBZ-D10. Methanol was used as solvent for CBZ and EE2. Atrazine, chlorpyrifos, β-HCH, γ-HCH, and (DDT) were dissolved in acetone. If not stated otherwise, all solutions and dilutions containing the reference materials in this work were prepared using these stock solutions.

Table 11: Reference materials used in this work. Solvent of BPA-D16 and CBZ-D10 was acetonitrile.

Substance	Abbreviation	Purity	Supplier
Atrazine	n/a	98.0%	Riedel-de-Hän; Seelze Germany
Bisphenol A D16	BPA-D16	100 µg mL^{-1}	Neochema, Bodenheim, Germany
Carbamazepine	CBZ	99.1%	Sigma Aldrich, St Louis, USA
Carbamazepine D10	CBZ-D10	100 µg mL^{-1}	Neochema, Bodenheim, Germany
Chlorpyrifos	n/a	99.0%	Dr. Ehrenstorfer, Augsburg, Germany
o,p-Dichlordiphenyltrichlorethan	DDT	97.5%	Dr. Ehrenstorfer, Augsburg, Germany
17α-Ethinylestradiol	EE2	99.0%	Sigma Aldrich, St Louis, USA
β-Hexachlorocyclohexane	β-HCH	99.1%	Dr. Ehrenstorfer, Augsburg, Germany
γ-Hexachlorocyclohexane	γ-HCH	99.8%	Riedel-de-Hän; Seelze Germany

9.1.5 Separation of microplastics from shore sediments

The water level of the river Rhine was determined in Mainz, Germany (50° 0.240' N, 8° 16.519' E) and the water level of the River Main was obtained in Raunheim, Germany (50° 0.240' N, 8° 16.519' E). Detailed coordinates of the sampling sites located in the Rhine-Main area of Germany are shown in Table 12.

Table 12: Sampling sites at the river Rhine, the river Main, and the stream Schwarzbach with abbreviation used and coordinates of the sites.

Abbreviation	Location	Coordinates
S1	Astheim	49°56'01.3"N 8°22'03.6"E
S2	Ginsheim	49°57'43.5"N 8°20'52.6"E
R1	Ginsheim-Gustavsburg	49°58'18.6N 8°19'39.7"E
R2	Mainz-Kastel	50°00'22.5"N 8°16'49.7"E
R3	Mainz-Kastel	50°01'24.4"N 8°15'51.1"E
R4	Wiesbaden-Biebrich	50°02'14.7"N 8°13'48.6"E
R5	Wiesbaden-Schierstein	50°02'14.3"N 8°10'45.7"E
R6	Walluf	50°01'55.2"N 8°09'26.5"E
R7	Erbach	50°01'03.5"N 8°05'16.0"E
R8	Geisenheim	49°58'52.5"N 7°58'19.0"E

Abbreviation	Location	Coordinates
M1	Mainz-Kostheim	49°59'57.3"N 8°18'25.9"E
M2	Mainz-Kostheim	50°00'08.0"N 8°19'33.7"E

9.1.6 Sorption isotherm experiments

Concentration prepared for the sorption isotherms and respective sampling volumes of the supernatant for the substances CBZ, γ-HCH, and chlorpyrifos are shown in Table 13.

Table 13: Concentration and sampled volume of CBZ, γ-HCH, and chlorpyrifos in the sorption isotherm experiments.

Concentration of the contaminant [ng mL^{-1}]	Sample volume of the supernatant [mL]		
	CBZ	**γ-HCH**	**Chlorpyrifos**
5	0.9	8.0	8.0
10	0.9	8.0	8.0
20	0.9	5.0	5.0
40	0.9	5.0	5.0
75	0.9	2.0	2.0
100	0.1	2.0	2.0
200	0.1	1.0	1.0
350	0.1	1.0	1.0
550	0.1	0.5	0.5
800	0.1	0.5	0.5

9.1.7 Instrument parameters

9.1.7.1 GPC Parameters

The parameters that were used for the GPC clean-up are shown in Table 14. A volume of 100 µL sample was injected into the system.

Table 14: Conditions of the GPC clean-up for the extraction of contaminants from THF-soluble polymer particles

Parameter	Condition
Eluent	THF
Flow rate	1 mL min
Column	PSS SDV Linear M
Detector	off
Fraction collection	9.7-11.3 min
Run time	13 min

9.1.7.2 LC-MS/MS analysis

9.1.7.2.1 LC-MS/MS analysis for the determination of sorption kinetics and sorption isotherms

All LC-MS/MS measurements were carried out on an Agilent 1100 HPLC system coupled to an AB Sciex API 2000 mass spectrometer. The modules used in this setup are described in Table 10. Nitrogen used for the instrument was generated by membrane nitrogen generator NGM-22-LC/MS. The data acquisition and the operation of the instrument were carried out by the Analyst Software (V1.5). For the development of a MRM method to analyze CBZ and EE2, an optimization of the MS parameters was performed by syringe pump injection and by flow injection analysis. The optimization via syringe pump injection was carried out with solutions at a concentration of 1 µg/mL (CBZ) and 5 µg/mL (EE2) in methanol:water 1:1 (v:v), respectively. The optimization was performed manually by the variation of the parameters "declustering potential" (DP), "entering potential", "focusing potential", "collision energy" (CE), and "collision cell exit potential". Flow injection analysis was performed automatically with a solution of CBZ and EE2 at a concentration of 200 ng mL^{-1}, which was injected by the autosampler in a stream of eluent. The flow rate was set to 200 µL min^{-1}. Flow injection analysis was used to optimize the MS parameters "Ion pray voltage", "temperature", "curtain gas", "nebulizer gas", "turbo gas", and "CAD gas". All MS parameter settings are shown in Table 15.

Table 15: Settings of MS parameters used for the analysis of CBZ, EE2, and the mass-labeled internal standards CBZ-D10 and BPA-D16.

Setting	**Value**			
	CBZ	**CBZ-D10**	**EE2**	**BPA-D16**
Ion Spray Voltage [V]	3500	4500	-4500	-4500
Temperature [°C]	400	400	400	400
Curtain Gas [PSI]	25	25	25	25
Nebulizer Gas [PSI]	60	60	55	55
Turbo Gas [PSI]	60	60	65	65
CAD Gas	4	4	6	6
Interface heater	on	on	on	on
Q1 mass (*m/z*)	237	247	295	241
Declustering Potential [V]	30	30	-35	-42
Entering Potential [V]	10	10	-10	-10
Focussing Potential [V]	400	400	-400	-400
Q2 mass (*m/z*)	194 192	204 202	145 143	223 142
Collision Energy [V]	30 34	33 34	-50 -70	-28 -36
Collision Cell Exit Potential [V]	8 5	8 8	-8 -7	-5 -5

The chromatographic conditions were optimized throughout the thesis. For this reason only the final method is presented here.

A MZ Aqua Perfect C18 analytical column (50x2.1 mm, 5 µm) was used for the separation of CBZ and EE2. The injection volume was 25 µL and the flow rate was set to 200 µL min^{-1} for both, CBZ and 40 µL EE2 respectively. For the analysis of CBZ, eluent A consisted of water:methanol 80:20 (v:v) and eluent B consisted of water:methanol 5:95 (v:v). Both eluents contained 5 mM ammonium acetate. EE2 was analyzed with water as eluent A and acetonitrile as eluent B. The chromatographic gradients for both substances are shown in Table 16.

Table 16: Gradients for the chromatographic separation of CBZ and EE2.

CBZ		**EE2**	
Time [min]	Conditions	Time [min]	Conditions
0-2	80% A	0-5	70% A
2-12	80→0% A	5-10	70→20% A
12-14	0% A	10-15	20% A
14-17	0→80% A	15-20	20→70% A
17-27	80% A	20-28	70% A

9.1.7.2.2 LC-MS/MS parameters for the target screening of extracted microplastics

The chromatographic conditions of the target screening method are shown in Table 17. Eluent A consisted of water:methanol 95:5 (v:v) and eluent B consisted of water:methanol 5:95 (v:v), both containing 5 mM ammonium acetate. The flow rate was 200 µL min^{-1}, and the injection volume was set to 20 µL.

Table 17: Chromatographic conditions of the LC-MS/MS target screening method.

Time [min]	**Conditions**
0-1	100% A
1-12	100→0% A
12-22	0% A
22-27	0→100% A
27-37	100% A

The settings of the ion source were equal for all substances and are shown in Table 18.

Table 18: Ion source parameters of the LC-MS/MS target screening method.

Parameter	**CBZ**
Ion Spray Voltage [V]	5500
Temperature [°C]	400
Curtain Gas [PSI]	25
Nebulizer Gas [PSI]	60
Turbo Gas [PSI]	60
CAD Gas	4
Interface heater	on

For each target analyte separate settings for the parameters DP and CE were used to measure the two most intense ions (qualifier and quantifier ions). Parameters and resulting *m/z* ratios used in the MRM method are shown in Table 19. For all substances the same settings were used for "entering potential" (10 V), "focusing potential" (400 V), and "collision cell exit potential" (6V).

Table 19: MRM parameters of the LC-MS/MS screening method including substance name, *m/z* ratios selected in Q1 and Q3, as quantifier and qualifier ion, respectively, as well as the respective declustering potential (DP), and collision energy (CE).

Substance	**Q1/Q3 quantifier [*m/z*]**	**DP [V]**	**CE_{quan} [V]**	**Q1/Q3 qualifier [*m/z*]**	**CE_{qual} [V]**
Furmecyclox	252/170	41	17	252/83	29
Terbutryn	242/186	25	25	242/68	57
Cycloxydim	326/280	61	19	326/180	29
Dithianon	314/162	26	23	314/119	49
Fenhexamide	302/97	91	33	302/55	57
Flurtamon	334/247	51	35	334/247	57
Napropamide	272/129	31	21	272/171	23
Bupropion	240/184	20	15	240/166	25
Fluoxetine	310/148	52	15	310/44	30
Ketoconazol	531/489	76	50	531/82	50
Ranitidine	315/176	36	25	315/130	30
Tramadol	264/246	21	10	264/58	33
Venlafaxine	278/260	21	33	278/121	29
Bixafen	414/394	36	19	414/266	29
Acetyl-sulfadiazine	293/134	41	31	293/108	35
Desmethylvenlafaxine	264/133	43	30	264/107	30

Substance	Q1/Q3 quantifier [*m/z*]	DP [V]	CE_{quan} [V]	Q1/Q3 qualifier [*m/z*]	CE_{qual} [V]
Ivermectine	892/145	25	47	892/113	67
Hydroxybuptopion	256/238	21	15	256/139	37
ABI	134/92	48	31	134/65	41
Batoparazine	232/188	60	37	232/131	69
Amisulprid	370/242	53	37	370/196	55
Bicalutamide	431/217	41	23	431/95	69
CBZ	237/194	30	30	237/192	34
Citalopram	325/262	26	41	325/109	56
Climbazol	293/197	32	21	293/69	31
Desaminometribuzine	200/172	41	23	200/116	31
Fluconazol	307/238	29	21	307/220	21
Irbesartan	429/207	44	33	429/180	64
Lidocain	235/86	44	21	235/58	58
Moclobemid	269/182	32	43	269/139	43
Sulfadiazin	251/156	31	19	251/108	31
Tritosulfaron	446/195	36	25	446/145	50
Benzotriazol	120/92	35	16	120/65	19

9.1.7.3 GC/MS analysis

9.1.7.3.1 GC/MS method for the analysis of the laboratory sorption experiments

The analysis for samples containing β-HCH, γ-HCH, chlorpyrifos, and DDT was carried out on an Agilent 6890N GC system coupled to the mass spectrometer Agilent MSD 5973 inert. As stated for the LC-MS/MS analysis in 9.1.7.2.2, conditions for the GC/MS measurements were also optimized throughout the thesis and only the final methods are presented here. For the identification of the analytes, standard solutions for each compound at a concentration of 100 ng mL^{-1} were injected. The MS was operated in Scan mode to collect mass spectra of each compound. The two most intense peaks were selected from the mass spectra and used as quantifier ion and qualifier ion in a SIM method. All GC/MS parameters used and selected *m/z* ratios are shown in Table 20.

Table 20: Parameters for the GC/MS analysis.

Parameter	β-HCH	γ-HCH	Chlorpyrifos	DDT
Quantifier ion	181	181	314	235
Qualifier ion	219	219	199	237

Parameter	Value
Carrier Gas	Helium
Inlet	Pulsed Splitless
Heater	250 °C
Injection pulse pressure	100 kPa
Injection volume	1 µL
Purge flow to split	60 mL/min
Oven profile	50 °C for 0.75 min, 20 °C/min to 120 °C; 4 °C/min to 230 °C, 10 °C/min to 290 °C Post run: 290 °C for 10 min
Mode	Constant Flow
Column	HP-5MS, 0.25 mm x 30 m x 0.25 µm
MSD	5973 inert
Transfer line temperature	280 °C
Source temperature	230 °C
Solvent delay	10 min

9.1.7.3.2 GC/MS screening method for analysis of microplastic extracts in SIM mode and Scan mode

The analysis of extracts from PE and PS particles that were separated from sediments was carried out by GC/MS in SIM mode and SCAN mode, respectively. The parameters of the SIM method are shown in Table 21.

Table 21: GC parameters used in the SIM method.

Parameter	Value
Carrier Gas	Helium
Inlet	Pulsed Splitless
Heater	250 °C
Injection pulse pressure	60 kPa
Injection volume	1 µL
Purge flow to split	60 mL/min
Oven profile	50 °C for 0.75 min, 20 °C/min to 120 °C; 1.5 °C/min to 230 °C, 10 °C/min to 290 °C Post run: 290 °C for 10 min
Mode	Constant Flow
Column	HP-5MS, 0.25 mm x 30 m x 0.25 µm
MSD	5973 inert
Transfer line temperature	280 °C

Source temperature	230 °C
Solvent delay	10 min

The *m/z* ratios that were used for the identification of the substances as quantifier and qualifier ions are shown in Table 22.

Table 22: Substances comprised and *m/z* ratios used in the GC/MS screening method as quantifier and qualifier ions.

Name	**Quantifier ion [*m/z*]**	**Qualifier ion [*m/z*]**
Alachlor	188	160
Ametryn	227	212
Azinphos-ethyl	160	132
Azinphos-methyl	160	132
Bifenox	281	341
Chlordane	373	375
Chlorfenvinphos	323	267
Chlorpyrifos	314	199
Coumaphos	226	362
Cyprodinil	225	224
DDT	235	237
Diethyltoluolamide	19	119
Demethon-S	170	88
Desmetryn	213	198
Dichlobenil	171	173
Dichlorovos	185	109
Diclofol	139	250
Dimethoate	125	87
Disulfoton	186	88
Endosulfan	241	195
Endosulfansulfate	387	272
Etrimfos	292	168
Fenitrothion	277	260
Fenprophimorph	303	128
Fenthion	278	169
Fluchoralin	326	306
Fluralaxyl	242	95
β-HCH	181	219
γ-HCH	181	219
Heptachlor	272	274
Heptachlorepoxid	353	355

Name	Quantifier ion [*m/z*]	Qualifier ion [*m/z*]
Iprodion	314	316
Kresoxim-methyl	131	116
Malathion	173	125
Methidathion	145	85
Mevinphos	127	109
Parathion-ethyl	291	109
Parathion-methyl	263	128
Pentimethalin	252	162
Pentobarbital	156	141
Phenobarbital	204	117
Phenanthrene	178	176
Picolinafen	238	376
Propham	179	93
Pyrene	202	201
Quinoxyfen	72	237
TBP	155	99
TCEP	249	251
TDCP	191	381
TPP	326	77
TPPO	277	125
Trazophos	208	161
Trifluralin	306	264
Vinclozolin	285	212

Additionally to the GC/MS analysis in SIM mode, all PE and PS particles were analyzed via GC/MS operated in Scan mode. The parameters for the GC/MS analysis are shown in Table 23.

Table 23: GC/MS parameters for the GC/MS analysis in Scan mode

Parameter	Value
Carrier Gas	Helium
Inlet	Pulsed Splitless
Heater	250 °C
Injection pulse pressure	100 kPa
Injection volume	1 µL
Purge flow to split	60 mL/min
Oven profile	60 °C for 0.75 min, 20 °C/min to 120 °C; 2 °C/min to 230 °C, 10 °C/min to 290 °C

Parameter	**Value**
	Post run: 290 °C for 10 min
Mode	Constant Flow
Column	HP-5MS, 0.25 mm x 30 m x 0.25 µm
MSD	5973 inert
Transfer line temperature	280 °C
Source temperature	230 °C
Solvent delay	10 min
Scan range	*m/z* 60 to *m/z* 450
Threshold	150 counts

9.2 Investigations on microplastic abundance in river shore sediments

9.2.1 Identification of microplastics via FTIR

Figure 38 shows exemplary FTIR spectra obtained for the identification of polymer particles of the size fraction 630-5000 µm via FTIR.

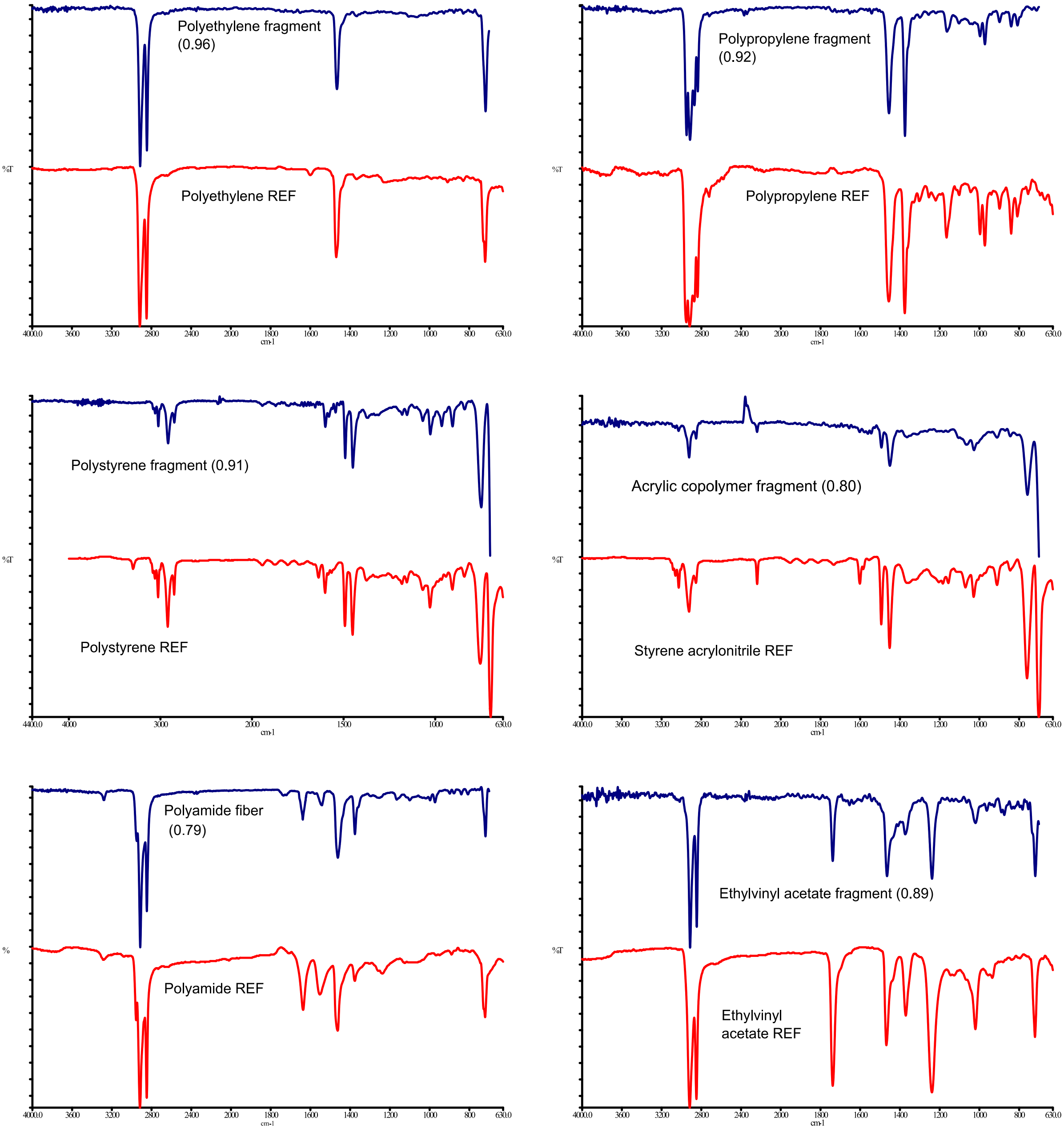

Figure 38: IR spectra of PE, PP, PS, acrylic polymer, PA, and EVA, compared to reference spectra (REF). Match factors are shown in brackets.

9.2.2 Investigations on blank values

Blank samples were determined for every step involved in the analysis of microplastics (refer to 4.2.6.1). Blank values were very low, except for the size fraction smaller than 63 µm that was therefore not included in the analysis of the sediment samples (Table 24). Control samples that were used to determine the blank values consisted of commercially available clean sand. Blanks were analyzed for single steps in the method, such as the density separation or combined steps such as sieving followed by a density separation or the complete sample preparation including the destruction of natural debris. To estimate a possible contamination of the wide-neck cans used for the sampling of sediments, clean sand was analyzed after storage and shaking in the wide-neck can.

Table 24: Blank values obtained after sieving of clean sand, shaking of wide-neck cans filled with clean sand, blank values of the density separation only and the blank values of the complete method. Control samples that were analyzed with the sediment samples are shown as "Mean blank value". Blank values are given as absolute particle numbers. Standard deviation is shown in parentheses.

	< 63 µm	63-200 µm	200-630 µm	630-5000 µm
Density separation	55 (21)	2 (3)	1 (1)	0 (0)
Shaking of wide-neck cans	45 (56)	3 (1)	0 (0)	0 (0)
Sieving of clean sand	74 (45)	1 (2)	1 (1)	0 (0)
Complete method	85 (41)	2 (2)	0 (0)	0 (0)
Mean blank value	n/a	3 (2)	1 (1)	0 (0)

9.2.3 Analysis of microplastics in shore sediments

Exact values for the microplastic concentrations that were separated from river shore sediments are provided in Table 25 and Table 26.

Table 25: Mass fraction of plastic in the sediments analyzed. All values are given in mg kg^{-1}.

Size fraction		63-200 µm	200-630 µm	630-5000 µm	Total
Sample location	S1	0.9	1.1	16.0	18.2
	S2	1.1	1.3	89	91.4
	R1	1.5	4.4	109.8	115.7
	M1	2.5	2.7	38.3	43.5
	M2	5.2	55.4	398.9	459.4
	R2	7.0	4.3	500.6	511.9
	R3	7.0	135.2	791.3	933.5
	R4	2.5	3.4	228.7	234.6
	R5	1.2	3.2	63.2	67.6
	R6	1.4	3.7	47.7	52.8
	R7	2.1	3.8	15.9	21.8
	R8	1.9	7.2	111.6	120.7

Moreover, in Table 26 an estimation of the particle number per m² is shown. To estimate area-related results for this study, the sediment mass-related values were transformed. This was done by the known sampled volume of sediment that was approximately 2.5 L, given by the sampling vessels. The volume was transformed to an area with the lowest sampling depth (2 cm) resulting in an area of 0.125 m². Thus, the transformation of the “particles kg^{-1}” to “particles m^{-2}” was done by multiplying the results with a factor of eight.

Table 26: Number of plastic items in the sediments analyzed. All values are given as plastic particles kg^{-1} except the estimation of total amount of microplastics for area-related results. Although exact numbers are provided, these should be considered as estimation.

Size fraction		63-200 µm	200-630 µm	630-5000 µm	Total	Total (particle m^{-2})
Sample location	S1	110	51	6	167	1336
	S2	178	111	18	307	2456
	R1	189	134	36	359	2870
	M1	685	75	27	786	6289
	M2	727	565	76	1368	10945
	R2	564	192	126	881	7054
	R3	2448	923	393	3763	30106
	R4	433	122	66	620	4966
	R5	145	99	24	268	2144
	R6	129	78	16	228	1784
	R7	217	90	8	314	2512
	R8	258	159	37	455	3632

9.3 Investigation on sorption of contaminants on microplastics

9.3.1 Polymer particle characterization

Particle size measurements were done via microscopy to determine the particle size of the polymers that are used for the laboratory scale sorption experiments. Therefore the polymer powders were ground to homogenize the powders prior the size determination. The measurements were carried out essentially as the measurements of the microplastic particles from sediment samples. Particle size distribution Q_0 of the polymers PC, PMMA, PS, and PVC was calculated by the equation

$$Q_0(x_i) = \frac{N_i}{N}$$

where N_i is the number of particles smaller or equal to the particle diameter x_i, and N is the total particle number.

The resulting particle size distributions based on the particle numbers are shown in Figure 39.

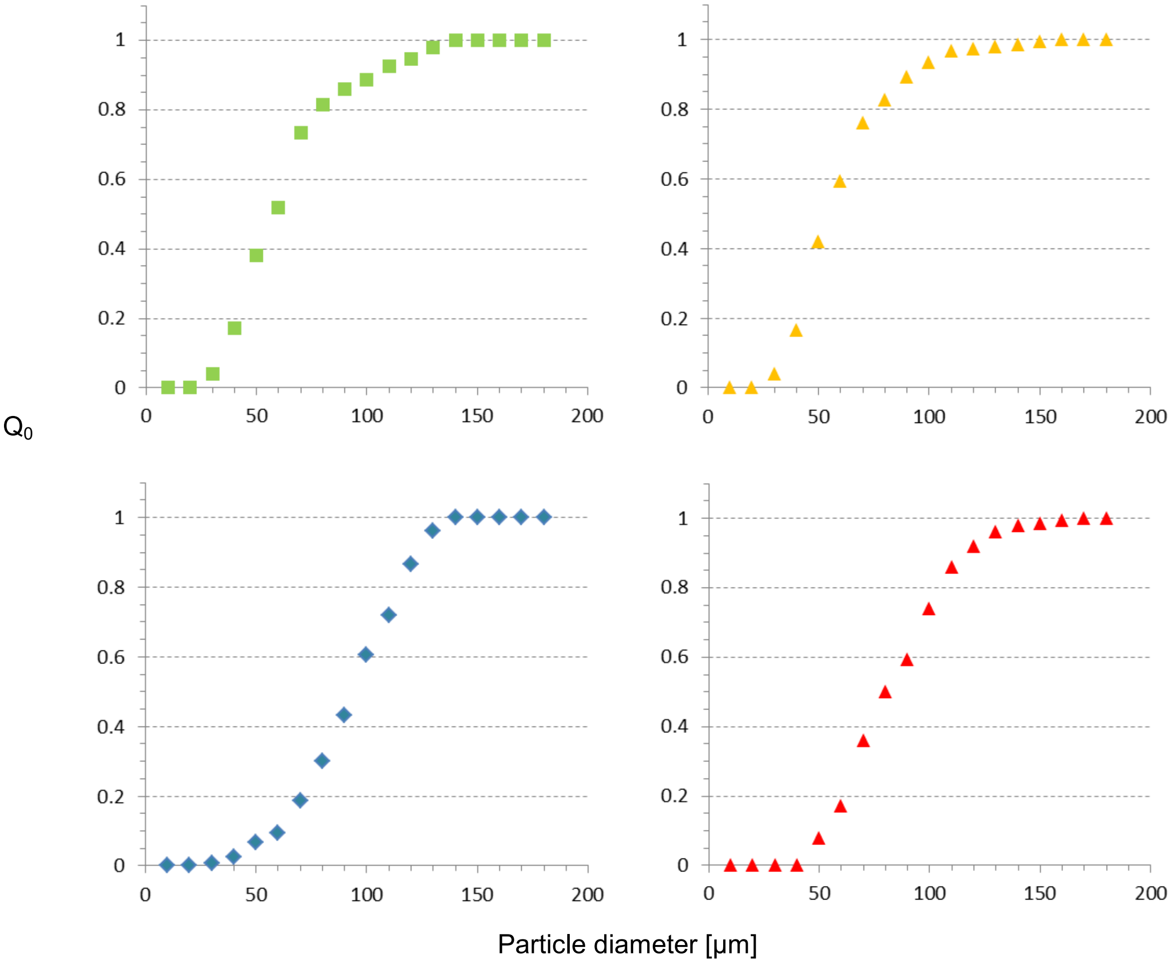

Figure 39: Particle size distribution based on the particle number of the polymer powders PC (green) PMMA (yellow), PS (teal), and PVC (red). Size distributions were obtained by microscopic measurement of 200 particles.

The corresponding particle density distributions are shown in Figure 40. The particle size analysis showed that all polymer powders used for the sorption experiments were of comparable size after grinding of the powder. Microscopic analysis showed an equal surface structure. Thus, it can be assumed that all dry polymer powder had a comparable surface area. It need to be addressed that the polymers tend to aggregate and were floating on the water surface. Therefore, the surface of the polymer powder in an aqueous solution could not be estimated exactly, and all results concerning sorption are referred to the particle weight only.

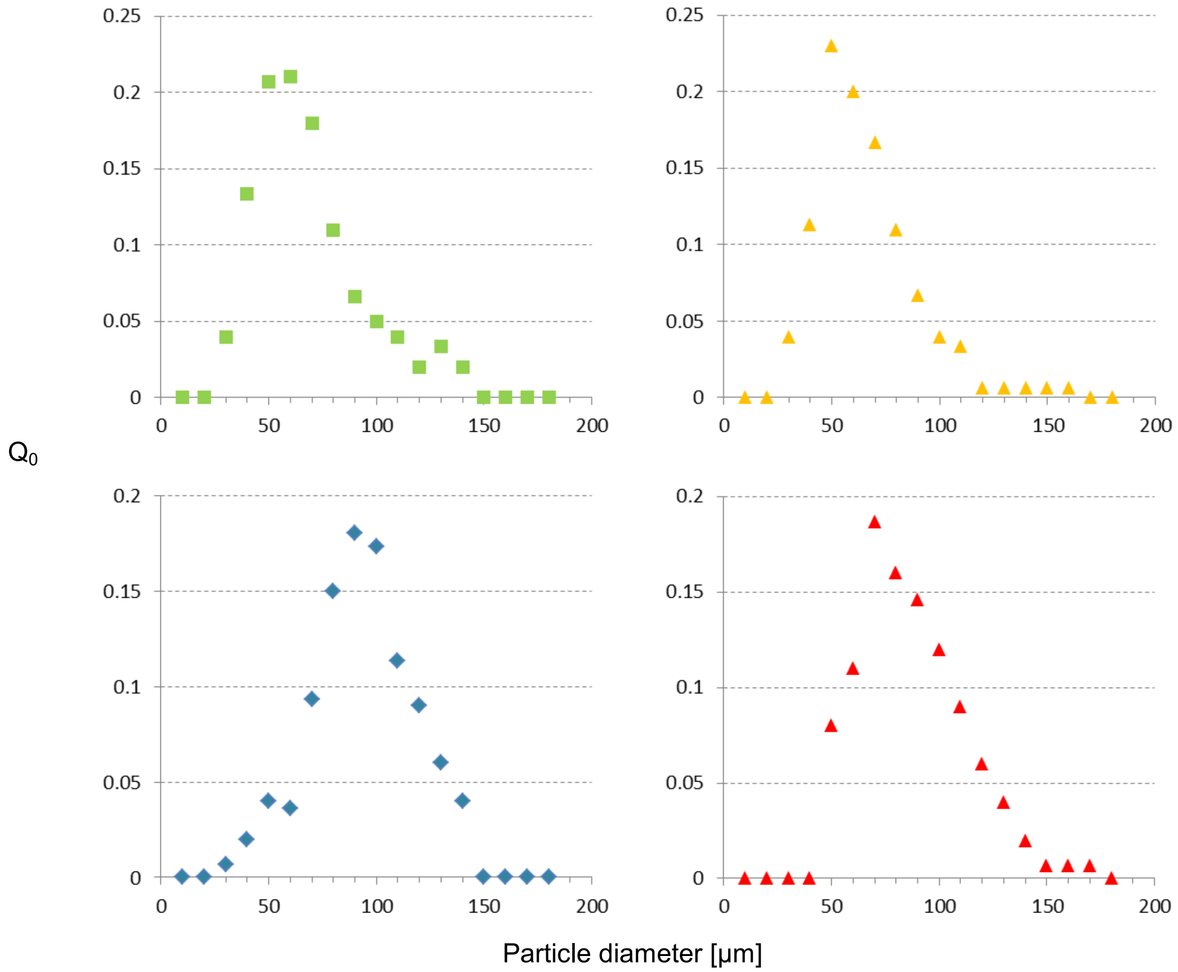

Figure 40: Particle density distribution based on the particle number of the polymer powders PC (green) PMMA (yellow), PS (teal), and PVC (red). The particle density distributions were obtained by microscopic measurement of 200 particles.

9.3.2 Control samples of the sorption kinetics experiments

The detailed trend of the control samples of the sorption kinetics experiments are shown in Figure 41. The control samples were prepared and treated the same as the sorption batch experiments with polymers, but did not contain polymer particles. The aqueous concentration of each substance stayed constant at the initial concentration except for β-HCH and DDT. Here the aqueous concentration dropped to approximately 20% or 5% of the initial concentration of β-HCH or DDT, respectively. As discussed for the experiments of EE2 with polymer particles, the determination of EE2 was

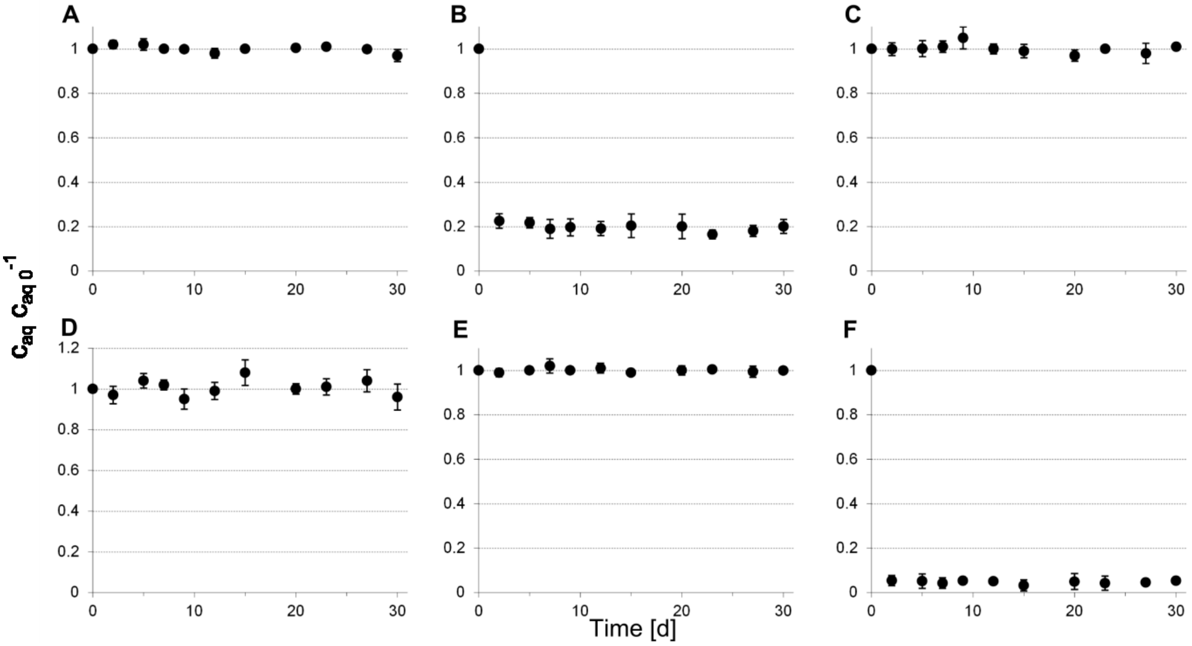

Figure 41: Control samples of the sorption kinetics experiments of CBZ **(A)**, β-HCH **(B)**, γ-HCH **(C)**, EE2 **(D)**, chlorpyrifos **(E)**, and DDT **(F)**. Measurements were done with two independent controls samples for each substance.

9.3.3 Determination of sorption kinetics

Detailed model curves of a pseudo-first-order rate law for the sorption of CBZ, γ-HCH, EE2, and chlorpyrifos to the polymers PC, PMMA, EPS, and PVC are provided in Figure 42Figure 44.

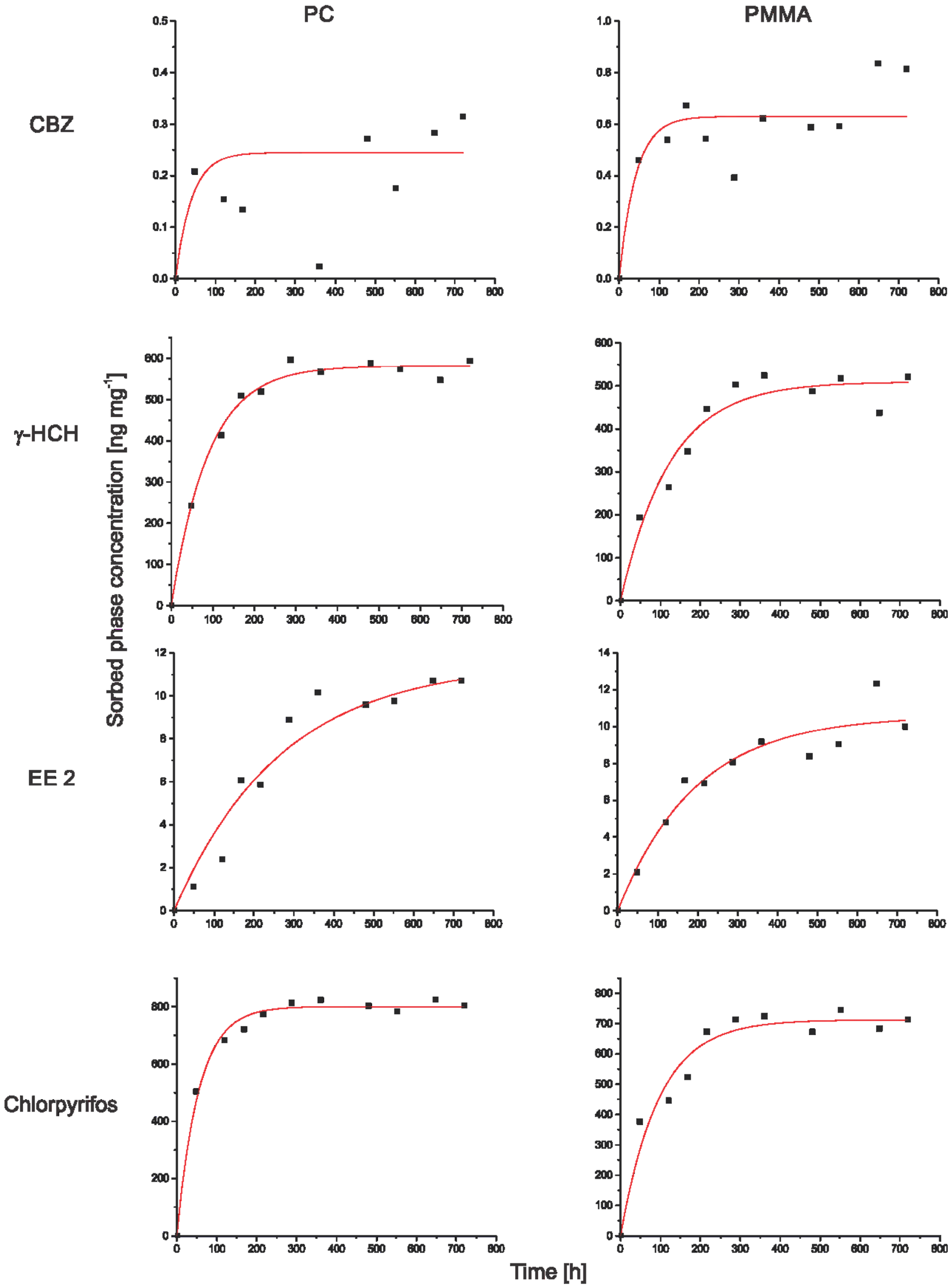

Figure 42: Sorption kinetics model curves applying a pseudo-first-order rate law for the polymers PMMA and PVC and the model substances CBZ, γ-HCH, EE2, and chlorpyrifos.

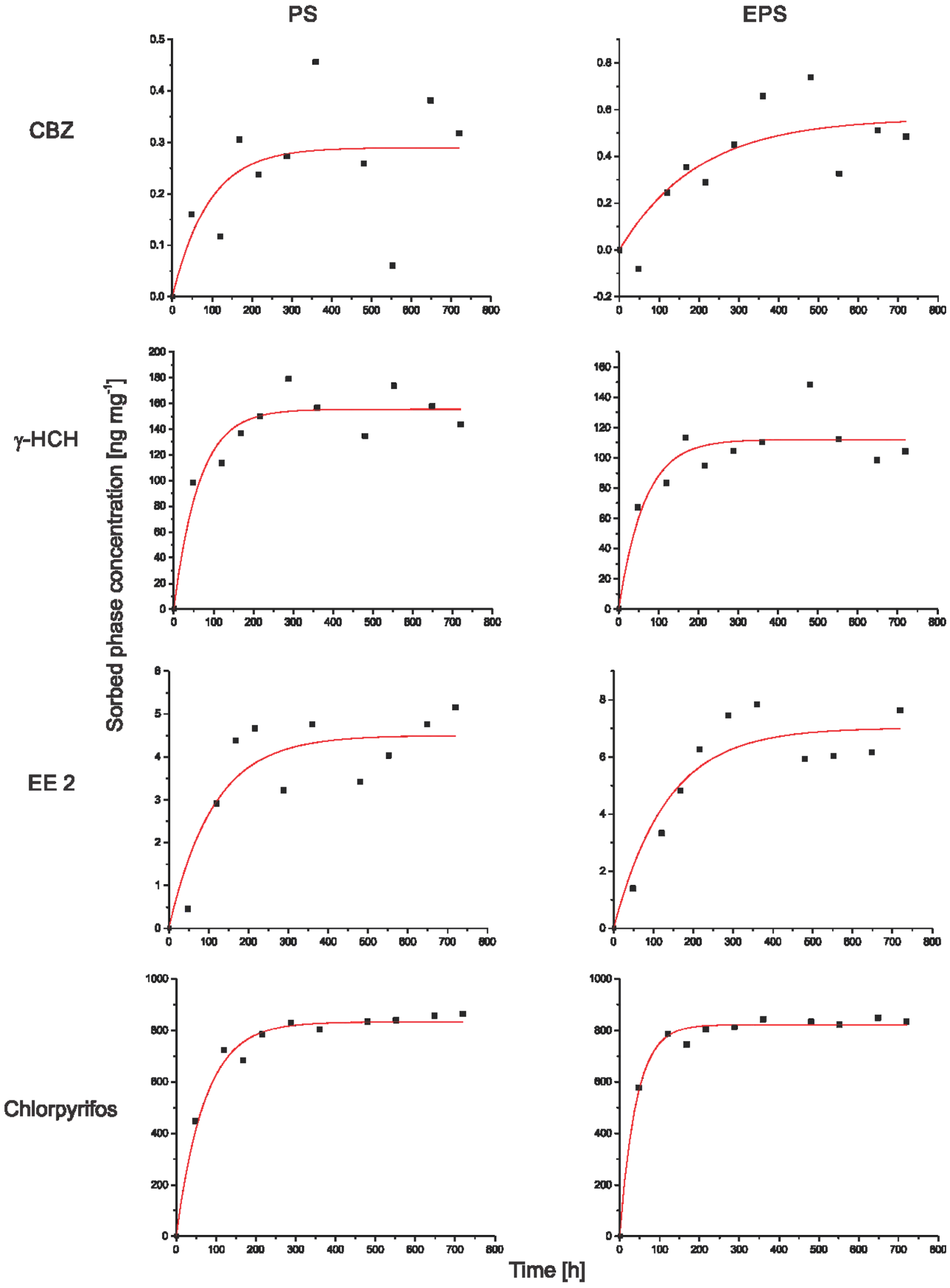

Figure 43: Sorption kinetics model curves applying a pseudo-first-order rate law for the polymers PS and EPS and the model substances CBZ, γ-HCH, EE2, and chlorpyrifos.

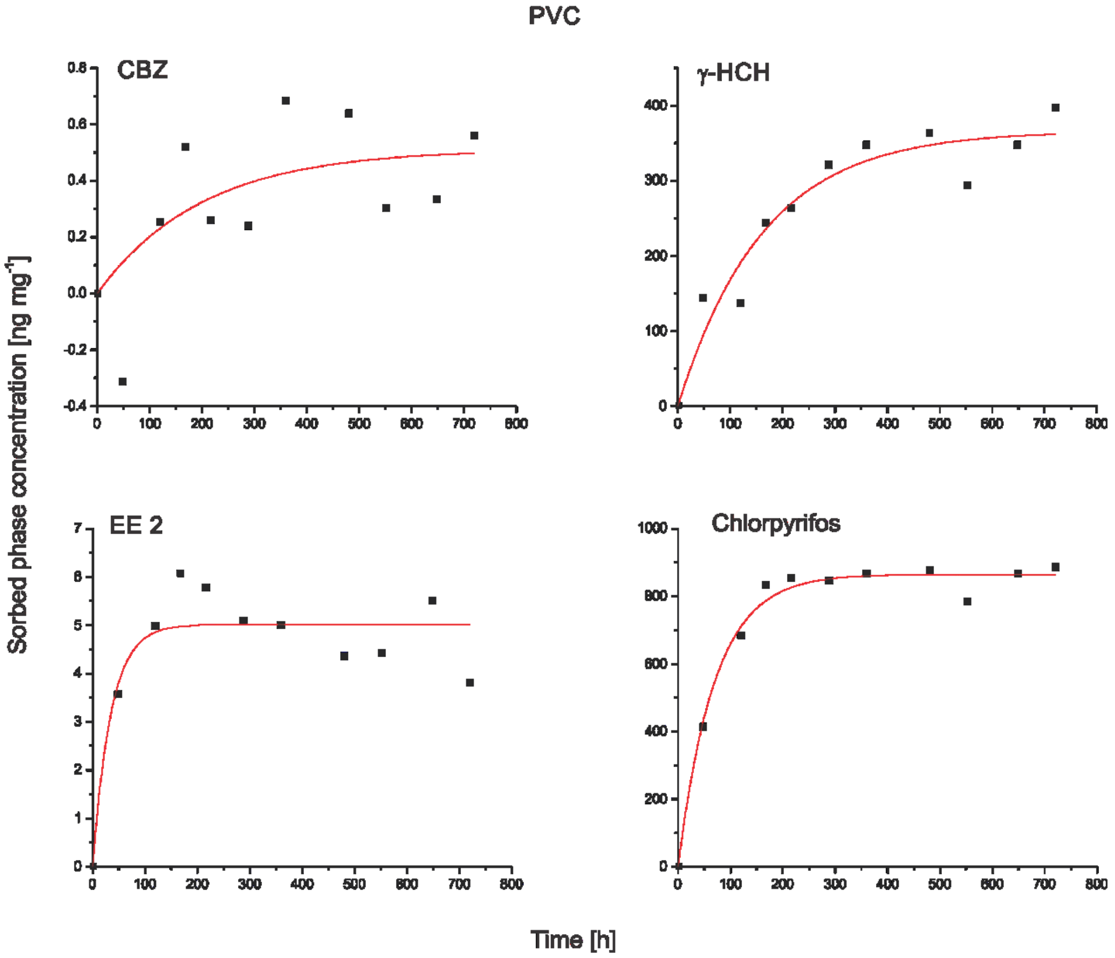

Figure 44: Sorption kinetics model curves applying a pseudo-first-order rate law for the polymer PVC and the model substances CBZ, γ-HCH, EE2, and chlorpyrifos.

9.4 Extraction via dissolution with subsequent GPC clean-up

Extraction of plastic particles via dissolution is a viable technique and often used for the extraction of e.g. polymer additives. Therefore the polymer is dissolved in a suitable solvent, resulting in a complete extraction of the particle. For the analysis of the extracted compounds a clean-up step needed to be carried out to reduce the amount of matrix that is interfering during the chromatographic separation or the detection of the analyte.

GPC offers the possibility to separate the large polymer molecules that represent most of the interfering matrix. To develop a fast clean up method the elution time of small particles was determined after injection of a standard solution containing 1 µm mL^{-1} in a GPC system (parameters of the GPC are shown in Table 14. Twelve Fractions were collected in intervals of 20 s between 8.5 and 12.5 min. Each of the fractions was prepared as described in 4.3.1.3 and subsequently analyzed via LC-MS/MS. The elution of CBZ is shown in Figure 45 and was calculated via the recovered CBZ in each fraction.

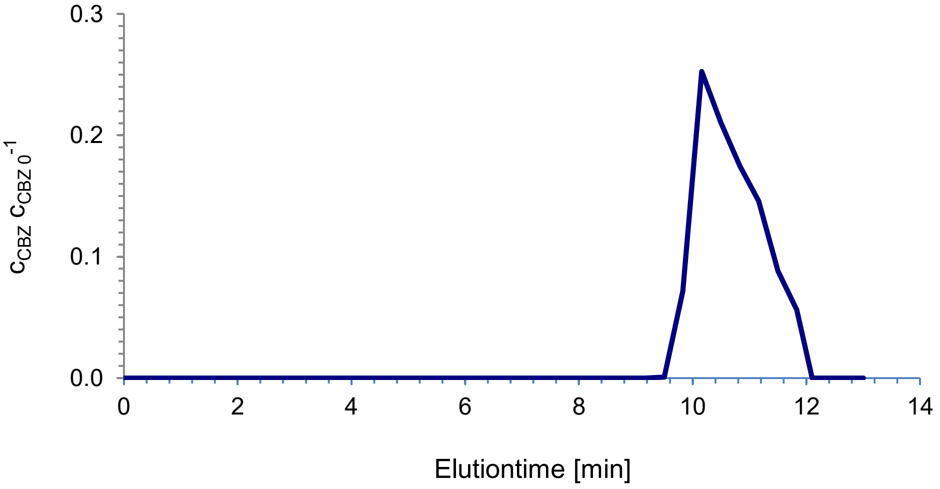

Figure 45: Elution time of CBZ on a GPC system equipped with a PSS SDV linear M column using THF as eluent. CBZ was measured by LC-MS/MS after collecting 12 fractions between 8.5 and 12.5 min.

CBZ showed a relatively broad peak between 9-12 min. To determine a suitable collection time for the clean-up procedure and evaluate the separation power of this method, CBZ was spiked to PMMA particles that were used for the sorption experiments. PMMA (10 mg) was dissolved in THF and CBZ (10 µg L^{-1}) was spiked to the solution and mixed vigorously. The solution was injected into the GPC system as described previously. A sufficient separation of the low molecular weight polymer ($M_{W\ PMMA}$ 3471 g mol^{-1}) and the model substance CBZ was observed (Figure 46A). Both peaks are not baseline separated, but fraction collection between 9.7-11.3 min resulted in reproducible results. As this interval does not cover 100% of the elution time of the model substance CBZ, the use of an internal standard is mandatory. Subsequent LC-MS/MS measurement of the purified extract after solvent change to methanol/water resulted in clean chromatograms of CBZ. For the lowest tested concentration (0.1 ng mg^{-1}) of CBZ a signal-to-noise ratio of 21 was observed, indicating the good applicability of the extraction method (Figure 46B).

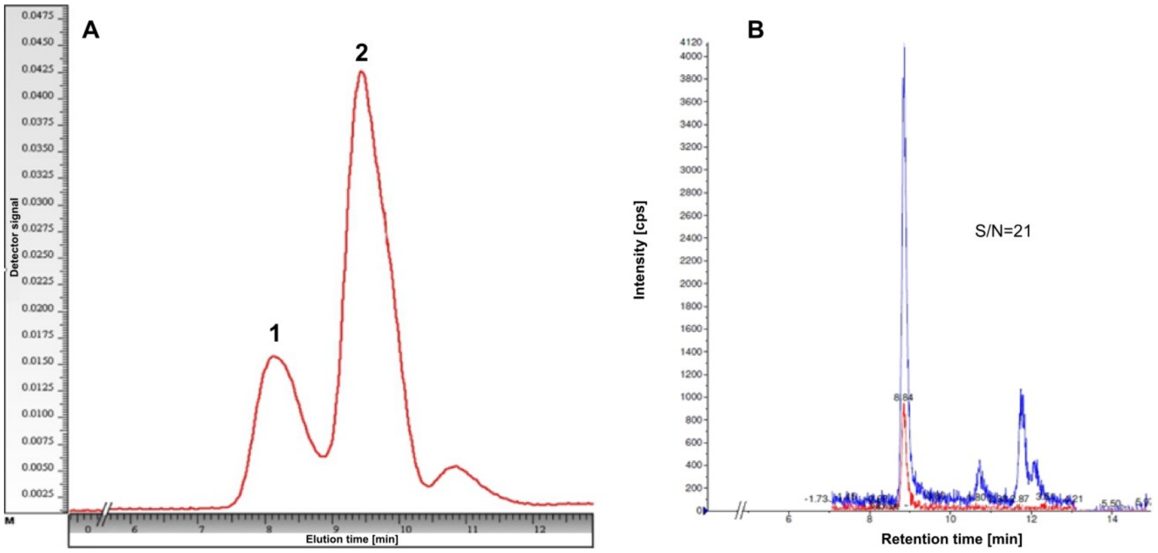

Figure 46: (A) GPC chromatogram of the separation of PMMA (1) and CBZ (2) after detection by a refractive index detector. **(B)** LC-MS/MS chromatogram of 0.1 ng mg^{-1} CBZ after measured after GPC separation from PMMA. Chromatograms of the quantifier ion (blue line) and the qualifier ion (red line) including the signal-to-noise ratio (S/N) of the quantifier ion are shown.

The method was validated by spiking each of the model substances (CBZ, β-HCH, γ-HCH, EE2, chlorpyrifos, and DDT) at a concentration close to the respective limit of quantification to polystyrene particles (PS168). The substances were extracted from PS via dissolution and subsequent GPC clean-up and analyzed via LC-MS/MS or GC/MS. Recoveries of the substances were determined with and without the use of internal standards. Additionally, substances that were analyzed via GC/MS were quantified using an internal calibration (refer to 4.4.1). The recovery experiments revealed good recoveries (89-101%) for all substances if using an internal standard except DDT (52%). Comparable low recovery without the application of an internal standard (47-81%) can be explained by the fraction collection period that did not cover the entire elution time of the analyte. However, the recovery of DDT did not improve if using an internal standard. This could be related to structural differences between the internal standard (atrazine) and the analyte. DDT possibly interacts with the column material of the GPC column that is made of styrene-divinylbenzene via hydrophobic or π-π interactions, resulting in a prolonged elution time. The extension of the fraction collection window by 1 min did not increase the recovery of DDT significantly (61%). Nevertheless, an acceptable recovery for was obtained

Table 27: Recovery of the substances CBZ, β-HCH, γ-HCH, EE2, chlorpyrifos, and DDT after GPC clean-up and analysis by LC-MS/MS or GC/MS, respectively. Recovery was determined with and without the use of an internal standard (ISTD). GC/MS analysis was additionally carried out with an internal calibration. Standard deviation of a triplicate analysis is shown in parentheses.

Substance	**Recovery [%]**		
	w/o ISTD	**with ISTD**	**with Internal calibration**
CBZ	81.1 (7.5)	93.3 (5.7)	n/a
β-HCH	75.3 (8.1)	100.7 (6.4)	99.6 (3.4)
γ-HCH	78.4 (9.2)	99.8 (3.3)	99.5 (2.1)
EE2	69.1 (9.5)	89.0 (5.8)	n/a
chlorpyrifos	71.2 (9.2)	91.8 (4.3)	92.9 (4.2)
DDT	46.5 (5.6)	51.6 (2.2)	89.4 (5.8)

10 References

1. Koltzenburg, S.; Maskos, M.; Nuyken, O., *Polymere: Synthese, Eigenschaften und Anwendungen*. Springer: **2014**.

2. Andrady, A. L.; Neal, M. A., Applications and societal benefits of plastics. *Philosophical transactions of the Royal Society of London. Series B, Biological sciences* **2009,** *364*, (1526), 1977-84.

3. PlasticsEurope, Plastics - The Facts 2014/2015: An analysus of European plastics production, demand and waste date. *Association of Plastic Manufacturers* **2015**.

4. Hidalgo-Ruz, V.; Gutow, L.; Thompson, R. C.; Thiel, M., Microplastics in the marine environment: a review of the methods used for identification and quantification. *Environ. Sci. Technol.* **2012,** *46*, (6), 3060-75.

5. Automation Creations, Inc., MatWeb - Material Property Data. In **2015**.

6. Carpenter, E. J.; Smith, K. L., Plastics on the Sargasso Sea Surface. *Science* **1972,** *175*, (4027), 1240-1241.

7. Carpenter, E. J.; Anderson, S. J.; Harvey, G. R.; Miklas, H. P.; Peck, B. B., Polystyrene Spherules in Coastal Waters. *Science* **1972,** *178*, (4062), 749-750.

8. Colton, J. B.; Burns, B. R.; Knapp, Frederick D., Plastic Particles in Surface Waters of the Northwestern Atlantic. *Science* **1974,** *185*, (4150), 491-497.

9. Gregory, M. R., Plastics and South Pacific Island shores: environmental implications. *Ocean Coast Manage* **1999,** *42*, (6–7), 603-615.

10. Convey, P.; Barnes, D. K. A.; Morton, A., Debris accumulation on oceanic island shores of the Scotia Arc, Antarctica. *Polar Biol* **2002,** *25*, (8), 612-617.

11. Derraik, J. G. B., The pollution of the marine environment by plastic debris: a review. *Mar Pollut Bull* **2002,** *44*, (9), 842-852.

12. Cunningham, D. J.; Wilson, S. P., Marine debris on beaches of the Greater Sydney Region. *J Coastal Res* **2003,** *19*, (2), 421-430.

13. Barnes, D. K. A.; Walters, A.; Goncalves, L., Macroplastics at sea around Antarctica. *Mar Environ Res* **2010,** *70*, (2), 250-252.

14. Thiel, M.; Hinojosa, I.; Vasquez, N.; Macaya, E., Floating marine debris in coastal waters of the SE-Pacific (Chile). *Mar Pollut Bull* **2003,** *46*, (2), 224-231.

15. Moore, C. J.; Moore, S. L.; Leecaster, M. K.; Weisberg, S. B., A comparison of plastic and plankton in the North Pacific central gyre. *Mar Pollut Bull* **2001,** *42*, (12), 1297-1300.

16. Law, K. L.; Moret-Ferguson, S.; Maximenko, N. A.; Proskurowski, G.; Peacock, E. E.; Hafner, J.; Reddy, C. M., Plastic Accumulation in the North Atlantic Subtropical Gyre. *Science* **2010,** *329*, (5996), 1185-1188.

17. Eriksen, M.; Cummins, A.; Maximenko, N.; Thiel, M.; Lattin, G.; Wilson, S.; Hafner, J.; Zellers, A.; Rifman, S., Plastic Pollution in the South Pacific Subtropical Gyre. *Plast Eng* **2013,** *69*, (5), 38-+.

18. Donohue, M. J., Eastern Pacific Ocean source of Northwestern Hawaiian Islands marine debris supported by errant fish aggregating device. *Mar Pollut Bull* **2005,** *50*, (8), 886-888.

19. Michelle Allsopp, A. W., David Santillo, Paul Johnston *Plastic Debris in the World's Oceans*; Greenpeace International: Amsterdam, **2006**.

20. Jambeck, J. R.; Geyer, R.; Wilcox, C.; Siegler, T. R.; Perryman, M.; Andrady, A.; Narayan, R.; Law, K. L., Plastic waste inputs from land into the ocean. *Science* **2015,** *347*, (6223), 768-771.

21. Rech, S.; Macaya-Caquilpán, V.; Pantoja, J. F.; Rivadeneira, M. M.; Jofre Madariaga, D.; Thiel, M., Rivers as a source of marine litter – A study from the SE Pacific. *Mar Pollut Bull* **2014,** *82*, (1–2), 66-75.

22. Gregory, M. R., Environmental implications of plastic debris in marine settings-entanglement, ingestion, smothering, hangers-on, hitch-hiking and alien invasions. *Philos T R Soc B* **2009,** *364*, (1526), 2013-2025.

23. Barnes, D. K. A., Biodiversity - Invasions by marine life on plastic debris. *Nature* **2002,** *416*, (6883), 808-809.

24. Gonzalez-Zevallos, D.; Yario, P.; Caille, G., Seabird mortality at trawler warp cables and a proposed mitigation measure: A case of study in Golfo San Jorge, Patagonia, Argentina. *Biol Conserv* **2007,** *136*, (1), 108-116.

25. Copello, S.; Quintana, F., Marine debris ingestion by Southern Giant Petrels and its potential relationships with fisheries in the Southern Atlantic Ocean. *Mar Pollut Bull* **2003,** *46*, (11), 1513-1515.

26. Colabuono, F. I.; Barquete, V.; Domingues, B. S.; Montone, R. C., Plastic ingestion by Procellariiformes in Southern Brazil. *Mar Pollut Bull* **2009,** *58*, (1), 93-96.

27. Mrosovsky, N.; Ryan, G. D.; James, M. C., Leatherback turtles: The menace of plastic. *Mar Pollut Bull* **2009,** *58*, (2), 287-289.

28. Davison, P.; Asch, R. G., Plastic ingestion by mesopelagic fishes in the North Pacific Subtropical Gyre. *Mar Ecol-Prog Ser* **2011,** *432*, 173-180.

29. Mallory, M. L.; Roberston, J.; Moenting, A., Marine plastic debris in northern fulmars from Davis Strait, Nunavut, Canada. *Mar Pollut Bull* **2006,** *52*, (7), 813-815.

30. Eubeler, J. P.; Zok, S.; Bernhard, M.; Knepper, T. P., Environmental biodegradation of synthetic polymers I. Test methodologies and procedures. *TrAC, Trends Anal. Chem.* **2009,** *28*, (9), 1057-1072.

31. Eubeler, J. P.; Bernhard, M.; Knepper, T. P., Environmental biodegradation of synthetic polymers II. Biodegradation of different polymer groups. *Trac-Trend Anal Chem* **2010,** *29*, (1), 84-100.

32. Andrady, A. L., Microplastics in the marine environment. *Mar Pollut Bull* **2011,** *62*, (8), 1596-605.

33. Andrady, A. L.; Pegram, J. E.; Song, Y., Studies on enhanced degradable plastics. II. Weathering of enhanced photodegradable polyethylenes under marine and freshwater floating exposure. *J Environ Polym Degr* **1993,** *1*, (2), 117-126.

34. Anderson, D. A.; Freeman, E. S., The kinetics of the thermal degradation of polystyrene and polyethylene. *Journal of Polymer Science* **1961,** *54*, (159), 253-260.

35. McNeill, I. C.; Leiper, H. A., Degradation studies of some polyesters and polycarbonates—2. Polylactide: Degradation under isothermal conditions, thermal degradation mechanism and photolysis of the polymer. *Polym. Degrad. Stab.* **1985,** *11*, (4), 309-326.

36. Duwez, A. S.; Nysten, B., Mapping Aging Effects on Polymer Surfaces: Specific Detection of Additives by Chemical Force Microscopy. *Langmuir : the ACS journal of surfaces and colloids* **2001,** *17*, (26), 8287-8292.

37. Gu, J.-D., Microbiological deterioration and degradation of synthetic polymeric materials: recent research advances. *Int Biodeter Biodegr* **2003,** *52*, (2), 69-91.

38. Arthur, C., Baker, J., and Bamford, H., Proceedings of the International Research Workshop on the Occurrence, Effects, and Fate of Micro-plastic Marine Debris. In NOAA Technical Memorandum NOS-OR&R-30: **2009**.

39. Claessens, M.; Meester, S. D.; Landuyt, L. V.; Clerck, K. D.; Janssen, C. R., Occurrence and distribution of microplastics in marine sediments along the Belgian coast. *Mar Pollut Bull* **2011,** *62*, (10), 2199-2204.

40. Van Cauwenberghe, L.; Claessens, M.; Vandegehuchte, M. B.; Mees, J.; Janssen, C. R., Assessment of marine debris on the Belgian Continental Shelf. *Mar Pollut Bull* **2013,** *73*, (1), 161-169.

41. Wright, S. L.; Thompson, R. C.; Galloway, T. S., The physical impacts of microplastics on marine organisms: A review. *Environmental Pollution* **2013,** *178*, 483-492.

42. European Parliament and the Council, Directive 2008/56/EC of the European Parliament and of the Council of 17 June 2008 establishing a framework for community action in the field of marine environmental policy (Marine Strategy Framework Directive). In Brussels, **2008**.

43. Imhof, H. K.; Schmid, J.; Niessner, R.; Ivleva, N. P.; Laforsch, C., A novel, highly efficient method for the separation and quantification of plastic particles in sediments of aquatic environments. *Limnol Oceanogr-Meth* **2012,** *10*, 524-537.

44. Imhof, H. K.; Ivleva, N. P.; Schmid, J.; Niessner, R.; Laforsch, C., Contamination of beach sediments of a subalpine lake with microplastic particles. *Current biology : CB* **2013,** *23*, (19), R867-R868.

45. Dekiff, J. H.; Remy, D.; Klasmeier, J.; Fries, E., Occurrence and spatial distribution of microplastics in sediments from Norderney. *Environ. Pollut.* **2014,** *186*, 248-56.

46. Heo, N.; Hong, S.; Han, G.; Hong, S.; Lee, J.; Song, Y.; Jang, M.; Shim, W., Distribution of small plastic debris in cross-section and high strandline on Heungnam beach, South Korea. *Ocean Sci. J.* **2013,** *48*, (2), 225-233.

47. Lee, J.; Hong, S.; Song, Y. K.; Hong, S. H.; Jang, Y. C.; Jang, M.; Heo, N. W.; Han, G. M.; Lee, M. J.; Kang, D.; Shim, W. J., Relationships among the abundances of plastic debris in different size classes on beaches in South Korea. *Mar Pollut Bull* **2013,** *77*, (1–2), 349-354.

48. Isobe, A.; Kubo, K.; Tamura, Y.; Kako, S. i.; Nakashima, E.; Fujii, N., Selective transport of microplastics and mesoplastics by drifting in coastal waters. *Mar Pollut Bull* **2014,** *89*, (1–2), 324-330.

49. Collignon, A.; Hecq, J.-H.; Galgani, F.; Collard, F.; Goffart, A., Annual variation in neustonic micro- and meso-plastic particles and zooplankton in the Bay of Calvi (Mediterranean–Corsica). *Mar Pollut Bull* **2014,** *79*, (1–2), 293-298.

50. Gregory, M. R., Virgin plastic granules on some beaches of Eastern Canada and Bermuda. *Mar Environ Res* **1983,** *10*, (2), 73-92.

51. Doyle, M. J.; Watson, W.; Bowlin, N. M.; Sheavly, S. B., Plastic particles in coastal pelagic ecosystems of the Northeast Pacific ocean. *Mar Environ Res* **2011,** *71*, (1), 41-52.

52. Gregory, M. R., Plastic ‘scrubbers’ in hand cleansers: a further (and minor) source for marine pollution identified. *Mar Pollut Bull* **1996,** *32*, (12), 867-871.

53. Fendall, L. S.; Sewell, M. A., Contributing to marine pollution by washing your face: microplastics in facial cleansers. *Mar Pollut Bull* **2009,** *58*, (8), 1225-8.

54. Browne, M. A.; Crump, P.; Niven, S. J.; Teuten, E.; Tonkin, A.; Galloway, T.; Thompson, R., Accumulation of Microplastic on Shorelines Woldwide: Sources and Sinks. *Environmental Science & Technology* **2011,** *45*, (21), 9175-9179.

55. Thompson, R. C.; Olsen, Y.; Mitchell, R. P.; Davis, A.; Rowland, S. J.; John, A. W. G.; McGonigle, D.; Russell, A. E., Lost at sea: Where is all the plastic? *Science* **2004,** *304*, (5672), 838-838.

56. Nuelle, M. T.; Dekiff, J. H.; Remy, D.; Fries, E., A new analytical approach for monitoring microplastics in marine sediments. *Environ. Pollut.* **2014,** *184*, 161-9.

57. Vianello, A.; Boldrin, A.; Guerriero, P.; Moschino, V.; Rella, R.; Sturaro, A.; Da Ros, L., Microplastic particles in sediments of Lagoon of Venice, Italy: First observations on

occurrence, spatial patterns and identification. *Estuarine, Coastal and Shelf Science* **2013,** *130*, (0), 54-61.

58. Liebezeit, G.; Dubaish, F., Microplastics in Beaches of the East Frisian Islands Spiekeroog and Kachelotplate. *Bull Environ Contam Toxicol* **2012**.

59. Claessens, M.; Van Cauwenberghe, L.; Vandegehuchte, M. B.; Janssen, C. R., New techniques for the detection of microplastics in sediments and field collected organisms. *Mar Pollut Bull* **2013,** *70*, (1-2), 227-233.

60. Yonkos, L. T.; Friedel, E. A.; Perez-Reyes, A. C.; Ghosal, S.; Arthur, C. D., Microplastics in Four Estuarine Rivers in the Chesapeake Bay, U.S.A. *Environmental Science & Technology* **2014**.

61. Cole, M.; Webb, H.; Lindeque, P. K.; Fileman, E. S.; Halsband, C.; Galloway, T. S., Isolation of microplastics in biota-rich seawater samples and marine organisms. *Sci. Rep.* **2014,** *4*.

62. Karapanagioti, H. K.; Klontza, I., Investigating the properties of plastic resin pellets found in the coastal areas of lesvos island. *Global Nest J* **2007,** *9*, (1), 71-76.

63. Van Cauwenberghe, L.; Vanreusel, A.; Mees, J.; Janssen, C. R., Microplastic pollution in deep-sea sediments. *Environmental Pollution* **2013,** *182*, (0), 495-499.

64. Gilfillan, L. R.; Ohman, M. D.; Doyle, M. J.; Watson, W., Occurrence of Plastic Micro-Debris in the Southern California Current System. *Cal Coop Ocean Fish* **2009,** *50*, 123-133.

65. Browne, M. A.; Galloway, T. S.; Thompson, R. C., Spatial patterns of plastic debris along Estuarine shorelines. *Environ. Sci. Technol.* **2010,** *44*, (9), 3404-9.

66. Harrison, J. P.; Ojeda, J. J.; Romero-Gonzalez, M. E., The applicability of reflectance micro-Fourier-transform infrared spectroscopy for the detection of synthetic microplastics in marine sediments. *The Science of the total environment* **2012,** *416*, 455-63.

67. Rocha-Santos, T.; Duarte, A. C., A critical overview of the analytical approaches to the occurrence, the fate and the behavior of microplastics in the environment. *TrAC, Trends Anal. Chem.* **2015,** *65*, (0), 47-53.

68. Trimpin, S.; Wijerathne, K.; McEwen, C. N., Rapid methods of polymer and polymer additives identification: Multi-sample solvent-free MALDI, pyrolysis at atmospheric pressure, and atmospheric solids analysis probe mass spectrometry. *Anal. Chim. Acta* **2009,** *654*, (1), 20-25.

69. Eriksen, M.; Mason, S.; Wilson, S.; Box, C.; Zellers, A.; Edwards, W.; Farley, H.; Amato, S., Microplastic pollution in the surface waters of the Laurentian Great Lakes. *Mar Pollut Bull* **2013,** *77*, (1–2), 177-182.

70. Eriksen, M.; Lebreton, L. C. M.; Carson, H. S.; Thiel, M.; Moore, C. J.; Borerro, J. C.; Galgani, F.; Ryan, P. G.; Reisser, J., Plastic Pollution in the World's Oceans: More than 5 Trillion Plastic Pieces Weighing over 250,000 Tons Afloat at Sea. *Plos One* **2014,** *9*, (12).

71. Gregory, M. R., Accumulation and distribution of virgin plastic granules on New Zealand beaches. *New Zeal J Mar Fresh* **1978,** *12*, (4), 399-414.

72. Shiber, J. G., Plastic pellets on the coast of Lebanon. *Mar Pollut Bull* **1979,** *10*, (1), 28-30.

73. Shiber, J. G., Plastic pellets and tar on Spain's Mediterranean beaches. *Mar Pollut Bull* **1987,** *18*, (2), 84-86.

74. Ng, K. L.; Obbard, J. P., Prevalence of microplastics in Singapore's coastal marine environment. *Mar Pollut Bull* **2006,** *52*, (7), 761-7.

75. Martins, J.; Sobral, P., Plastic marine debris on the Portuguese coastline: A matter of size? *Mar Pollut Bull* **2011,** *62*, (12), 2649-2653.

76. Corcoran, P. L.; Biesinger, M. C.; Grifi, M., Plastics and beaches: A degrading relationship. *Mar Pollut Bull* **2009,** *58*, (1), 80-84.

77. Ivar do Sul, J. A.; Spengler, Â.; Costa, M. F., Here, there and everywhere. Small plastic fragments and pellets on beaches of Fernando de Noronha (Equatorial Western Atlantic). *Mar Pollut Bull* **2009,** *58*, (8), 1236-1238.

78. Karapanagioti, H. K.; Endo, S.; Ogata, Y.; Takada, H., Diffuse pollution by persistent organic pollutants as measured in plastic pellets sampled from various beaches in Greece. *Mar Pollut Bull* **2011,** *62*, (2), 312-317.

79. Lechner, A.; Keckeis, H.; Lumesberger-Loisl, F.; Zens, B.; Krusch, R.; Tritthart, M.; Glas, M.; Schludermann, E., The Danube so colourful: A potpourri of plastic litter outnumbers fish larvae in Europe's second largest river. *Environmental Pollution* **2014,** *188*, (0), 177-181.

80. von Moos, N.; Burkhardt-Holm, P.; Köhler, A., Uptake and Effects of Microplastics on Cells and Tissue of the Blue Mussel Mytilus edulis L. after an Experimental Exposure. *Environmental Science & Technology* **2012,** *46*, (20), 11327-11335.

81. Besseling, E.; Wegner, A.; Foekema, E. M.; van den Heuvel-Greve, M. J.; Koelmans, A. A., Effects of Microplastic on Fitness and PCB Bioaccumulation by the Lugworm Arenicola marina (L.). *Environmental Science & Technology* **2013,** *47*, (1), 593-600.

82. Lusher, A. L.; McHugh, M.; Thompson, R. C., Occurrence of microplastics in the gastrointestinal tract of pelagic and demersal fish from the English Channel. *Mar Pollut Bull* **2013,** *67*, (1-2), 94-99.

83. Watts, A. J.; Lewis, C.; Goodhead, R. M.; Beckett, S. J.; Moger, J.; Tyler, C. R.; Galloway, T. S., Uptake and retention of microplastics by the shore crab Carcinus maenas. *Environ. Sci. Technol.* **2014,** *48*, (15), 8823-30.

84. Cole, M.; Lindeque, P.; Fileman, E.; Halsband, C.; Goodhead, R.; Moger, J.; Galloway, T. S., Microplastic Ingestion by Zooplankton. *Environmental Science & Technology* **2013,** *47*, (12), 6646-6655.

85. Hamer, J.; Gutow, L.; Kohler, A.; Saborowski, R., Fate of microplastics in the marine isopod Idotea emarginata. *Environ. Sci. Technol.* **2014,** *48*, (22), 13451-8.

86. Setala, O.; Fleming-Lehtinen, V.; Lehtiniemi, M., Ingestion and transfer of microplastics in the planktonic food web. *Environ. Pollut.* **2014,** *185*, 77-83.

87. Van Cauwenberghe, L.; Janssen, C. R., Microplastics in bivalves cultured for human consumption. *Environ. Pollut.* **2014,** *193*, 65-70.

88. Rochman, C. M.; Hoh, E.; Kurobe, T.; Teh, S. J., Ingested plastic transfers hazardous chemicals to fish and induces hepatic stress. *Sci. Rep.* **2013,** *3*.

89. de Sa, L. C.; Luis, L. G.; Guilhermino, L., Effects of microplastics on juveniles of the common goby (Pomatoschistus microps): Confusion with prey, reduction of the predatory performance and efficiency, and possible influence of developmental conditions. *Environ. Pollut.* **2014,** *196C*, 359-362.

90. Hollender, J.; Bourgin, M.; Fenner, K. B.; Longrée, P.; McArdell, C. S.; Moschet, C.; Ruff, M.; Schymanski, E. L.; Singer, H. P., Exploring the Behaviour of Emerging Contaminants in the Water Cycle using the Capabilities of High Resolution Mass Spectrometry. *CHIMIA International Journal for Chemistry* **2014,** *68*, (11), 793-798.

91. Rolf, H.; Nick van de, G.; Corine, J. H., Medicinal footprint of the population of the Rhine basin. *Environmental Research Letters* **2013,** *8*, (4), 044057.

92. Peschka, M.; Müller, J.; Knepper, T. P.; Seel, P., Trends in Pesticide Transport into the River Rhine. In *The Rhine*, Knepper, T., Ed. Springer Berlin Heidelberg: 2006; Vol. 5L, pp 155-175.

93. Yang, Y.; Ligouis, B.; Pies, C.; Grathwohl, P.; Hofmann, T., Occurrence of coal and coal-derived particle-bound polycyclic aromatic hydrocarbons (PAHs) in a river floodplain soil. *Environmental Pollution* **2008,** *151*, (1), 121-129.

94. Fries, E.; Zarfl, C., Sorption of polycyclic aromatic hydrocarbons (PAHs) to low and high density polyethylene (PE). *Environ Sci Pollut Res* **2012,** *19*, (4), 1296-1304.

95. Fox, A. J.; Collier, P. F., Mortality experience of workers exposed to vinyl chloride monomer in the manufacture of polyvinyl chloride in Great Britain. *British Journal of Industrial Medicine* **1977,** *34*, (1), 1-10.

96. Sajiki, J.; Yonekubo, J., Leaching of bisphenol A (BPA) to seawater from polycarbonate plastic and its degradation by reactive oxygen species. *Chemosphere* **2003,** *51*, (1), 55-62.

97. Mato, Y.; Isobe, T.; Takada, H.; Kanehiro, H.; Ohtake, C.; Kaminuma, T., Plastic resin pellets as a transport medium for toxic chemicals in the marine environment. *Environmental Science & Technology* **2001,** *35*, (2), 318-324.

98. Endo, S.; Takizawa, R.; Okuda, K.; Takada, H.; Chiba, K.; Kanehiro, H.; Ogi, H.; Yamashita, R.; Date, T., Concentration of polychlorinated biphenyls (PCBs) in beached resin

pellets: Variability among individual particles and regional differences. *Mar Pollut Bull* **2005,** *50*, (10), 1103-1114.

99. Frias, J. P.; Sobral, P.; Ferreira, A. M., Organic pollutants in microplastics from two beaches of the Portuguese coast. *Mar Pollut Bull* **2010,** *60*, (11), 1988-92.

100. Fisner, M.; Taniguchi, S.; Moreira, F.; Bicego, M. C.; Turra, A., Polycyclic aromatic hydrocarbons (PAHs) in plastic pellets: Variability in the concentration and composition at different sediment depths in a sandy beach. *Mar Pollut Bull* **2013,** *70*, (1-2), 219-226.

101. Endo, S.; Yuyama, M.; Takada, H., Desorption kinetics of hydrophobic organic contaminants from marine plastic pellets. *Mar Pollut Bull* **2013,** *74*, (1), 125-131.

102. Wurl, O.; Obbard, J. P., A review of pollutants in the sea-surface microlayer (SML): a unique habitat for marine organisms. *Mar Pollut Bull* **2004,** *48*, (11–12), 1016-1030.

103. Teuten, E. L.; Rowland, S. J.; Galloway, T. S.; Thompson, R. C., Potential for plastics to transport hydrophobic contaminants. *Environ. Sci. Technol.* **2007,** *41*, (22), 7759-64.

104. Bakir, A.; Rowland, S. J.; Thompson, R. C., Enhanced desorption of persistent organic pollutants from microplastics under simulated physiological conditions. *Environ. Pollut.* **2014,** *185*, 16-23.

105. Koelmans, A. A.; Besseling, E.; Wegner, A.; Foekema, E. M., Plastic as a Carrier of POPs to Aquatic Organisms: A Model Analysis. *Environmental Science & Technology* **2013,** *47*, (14), 7812-7820.

106. Koelmans, A. A.; Besseling, E.; Foekema, E. M., Leaching of plastic additives to marine organisms. *Environmental Pollution* **2014,** *187*, 49-54.

107. Falbe, J.; Regitz, M., Römpp Chemie Lexikon, 9. erweiterte und neubearbeitete Auflage. In Georg Thieme Verlag, Stuttgart: 1995.

108. Wienberg, R., Adsorption und Desorption. *Handbuch zur Erkundung des Untergrundes von Deponien und Altlasten* **1998,** *5*, 209-222.

109. Sposito, G., *The chemistry of soils*. Oxford university press: 2008.

110. Worch, E., *Adsorption technology in water treatment: fundamentals, processes, and modeling*. Walter de Gruyter: **2012**.

111. Kümmel, R.; Worch, E., *Adsorption aus wässrigen Lösungen: mit 23 Tabellen*. Dt. Verlag für Grundstoffindustrie: **1990**.

112. Luckner, L., *Migration processes in the soil and groundwater zone*. CRC Press: 1991.

113. Kinniburgh, D. G., General purpose adsorption isotherms. *Environmental Science & Technology* **1986,** *20*, (9), 895-904.

114. Brunauer, S.; Emmett, P. H.; Teller, E., Adsorption of Gases in Multimolecular Layers. *J. Am. Chem. Soc.* **1938,** *60*, (2), 309-319.

115. Lazaridis, N. K.; Asouhidou, D. D., Kinetics of sorptive removal of chromium(VI) from aqueous solutions by calcined Mg–Al–CO3 hydrotalcite. *Water Research* **2003,** *37*, (12), 2875-2882.

116. Tan, I. A. W.; Ahmad, A. L.; Hameed, B. H., Adsorption of basic dye on high-surface-area activated carbon prepared from coconut husk: Equilibrium, kinetic and thermodynamic studies. *J. Hazard. Mater.* **2008,** *154*, (1–3), 337-346.

117. Lin, K.; Pan, J.; Chen, Y.; Cheng, R.; Xu, X., Study the adsorption of phenol from aqueous solution on hydroxyapatite nanopowders. *J. Hazard. Mater.* **2009,** *161*, (1), 231-240.

118. Crini, G., Kinetic and equilibrium studies on the removal of cationic dyes from aqueous solution by adsorption onto a cyclodextrin polymer. *Dyes and Pigments* **2008,** *77*, (2), 415-426.

119. Lagergren, S., Zur Theorie der sogenannten Absorption gelöster Stoffe. *Kungliga Svenska Vetenskapsakademies. Handlingar* **1898,** *24*, (4), 1-39.

120. Yuh-Shan, H., Citation review of Lagergren kinetic rate equation on adsorption reactions. *Scientometrics* **2004,** *59*, (1), 171-177.

121. Rochman, C. M.; Manzano, C.; Hentschel, B. T.; Simonich, S. L. M.; Hoh, E., Polystyrene Plastic: A Source and Sink for Polycyclic Aromatic Hydrocarbons in the Marine Environment. *Environmental Science & Technology* **2013,** *47*, (24), 13976-13984.

122. Ho, Y.-S., Review of second-order models for adsorption systems. *J. Hazard. Mater.* **2006,** *136*, (3), 681-689.

123. Wan Ngah, W. S.; Teong, L. C.; Hanafiah, M. A. K. M., Adsorption of dyes and heavy metal ions by chitosan composites: A review. *Carbohydr. Polym.* **2011,** *83*, (4), 1446-1456.

124. Leboeuf, E. J.; Weber, W. J., Macromolecular characteristics of natural organic matter. 1. Insights from glass transition and enthalpic relaxation behavior. *Environmental Science & Technology* **2000,** *34*, (17), 3623-3631.

125. LeBoeuf, E. J.; Weber, W. J., A Distributed Reactivity Model for Sorption by Soils and Sediments. 8. Sorbent Organic Domains: Discovery of a Humic Acid Glass Transition and an Argument for a Polymer-Based Model. *Environmental Science & Technology* **1997,** *31*, (6), 1697-1702.

126. Rubio, J. A.; González-Mazo, E.; Gómez-Parra, A., Sorption of linear alkylbenzenesulfonates (LAS) on marine sediment. *Mar. Chem.* **1996,** *54*, (1–2), 171-177.

127. Xu, X.-R.; Li, X.-Y., Sorption behaviour of benzyl butyl phthalate on marine sediments: Equilibrium assessments, effects of organic carbon content, temperature and salinity. *Mar. Chem.* **2009,** *115*, (1–2), 66-71.

128. Cornelissen, G.; Gustafsson, Ö., Sorption of Phenanthrene to Environmental Black Carbon in Sediment with and without Organic Matter and Native Sorbates. *Environmental Science & Technology* **2004,** *38*, (1), 148-155.

129. Coulier, L.; Kaal, E. R.; Tienstra, M.; Hankemeier, T., Identification and quantification of (polymeric) hindered-amine light stabilizers in polymers using pyrolysis–gas chromatography–mass spectrometry and liquid chromatography–ultraviolet absorbance detection–evaporative light scattering detection. *J. Chromatogr. A* **2005,** *1062*, (2), 227-238.

130. Hosaka, A.; Watanabe, C.; Tsuge, S., Rapid Determination of Decabromodiphenyl Ether in Polystyrene by Thermal Desorption-GC/MS. *Anal Sci* **2005,** *21*, (10), 1145-1147.

131. Bart, J. C. J., Polymer/additive analysis by flash pyrolysis techniques1. *J. Anal. Appl. Pyrolysis* **2001,** *58–59*, (0), 3-28.

132. Jonker, M. T. O.; Koelmans, A. A., Extraction of Polycyclic Aromatic Hydrocarbons from Soot and Sediment: Solvent Evaluation and Implications for Sorption Mechanism. *Environmental Science & Technology* **2002,** *36*, (19), 4107-4113.

133. Parera, J.; Santos, F. J.; Galceran, M. T., Microwave-assisted extraction versus Soxhlet extraction for the analysis of short-chain chlorinated alkanes in sediments. *J. Chromatogr. A* **2004,** *1046*, (1–2), 19-26.

134. Bandh, C.; Björklund, E.; Mathiasson, L.; Näf, C.; Zebühr, Y., Comparison of Accelerated Solvent Extraction and Soxhlet Extraction for the Determination of PCBs in Baltic Sea Sediments. *Environmental Science & Technology* **2000,** *34*, (23), 4995-5000.

135. Lou, X.; Janssen, H.-G.; Cramers, C. A., Parameters Affecting the Accelerated Solvent Extraction of Polymeric Samples. *Anal Chem* **1997,** *69*, (8), 1598-1603.

136. Dunnivant, F.; Polansky, A.; Elzerman, A., Persistence and distribution of PCBs in the sediments of a reservoir (Lake Hartwell, South Carolina). *Bulletin of Environmental Contamination and Toxicology* **1989,** *43*, (6), 870-878.

137. Vrana, B.; Mills, G.; Greenwood, R.; Knutsson, J.; Svensson, K.; Morrison, G., Performance optimisation of a passive sampler for monitoring hydrophobic organic pollutants in water. *J Environ Monitor* **2005,** *7*, (6), 612-620.

138. Reingruber, E.; Buchberger, W., Analysis of polyolefin stabilizers and their degradation products. *J. Sep. Sci.* **2010,** *33*, (22), 3463-3475.

139. Zhang, Y.; Geißen, S.-U.; Gal, C., Carbamazepine and diclofenac: Removal in wastewater treatment plants and occurrence in water bodies. *Chemosphere* **2008,** *73*, (8), 1151-1161.

140. Karickhoff, S. W., Semi-empirical estimation of sorption of hydrophobic pollutants on natural sediments and soils. *Chemosphere* **1981,** *10*, (8), 833-846.

141. Weil, L.; Dure, G.; Quentin, K.-E., Water solubility of insecticide chlorinated hydrocarbons andpolychlorinated biphenyls in relation of water pollution with these compounds). *Z. Wasser-Abwasser-Forsch.* **1974,** *7*, (6), 169-175.

142. Platford, R. F., The environmental significance of surface films II. Enhanced partitioning of Lindane in thin films of octanol on the surface of water. *Chemosphere* **1981,** *10*, (7), 719-722.

143. Yu, Z.; Xiao, B.; Huang, W.; Peng, P. A., Sorption of steroid estrogens to soils and sediments. *Environ Toxicol Chem* **2004,** *23*, (3), 531-539.

144. Shareef, A.; Angove, M. J.; Wells, J. D.; Johnson, B. B., Aqueous Solubilities of Estrone, 17β-Estradiol, 17α-Ethynylestradiol, and Bisphenol A. *Journal of Chemical & Engineering Data* **2006,** *51*, (3), 879-881.

145. Racke, K. D., Environmental fate of chlorpyrifos. *Reviews of environmental contamination and toxicology* **1993,** *131*, 1-150.

146. Racke, K. D., *Environmental fate of chlorpyrifos*. Springer: **1993**.

147. Renner, R., The KOW Controversy. *Environmental Science & Technology* **2002,** *36*, (21), 410A-413A.

148. Kile, D. E.; Chiou, C. T., Water solubility enhancements of DDT and trichlorobenzene by some surfactants below and above the critical micelle concentration. *Environmental Science & Technology* **1989,** *23*, (7), 832-838.

149. Ogata, Y.; Takada, H.; Mizukawa, K.; Hirai, H.; Iwasa, S.; Endo, S.; Mato, Y.; Saha, M.; Okuda, K.; Nakashima, A.; Murakami, M.; Zurcher, N.; Booyatumanondo, R.; Zakaria, M. P.; Dung, L. Q.; Gordon, M.; Miguez, C.; Suzuki, S.; Moore, C.; Karapanagioti, H. K.; Weerts, S.; McClurg, T.; Burres, E.; Smith, W.; Van Velkenburg, M.; Lang, J. S.; Lang, R. C.; Laursen, D.; Danner, B.; Stewardson, N.; Thompson, R. C., International Pellet Watch: Global monitoring of persistent organic pollutants (POPs) in coastal Waters. 1. Initial phase data on PCBs, DDTs, and HCHs. *Mar Pollut Bull* **2009,** *58*, (10), 1437-1446.

150. Jayasiri, H. B.; Purushothaman, C. S.; Vennila, A., Plastic litter accumulation on high-water strandline of urban beaches in Mumbai, India. *Environ Monit Assess* **2013,** *185*, (9), 7709-7719.

151. JRC (Joint Research Centre), *Marine Litter - Technical Recommendations for the Implentation of MSFD Requirements*; 1831-9424; Institute for Environment and Sustainability: **2011**.

152. U.S. Environmental Protection Agency, *Plastic Pellets in The Aquatic Environment - Sorces And Recommendations*; Office of Water: **1993**.

153. Imhof, H. K.; Ivleva, N. P.; Schmid, J.; Niessner, R.; Laforsch, C., Supporting Information - Contamination of beach sediments of a subalpine lake with microplastic particles. *Current Biology* **2013,** *23*, (19).

154. Jung, J. H.; Ree, M.; Kim, H., Acid- and base-catalyzed hydrolyses of aliphatic polycarbonates and polyesters. *Catal. Today* **2006,** *115*, (1–4), 283-287.

155. Cole, M.; Webb, H.; Lindeque, P. K.; Fileman, E. S.; Halsband, C.; Galloway, T. S., Isolation of microplastics in biota-rich seawater samples and marine organisms. *Scientific reports* **2014,** *4*, 4528.

156. Lustiger, A., Understanding environmental stress cracking in polyethylene. *Medical plastics: degradation resistance & failure analysis* **1998**, 65-71.

157. Wik, A.; Dave, G., Occurrence and effects of tire wear particles in the environment – A critical review and an initial risk assessment. *Environmental Pollution* **2009,** *157*, (1), 1-11.

158. PlasticsEurope, Plastics - the Facts 2013: An analysis of European latest plastics production, demand and waste data. **2013**, 1-36.

159. Best, J. L., Sediment transport and bed morphology at river channel confluences. *Sedimentology* **1988,** *35*, (3), 481-498.

160. Frisch, H. L., Sorption and transport in glassy polymers–a review. *Polymer Engineering & Science* **1980,** *20*, (1), 2-13.

161. Pascall, M. A.; Zabik, M. E.; Zabik, M. J.; Hernandez, R. J., Uptake of Polychlorinated Biphenyls (PCBs) from an Aqueous Medium by Polyethylene, Polyvinyl Chloride, and Polystyrene Films. *J Agr Food Chem* **2005,** *53*, (1), 164-169.

162. Allan, I. J.; Booij, K.; Paschke, A.; Vrana, B.; Mills, G. A.; Greenwood, R., Field Performance of Seven Passive Sampling Devices for Monitoring of Hydrophobic Substances. *Environmental Science & Technology* **2009,** *43*, (14), 5383-5390.

163. Scheytt, T.; Mersmann, P.; Lindstädt, R.; Heberer, T., Determination of sorption coefficients of pharmaceutically active substances carbamazepine, diclofenac, and ibuprofen, in sandy sediments. *Chemosphere* **2005,** *60*, (2), 245-253.

164. Schwarzenbach, R. P.; Gschwend, P. M.; Imboden, D. M., Environmental Organic Chemistry. In John Wiley & Sons, Inc.: **2005**.

165. Schaffer, M.; Boxberger, N.; Börnick, H.; Licha, T.; Worch, E., Sorption influenced transport of ionizable pharmaceuticals onto a natural sandy aquifer sediment at different pH. *Chemosphere* **2012,** *87*, (5), 513-520.

166. Ternes, T. A.; Meisenheimer, M.; McDowell, D.; Sacher, F.; Brauch, H.-J.; Haist-Gulde, B.; Preuss, G.; Wilme, U.; Zulei-Seibert, N., Removal of Pharmaceuticals during Drinking Water Treatment. *Environmental Science & Technology* **2002,** *36*, (17), 3855-3863.

167. Weber Jr, W. J.; Miller, C. T., Modeling the sorption of hydrophobic contaminants by aquifer materials—I. Rates and equilibria. *Water Research* **1988,** *22*, (4), 457-464.

168. Sprynskyy, M.; Ligor, T.; Buszewski, B., Clinoptilolite in study of lindane and aldrin sorption processes from water solution. *J. Hazard. Mater.* **2008,** *151*, (2–3), 570-577.

169. Sotelo, J. L.; Ovejero, G.; Delgado, J. A.; Martínez, I., Adsorption of lindane from water onto GAC: effect of carbon loading on kinetic behavior. *Chem. Eng. J.* **2002,** *87*, (1), 111-120.

170. Nerin, C.; Tornes, A. R.; Domeno, C.; Cacho, J., Absorption of pesticides on plastic films used as agricultural soil covers. *J Agr Food Chem* **1996,** *44*, (12), 4009-4014.

171. Yu, Y. L.; Wu, X. M.; Li, S. N.; Fang, H.; Zhan, H. Y.; Yu, J. Q., An exploration of the relationship between adsorption and bioavailability of pesticides in soil to earthworm. *Environmental Pollution* **2006,** *141*, (3), 428-433.

172. Picer, M.; Picer, N.; Strohal, P., Evidence on behaviour of low concentration DDT in laboratory sorption experiments. *Science of The Total Environment* **1977,** *8*, (2), 159-164.

173. OECD, *Test No. 105: Water Solubility*. OECD Publishing.

174. Lee, C.-L.; Kuo, L.-J.; Wang, H.-L.; Hsieh, P.-C., Effects of ionic strength on the binding of phenanthrene and pyrene to humic substances: three-stage variation model. *Water Research* **2003,** *37*, (17), 4250-4258.

175. Qian, Y.; Posch, T.; Schmidt, T. C., Sorption of polycyclic aromatic hydrocarbons (PAHs) on glass surfaces. *Chemosphere* **2011,** *82*, (6), 859-865.

176. Kalbitz, K.; Popp, P.; Geyer, W.; Hanschmann, G., β-HCH mobilization in polluted wetland soils as influenced by dissolved organic matter. *Science of The Total Environment* **1997,** *204*, (1), 37-48.

177. Peijnenburg, W. J. G. M.; Struijs, J., Occurrence of phthalate esters in the environment of the Netherlands. *Ecotoxicology and Environmental Safety* **2006,** *63*, (2), 204-215.

178. Zhao, B.; Chu, Y.; Huang, Y.; Hardy, D. O.; Lin, S.; Ge, R.-S., Structure-dependent inhibition of human and rat 11β-hydroxysteroid dehydrogenase 2 activities by phthalates. *Chem. Biol. Interact.* **2010,** *183*, (1), 79-84.

179. Poon, R.; Lecavalier, P.; Mueller, R.; Valli, V. E.; Procter, B. G.; Chu, I., Subchronic oral toxicity of di-n-octyl phthalate and di(2-ethylhexyl) phthalate in the rat. *Food Chem. Toxicol.* **1997,** *35*, (2), 225-239.

180. Yunker, M. B.; Macdonald, R. W.; Vingarzan, R.; Mitchell, R. H.; Goyette, D.; Sylvestre, S., PAHs in the Fraser River basin: a critical appraisal of PAH ratios as indicators of PAH source and composition. *Org Geochem* **2002,** *33*, (4), 489-515.

181. Countway, R. E.; Dickhut, R. M.; Canuel, E. A., Polycyclic aromatic hydrocarbon (PAH) distributions and associations with organic matter in surface waters of the York River, VA Estuary. *Org Geochem* **2003,** *34*, (2), 209-224.

182. Gocht, T.; Moldenhauer, K.-M.; Püttmann, W., Historical record of polycyclic aromatic hydrocarbons (PAH) and heavy metals in floodplain sediments from the Rhine River (Hessisches Ried, Germany). *Appl. Geochem.* **2001,** *16*, (15), 1707-1721.

183. Karapanagioti, H. K.; Ogata, Y.; Takada, H., Eroded Plastic Pellets as Monitoring Tools for Polycyclic Aromatic Hydrocarbons (Pah): Laboratory and Field Studies. *Global Nest J* **2010,** *12*, (3), 327-334.

184. Zabaniotou, A.; Kassidi, E., Life cycle assessment applied to egg packaging made from polystyrene and recycled paper. *J Clean Prod* **2003,** *11*, (5), 549-559.

185. Kwon, E.; Castaldi, M. J., Investigation of Mechanisms of Polycyclic Aromatic Hydrocarbons (PAHs) Initiated from the Thermal Degradation of Styrene Butadiene Rubber (SBR) in N2 Atmosphere. *Environmental Science & Technology* **2008,** *42*, (6), 2175-2180.

186. Smith, E. J.; Davison, W.; Hamilton-Taylor, J., Methods for preparing synthetic freshwaters. *Water research* **2002,** *36*, (5), 1286-1296.